Acidic Catalyzed Ring-Opening (co)Polymerization of γ-lactones

Mariana Ferreira Monteiro

Thesis to obtain the Master Science Degree in

Chemical Engineering

Supervisors: Prof. Fréderic Peruch, Dr. Stephane Carlotti (LCPO)
Prof. Maria do Rosário Ribeiro (IST)

Examination Committee:

Chairperson: Prof. Sebastião Manuel Tavares da Silva Alves
Supervisor: Prof. Maria do Rosário Ribeiro
Members of the Committee: Prof. João Carlos Moura Bordado

June 2017

This work was done in collaboration with

Quote: “Life is too short to be afraid” Joana Peixoto

THIS PAGE WAS INTENTIONALLY LEFT BLANK

Acknowledgements

I express my gratitude to Professora Maria do Rosário Ribeiro, for the opportunity of developing this work at LCPO, and for the help during the revision of this work.

I want to thank my supervisors in LCPO, Frederic Peruch and Stéphane Carlotti, for all the support and dedication that they provided during the internship, and in the revision of this work. It was a pleasure to work with you both.

To LCPO department for the receiving welcome and for all the collaboration and affection during my time in LCPO. I want to thank Jeremie Granger for the help in the laboratory, friendship, for the French lessons and patience.

During this internship I met extraordinary people, that made me to integrate and to have great times in Bordeaux. To them: Dounia, Marie, Julie, Beste, Esra, Amelie, Sofiem, Quentin, Boris, Martin, Arthur, Jana, thank you.

I want to thank all my portuguese friends, that supported me and helped me in everything they can, especially the friends in Lisbon: João Cordeiro, João Loios, Filipe Costa, Joana Figueiredo, David Paulo, Francisco Ferreira.

Finally, but not less important my family. If it wasn't for you I didn't had strength to fight this alone. Thank you for all the support, love, affection, help. Without you none of this was possible.

This work is dedicated to a very special person to me: Joana Peixoto.

THIS PAGE WAS INTENTIONALLY LEFT BLANK

Abstract

The aim of this work was the study of several polymerization systems using lactones as monomers, such as, Ɛ-caprolactone and ɣ-butyrolactone, by a ring opening mechanism. The experiments were performed with acidic catalysts such as, methanesulfonic acid and triflic acid. As indicated in the literature, the ring opening polymerizations with these types of catalysts and ɣ-lactones were not possible under the operating conditions due to the thermodynamic stability of this type of monomer. Thus, to obtain an efficient system, the copolymerization of the two monomers, Ɛ-caprolactone and ɣ-butyrolactone, was performed at different temperatures (-40 °C to 30 °C) and with the two catalysts mentioned above. Novel copolymers, γ-butyrolactone-co-Ɛ-caprolactone were obtained at all tested temperatures showing the incorporation of ɣ-butyrolactone as desired.

KEYWORDS: Ɛ-caprolactone, ɣ-butyrolactone, Ring-opening Polymerization, lactones, copolymers

THIS PAGE WAS INTENTIONALLY LEFT BLANK

Resumo

O objetivo deste trabalho visa o estudo da polimerização por abertura de anel de lactonas, tais como, Ɛ-lactona e ɣ-lactona. Neste estudo utilizaram-se catalisadores ácidos nomeadamente o ácido metanosulfónico e o ácido tríflico. Tal como indicado na literatura, as reações de polimerização por abertura do anel de ɣ-lactonas, com este tipo de catalisadores, não foram possíveis nas condições operatórias usadas, dada a estabilidade termodinâmica deste tipo de monómeros. Assim, para se obter um sistema eficiente recorreu-se à copolimerização dos dois monómeros, Ɛ-caprolactona e ɣ-butirolactona, a diferentes temperaturas (-40ºC a 30ºC) e com os dois catalisadores supramencionados. Foram obtidos novos copolímeros, ɣ-butyrolactona-co-Ɛ-caprolactona, em todas as temperaturas testadas que mostram tal como pretendido a incorporação de y-butyrolactona.

PALAVRAS-CHAVE: Ɛ-caprolactona, ɣ-butyrolactona, Polimerização por abertura de anel, lactonas, copolímeros

THIS PAGE WAS INTENTIONALLY LEFT BLANK

Table of Contents

THIS PAGE WAS INTENTIONALLY LEFT BLANK

List of Figures

THIS PAGE WAS INTENTIONALLY LEFT BLANK

List of Tables

THIS PAGE WAS INTENTIONALLY LEFT BLANK

List of Abbreviations

$Ipeak_x$ Integration peak of x

Mn_{th} Theoretical molar mass

x_x conversion of x

^{1}H NMR Proton nuclear magnetic ressonanceresonance

4HV 4-hidroxyvaleratehydroxyvalerate

AOMEC 2-allyloxymethyl-2-ethyl-trimethylene carbonate

BnOH Benzyl alcohol

BPM Biphenyl-4-methanol

$CDCl_3$ Deuterated chlorophormchloroform

Đ Polydispersity Dispersity

DIPEA N,N-Diisopropylethylamine

DP Degree of polymerization

DPP Diphenyl phosphate

homoPMBL homopoly(α-methylene-γ-butyrolactone)

LA Lactide

LDPE Low density polyethylene

Lipase CC *Candida cylindracea lipase*

Lipase PF *Pseudomonas fluorescens lipase*

LLDPE Linear low-density polyethylene

MBL α-methylene-γ-butyrolactone

MeLi Methyllithium

Mn Number-average molar mass

mPEG methoxy polyethyleneglycol

MSA Methanesulfonic acid

PCL Polycaprolactone

PDL 15-pentadecanolactone

PGA Polyglycolic acid

PHA Polyhydroxyalkanoates

PHB Polyhydroxybutyrate

PLA Polylactide

PMBL-co-PCL poly(α-methylene-γ-butyrolactone-*co*-polyε-caprolactone)

PP Polypropylene

PPL *Porcine pancreatic lipase*

PVC Polyvinyl chloride

R Constant gas

RI Refractive Index

ROP Ring-Opening Polymerization

SEC Size exclusion chromatography

t-BuOK Tert-butoxide

t-BuP_4 Phosphazene

Tc Ceiling temperature

T_F Floor temperature

TFM Thermodynamic favored monomers

TfOH Triflic acid

THF Tetrahydrofuran

TIM Thermodynamic intermediate monomers

TMC Trimethylene carbonate

TUM Thermodynamic unfavored monomers

UV Ultraviolet

Ɛ-CL Ɛ-Caprolactone

ɣ-BL ɣ-Butyrolactone

ɣ-VL ɣ-Valerolactone

α-Br- ɣ-BL α-bromo-γ-butyrolactone

β-BL β-butyrolactone

δ-VL δ -valerolactone

ΔG_p Gibbs energy of polymerization

ΔH_p Enthalpy energy of polymerization

ΔS_p Entropy energy of polymerization

1. Introduction

Nowadays, plastics are used in an enormous and expanding range of products and markets, such as packaging, building and construction, electrical and electronic products. There is a large range of variety of plastics for different needs (PP, LDPE, LLDPE, PVC, etc.). In 2014, the world production of plastics was 314 million tons of which 59 million of tones was from Europe. The most alarming problem of the plastics is the ending up of this after being consumed. In 2014, 25.8 million tonnes of post-consumer plastics waste ended up in the waste upstream. 69.2% was recovered through recycling and energy recovery processes while 30.8% still went to landfill. Many of these plastics have a long time of degradation so there are a lot of environmental problems associated. [1]

To solve this problem, some investigators and researchers started to study the synthesis of biodegradable polymers. One of the most studied and the most important group of biodegradable polymers are polyesters. Thanks to their physical and chemical properties the range of applications can be varied. Biodegradable polyesters due to the characteristics of the main-chain structure and a certain extent of hydrophilicity can degrade easily in the environment. These attributes make them a leading candidate in biomedical and pharmaceutical industries. [2]

Two different approaches can be applied in the synthesis of these polyesters: Ring-Opening Polymerization (ROP) of cyclic esters and polycondensation.

In recent decades, Ring-Opening Polymerization of cyclic esters has been investigated to study new reaction pathways and new catalytic processes to create novel and high performing materials. Biodegradable and biocompatible polymers have become readily accessible by chemical synthesis via ROP from cyclic esters or lactones, with a big variety of applications or even be incorporated in another polymer in the form of blends or copolymers.

This thesis will focus on the synthesis of new biodegradable polyesters obtained by acidic catalyzed ring-opening polymerization of ɣ-butyrolactone, this lactone being described to be non-polymerizable because of unfavourable thermodynamics for the opening of the cycle.

Regarding the thesis outline, firstly a bibliographic review presents some relevant topics concerning biodegradable polymers, including the different approaches to obtain polyesters, the thermodynamic of ROP and some examples in particularly the ROP of ɣ-lactones (Chapter 1). The details about the experimental unit and the characterization apparatus are provided in Chapter 2. In Chapter 3 are presented the results of the homopolymerization and copolymerization of Ɛ-caprolactone and ɣ-butyrolactone, with two different catalysts methanesulfonic acid (MSA) and trifluoromethanesulfonic acid (TfOH) and biphenyl-4-methanol (BPM) as the initiator, performed at different temperatures and monomer ratios. In addition, the characterization of the polymers obtained by ^{1}H NMR and SEC is reported. Lastly, in Chapter 4 it can be found the main conclusions drawn along the project and the future perspectives for the remaining issues of this work.

THIS PAGE WAS INTENTIONALLY LEFT BLANK

2. Literature Review

2.1. Biodegradable Polymers

Biodegradable polymers have received an increasing attention in the last decades due to their ability to be ecofriendly and to their potential in a very wide range of applications such as, in the designing of resorbable materials, in disposable packages and in the designing of commodity thermoplastics from renewable resources. [3] The characteristics of the novel synthetic polymer materials can be very useful in the medical application, due to the mechanical and thermal properties and their non-toxicity. [2]

Biodegradable polymers can be divided in two large groups based on structure and synthesis: agro-polymers and biopolyesters (Figure 1).

Agro-polymers are derived from biomass including proteins and polysaccharides, such as: cellulose and starch, and biopolyesters are derived from microorganisms or synthetically made from either synthetic or natural monomers, such as: poly (lactic acid) (PLA), poly (glycolic acid) (PGA), poly (Ɛ-caprolactone) (PCL) and poly (hydroxyalkanoates) (PHA).

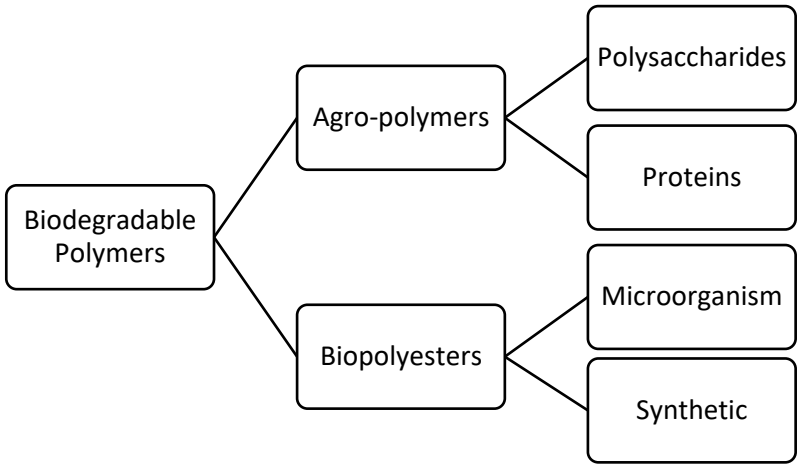

Figure 1 – Biodegradable polymers organization based on structure and occurrence.

Nowadays, the most popular and used biodegradable polymers are aliphatic polyesters (e.g. PCL, PLA, PGA and poly-3-hydroxybutyrate (PHB)). [4]

For example, biodegradable PLA exhibits properties which makes this polymer a very promising one for industrial application. PLA is used in medical, textile and packaging, although its brittleness and high price are a huge drawback and still limit its applications. The brittleness may be controlled in a certain extent using a plasticizer. The plasticizing of PLA was carried out with the help of chemicals, such as citrate esters and glucose monoesters, through the polar interactions between the ester groups in the plasticizer and PLA. Subsequently, it was detected that with the aging of the plasticized film materials, the low molar mass plasticizers tend to migrate to the film surface. [5] [6] [7] [8] [9] [10] Other investigations were also performed by blending this polymer with others more hydrophilic, to provide changes in terms of their miscibility, physical properties, morphology, biodegradability, drug release

properties and porous material preparation. An example of a hydrophilic polymer is PCL which is a ductile biodegradable polymer and tuned with PLA makes the last one, change from rigid to ductile. [4]

Polycaprolactone and its copolymers were popular in the 1970s and 1980s thanks to their advantages over other biopolymers: adaptable degradation kinetics and mechanical properties, ease of shaping and manufacture enabling pore sizes conducive to tissue-growth and the controlled delivery of drugs contained within their matrix. The functional groups added could also improve the properties of the polymer making it more hydrophilic, adhesive, or biocompatible. In the medical device industry, PCL did not have the mechanical properties suitable to high load bearing applications. Due to some limiting properties of PCL and with the appearance of other resorbable polymers, like PLA and PGA, polycaprolactone vanished from the investigations. PCL arose in the 21st century back into the biomedical field with rheological and viscoelastic characteristics better than other aliphatic polyesters, that allowed its application in a wide range of scaffold fabrication technologies. Its fabrication routes compared with other polyesters is inexpensive. [11]

Polyglycolide or poly (glycolic acid) (PGA) is also biodegradable and, when is implanted in tissue, has no toxicity. This polymer is highly crystalline, it has a high melting point and is hard to dissolve in most organic solvents. [12] [13] The first application of PGA was in 1970 with the production of a synthetic absorbable suture called Dexon^{TM} to be used in medical application. Since PGA has a hydrophilic nature, Dexon^{TM} tended to lose its mechanical strength over 2-4 weeks after implantation. [14] Copolymers of PLA and PGA were developed as an alternative for the sutures. This copolymerization can modify some morphological properties that in this case lead to a higher hydration and hydrolysis. In 1991, this copolymer was the most widely used in human medicine and drug delivery. [13]

2.2. Ring-Opening Polymerization vs Polycondensation

There are mainly two types of synthetic strategies applied to the synthesis of polyesters: stepwise polymerization (polycondensation) and chain growth polymerization (Ring-Opening Polymerization or ROP). [15] [16]

Polycondensation links monomers to obtain larger structural units, with the elimination of water and other alcohols. [17] A typical step-growth condensation is the reaction between a dicarboxylic acid and a diol, which results in a diester (AA + BB monomers in Scheme 1). This was developed in the late of 1920s by *Carothers et al.* who studied the synthesis of these degradable aliphatic polyesters. [18]

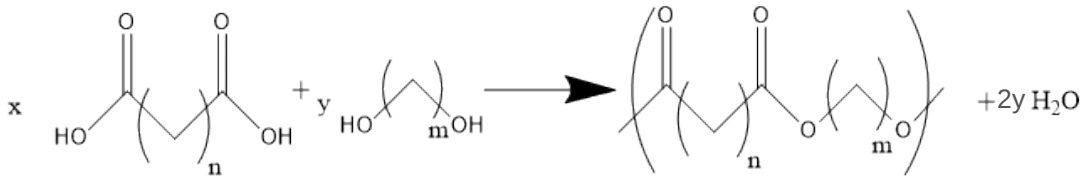

Scheme 1 – Step growth polymerization of a dibasic acid and a glycol.

Ring-opening polymerization (ROP) is a chain-growth polymerization and the reaction starts with an active centre. The reactive centre interacts with the cyclic monomer, opens the ring, and forms a long polymeric chain. The propagation centre can be anionic, cationic, or organometallic. A schematic representation of the ROP of a cyclic ester in the presence of an initiator is shown in Scheme 2. [2]

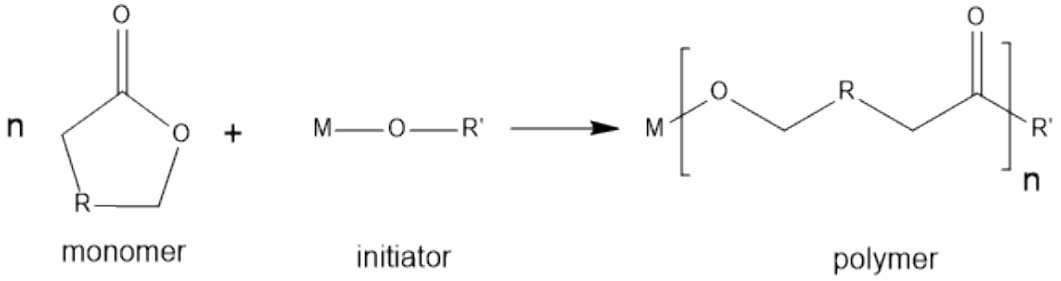

Scheme 2- ROP representation of a cyclic ester. $R = (CH_2)_{0-3}$ and/or $CHR', M = Zn,\ Sn(II), Al, Y, Sn\ (IV), Ti, etc$ and $R' = (CH_2)_x OH$

The comparison between the two types of polymerization is presented in Table 1, for better understanding.

Table 1 – Step growth-polymerization (condensation) vs chain-growth polymerization (ROP). *[19]*

Step-Growth Polymerization (Condensation)	***Chain-Growth Polymerization (ROP)***
All molecules present in the reaction (monomers, oligomers) can react with each other.	The monomers can only react with the active center.
Monomers are consumed early in the reaction.	Some monomer is still present even at very high conversion.
Steps of polymerization: -Initiation; -Propagation.	Steps of polymerization: -Initiation; -Propagation; -Termination (in some cases).
The rate of the reaction is higher in the beginning; Highest molar masses are obtained only at very high conversions.	The reaction rate depends on the concentration of initiator and high molar mass polymers form throughout the duration of the reaction. High molar masses can be obtained with high reaction time.
To synthesize long polymers with high molar masses, it requires high reaction times.	Long reaction times don't affect (much) the (average) molar mass, although it has high degrees of conversion.

The main drawback of step-growth polymerization is the lack of control (molar mass, tacticity, etc.) compared to chain-growth polymerization. In both cases, high temperatures and long reaction times generally favour the side reactions. Nevertheless, polycondensation is cheaper than ROP, but it is only possible to obtain polymers with low molar masses and not well-defined copolymers. [2] On the other hand, the ring-opening polymerization of lactones can yield to polymers with tailor-made properties and high molar masses, using lactones with different ring-size, substituted or not by functional groups. [20]

2.3. ROP mechanism

The first Ring-Opening Polymerization (ROP) was performed at the beginning of 1900s to synthesize polypeptides, by Leuchs [21]. Over the years, the ROP has been the focus of an intensive investigation to synthesize polysaccharides from anhydro sugars, obtaining various types of polysaccharides, like synthetic dextran. In the industrial application, many polymers are used that were obtained by ROP: poly (ethylene oxide), polyphosphazene, polynorbornene. Another polymer obtained by cationic ROP from aziridine monomers is polyethylenimine, which is highly branched. [22] Another example worthy of highlight is Nylon® -6, a textile fibre, since ROP had a big role in the production of this polyamide by Ɛ-caprolactam monomer. Consequently, the development of new catalytic processes allows the production of new copolymers, either between lactams, or between lactams and other (cyclic) monomers such as lactones. A little further, caprolactone became an interesting monomer because it has many interesting characteristics, like biodegradability and compatibility behaviour in blends with another polymer. [23]

Currently, researchers seek new ways to convert cyclic esters into new polymers. Synthetic aliphatic polyesters have several attributes that make them a leading candidate in pharmaceutical and biomedical industries, in addition to the numerous different polymers types with different degradation modes. Their synthesis is made in a numerous way, with different types of methodologies and catalytic systems. Their chain-ends can be controleld through initiation and termination. [2] The reaction can be carried out in solution, emulsion or dispersion, or in bulk (no solvent is used). The thermal stability and hydrolytic stability of the polyester is strongly dependent of the type of initiator used in the reaction. [24] [25]

The polymerization can proceed through different mechanisms, such as: anionic, coordination-insertion and cationic. In the following sections, these mechanisms will be reviewed. In addition, a discussion of the effect of the ring size of the lactone on its polymerizabilty, from a thermodynamic point of view, will be provided.

2.3.1. Thermodynamics

This subchapter will clarify how the ring size of lactones affects the thermodynamic equilibrium polymerization behaviour, among the different monomers. [16]

<u>Thermodynamics of equilibrium chain growth polymerization:</u>

The formal thermodynamic criterion of a given monomer polymerizability is related to the sign of the free enthalpy (called also Gibbs energy) of polymerization, in Equation 1: [26]

$$\Delta G_p = \Delta H_p - T\Delta S_p \quad (1)$$

If $\Delta G_p < 0$ the reaction is favored, but if $\Delta G_p > 0$ the reaction is not favored.

Snow and Frey [27] in 1940s, investigated the copolymerization behaviour between sulfur dioxide and olefins and concluded that depending on the type of olefin, as the reaction temperature increases, the rate of the polymerization decreases, reaching a temperature where there is no polymerization, called ceiling temperature. Dainton and Irvin [28] [29], concluded that this phenomenon was independent of the catalytic system but dependent on the monomer concentration. They proposed a thermodynamic description for this behaviour, the Dainton's equation (Equation 2).

$$T = \frac{\Delta H_p}{\Delta S_p + R\ln([M])_{eq}} \tag{2}$$

This equation states that at the equilibrium point, $\Delta G_p = 0$, there is a critical temperature called ceiling temperature (T_c) or floor temperature (T_F), depending on the thermodynamic features of the polymerization. At this point, the polymerization is finished, i.e., no conversion of monomer to polymer is obtained. [16]

Ring Size and Thermodynamic Polymerization Behaviour:

It is relevant to get some insight on the influence of the ring size and degree of substitution on the thermodynamic behaviour of the polymerization. Angle, conformation, and repulsion strain are three factors affecting the total strain of a ring. The total strain of a small lactone (4-7-membered) is high enough to allow polymerization to proceed in the presence of a good catalyst. This is demonstrated by a negative ΔH_p and an increased order of the system, indicative of a negative ΔS_p. When the magnitude of $T\Delta S_p$ surpass the ring strain, ΔH_p, the ceiling temperature is reached. For larger rings, with more than 9 atoms, an inverse temperature relation is observed. [16] Figure 2, shows the influence of the size of cyclic monomer in the standard thermodynamic parameters.

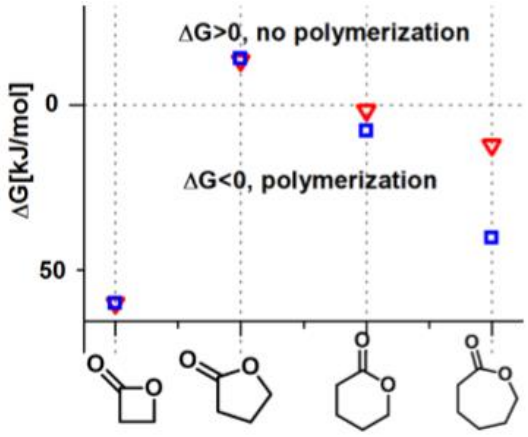

Figure 2 – Difference in ΔG as a function of ring-size ate normal pressure and at 25ºC: blue squares *[30]* and red triangles *[31]* represent different extracted values from the literature.

Difference in polymerization behaviour of lactones:

The ring size, addition of heteroatoms and degree of substitution are three factors that have a large influence on the thermodynamic polymerization behaviour of lactones. Among the factors previously indicated, the strain of the ring should not be considered as the main factor that influences the reaction: a larger substituent can increase the strain of the ring, even though the lactone suffers an overall decrease in equilibrium monomer conversion. This occurs due to an increase of the relative entropy associated to the larger substituent.

Figure 3 presents a division among different monomers that reflects their thermodynamic behaviour. This division was made from the perspective of practical synthesis and how it affects the synthetic behaviour. The proposed classes/intervals are as follows: Thermodynamic Unfavoured Monomers (TUM), Tc ≤ 0 °C; Thermodynamic Intermediate Monomers (TIM), 0 °C ≤ Tc ≤ 250 °C and Thermodynamic Favoured Monomers (TFM), Tc > 250 °C. It should be noticed that the interval considered does not mean that the polymerization is conducted at that temperature, but rather that the polymerization should be performed far below the Tc value of the monomer to get full conversion. It may be seen that ɣ-lactones are highly unfavoured thermodynamic monomeric species regard to the transition into the polymeric state. As it is written in the literature, the transition is however possible when used as a co-monomer together with a TIM or TFM. Under bulk conditions, the ɣ-lactones are thermodynamic intermediate monomers and thermodynamic unfavoured monomers, where the polymer to monomer equilibrium is easily altered by the temperature and concentration. [16]

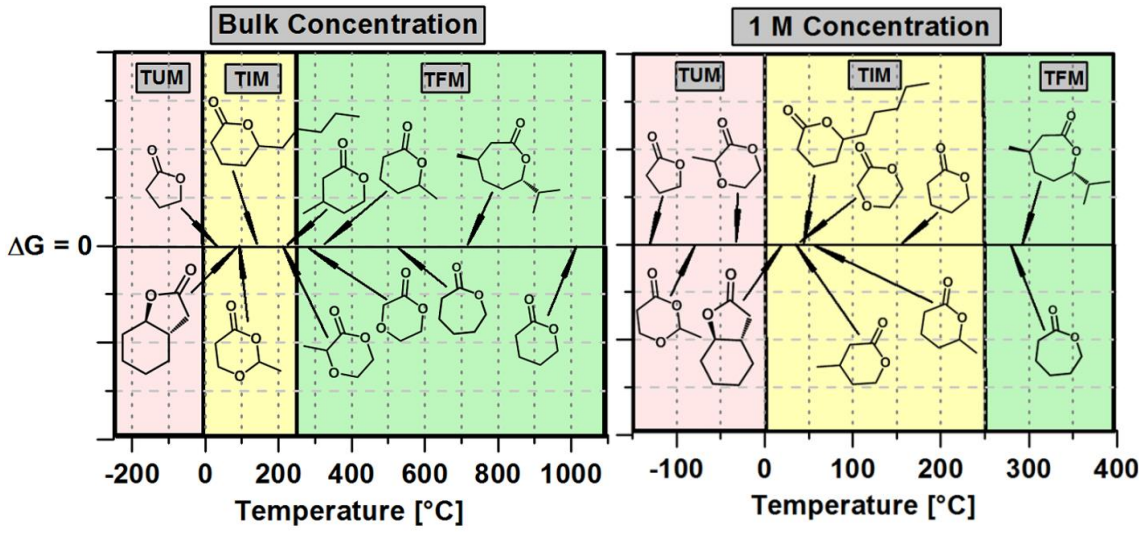

Figure 3 – Reflection of the thermodynamic behavior among the different monomers. The divisions are based upon a T_c interval in which the monomer is one the following: TUM (Thermodynamic Un-Favored Monomers), $T_c \leq 0^0C$; TIM (Thermodynamic Intermediate Monomers), $0^0C \leq T_c \leq 250^0C$ and TFM (Thermodynamic Favored Monomers), $T_c \geq 250^0C$, and how this relates to change in concentration: bulk (left) and 1M (right).

2.3.2. Coordination-Insertion ROP

The coordination-insertion mechanism has been investigated in the last few years and is shown in Scheme 3.

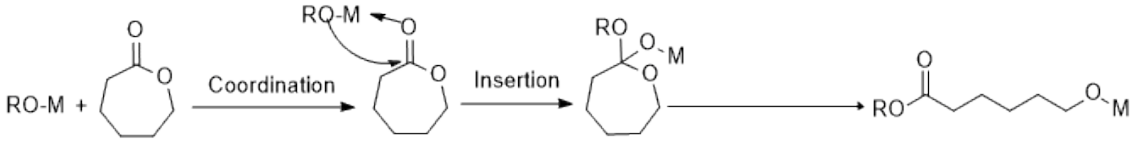

Scheme 3 - Coordination-insertion mechanism of lactone in the presence of a metal alkoxide (RO-M).

Metal alkoxides (RO-M) are typical initiators for this type of polymerization. In a first step, the alkoxide initiator coordinates the carbonyl of the monomer by a nucleophilic attack and subsequently the carbonyl bond is broken. An intermediate is formed, where the former carbonyl oxygen of the monomer is coordinated, while the carbonyl carbon assumes a sp3 bonding geometry. Secondly, the cleavage of the acyl-oxygen of the monomer occurs by opening the ring and forming a new alkoxide. [32] [33] [34]

Kricheldorf et al. [35] [36] [37], in 2000s, extended the concept of using aluminum alkoxides as initiators, to other types of metal alkoxides such as: tin (IV), titanium, and zirconium alkoxides. It is not possible to describe the huge number of different initiators and catalysts used in the different studies. However, the most used initiators are shown in Figure 4. These initiators predominance is due to their ability to produce stereoregular polymers with narrow and controllable molar masses and well-defined end groups. Aluminum-based initiators are more favourable in the synthesis of macromolecular structures than Tin initiators. [33]

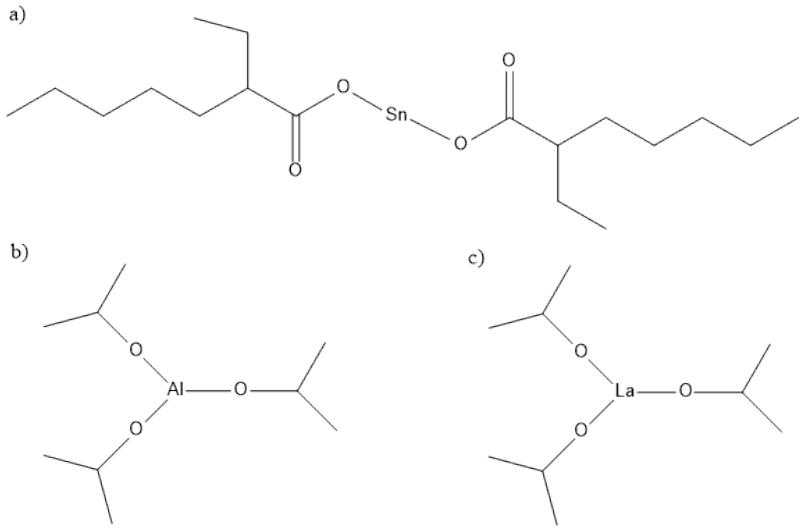

Figure 4 – Chemical structures of initiators used in ROP of lactones. a) stannous octoate; b) aluminium isopropoxide; c) lanthanide isopropoxide.

Some researchers studied the use of other initiators in the polymerization of lactones. For example, aluminoxanes were used as initiator, to polymerize racemic (R, S)-β-substituted-β-lactones

and to obtain isotactic polymers. However, this initiator when used in the polymerization of β-butyrolactone had some drawbacks, such as: long reaction time and a wide range of molar masses. [38]

More recently, β-diiminate metal alkoxides and rare-earth metal alkoxides (derived from yttrium and lanthanum) were successfully used as catalysts in the polymerization of cyclic esters, such as: β-butyrolactone, lactide and Ɛ-caprolactone. These catalysts/initiators were used in a large scale for the ROP of β-lactones, but only limited mechanistic and kinetic information were found. Most of the studies of the polymerization kinetics and mechanisms of larger lactones (Ɛ-caprolactone) were done, with covalent metal alkoxides. [39]

Regarding metal carboxylates, Tin (II) bis-(2-ethylhexanoate) (also referred as $Sn(Oct)_2$) is one of the most frequently used catalyst in the polymerization of cyclic esters. This catalyst is easily handled and relatively easy to purify. Penczek and coworkers studied the mechanism of polymerization of Ɛ-CL and LA/$Sn(Oct)_2$/primary amine (RNH_2) system which compared with the system Ɛ-CL and LA/$Sn(Oct)_2$/alcohol (ROH). They showed that they are similar. [40]

2.3.3. Anionic ROP

In anionic ROP of a cyclic ester, the reaction can follow living or nonliving characteristics depending on the initiators, monomers and reaction conditions used. The polymerization starts by a nucleophilic attack of an initiator on the carbon of the carbonyl group or on the alkyl-oxygen, opening the ring and obtaining a polymer, as shown in Scheme 4. The polymerization of β-lactones proceeds either through the cleavage of the alkyl-oxygen or the acyl-oxygen bond, thus obtaining both carboxylate and alkoxide end-groups, as it is shown in Scheme 4.

β-lactones polymerization was performed both with weak and strong bases as initiators. In the first case, the polymerization is carried out with the cleavage of the alkyl oxygen scission and the propagating species are carboxylate ions. In the second case, the polymerization in the presence of strong bases (alkali metal alkoxides) proceeds by an acyl-oxygen cleavage with an alkoxide as a propagating species. It was also claimed that the polymerization of β-lactones proceeds with the two cleavages simultaneously. [2] For the other lactones, it is only acyl-oxygen bond cleavage that occurs.

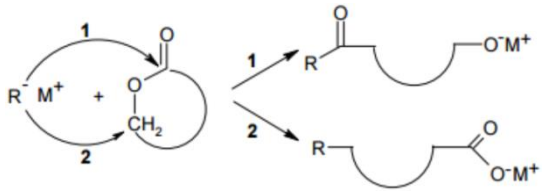

Scheme 4 – General reaction in a ROP for a cyclic ester. The reaction 1 describes the ROP of monomer by acyl-oxygen bond cleavage and the reaction 2 by alkyl-oxygen bond cleavage.

This route is one of the best to attain polymers with a high molar mass in a polar solvent. The effective initiators for anionic polymerization of lactones are alkali metals, alkali metal oxides, alkali metal naphthalenide complexes with crown ethers, etc.

Jedlinski *et al.* [41] [42] [43] [44] [45] [46] studied the anionic polymerization of β-lactones: β-propiolactone and β-butyrolactone using two different complexes, potassium methoxide and potassium tert-butoxide with 18-crown-6 as initiators. In their studies, the acyl-oxygen cleavage occurs to yield

potassium β-alkoxide ester and subsequently a potassium hydroxide and an unsaturated ester. The former potassium hydroxide reacts with another molecule of monomer, leading to the acyl-oxygen cleavage and forming a carboxylate ion and hydroxyl end-groups.

Organic bases such as: phosphines, pyridines, tertiary amines, and betaines, were among the first to be used for the ring-opening polymerization of β-lactones. More recently, other organic catalysts such as: carbenes, guanidine, amidine and phosphazenes, have proven to be effective for the polymerization of the same type of lactones, but also of lactones with a larger ring, Ɛ-CL.

One of the side reaction that can happen in anionic ROP is called back-biting giving polymers with lower molar mass. It arises when the alkoxide active centre attacks a carbonyl function of the polymeric chain forming cyclic oligomers (Scheme 5).

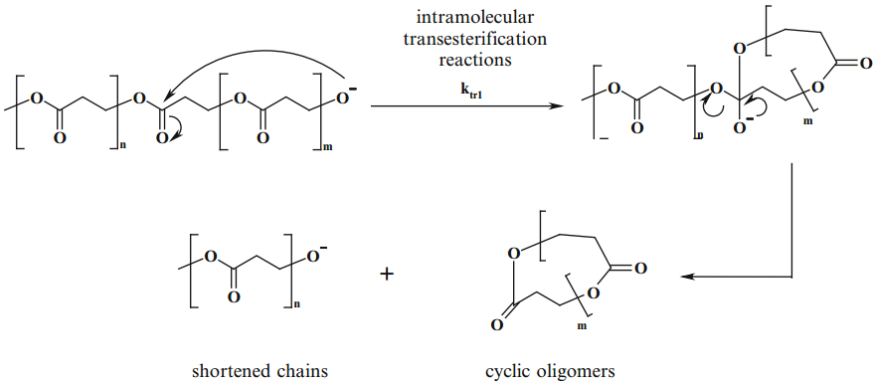

Scheme 5 - Intramolecular transesterification reactions, in an anionic ROP, resulting in cyclic oligomers and a shortened chain.

Transesterification reactions may also occur (Scheme 6) and will broaden the molar mass distribution. [26]

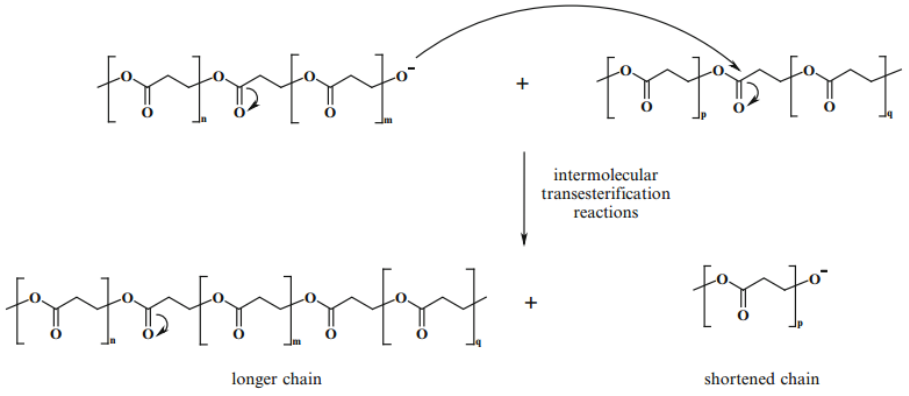

Scheme 6 - Intermolecular transesterification reactions, in an anionic ROP, resulting in a longer chain.

To control the molecular parameters, the transesterification reactions must be avoided. These reactions can be disfavoured by using less reactive initiators, to react with the more reactive ester groups of the cyclic monomer, and not with the less reactive ester groups along the chains. Backbiting reaction occurs when using potassium tert-butoxide in the polymerization of Ɛ-CL, forming large quantities of cyclic oligomers. Though, in the presence of lithium tert-butoxide in an apolar solvent, the oligomer

formation is reduced. The use of hindered ligands decreases the reactivity of the initiator, giving a better selectivity and consequently a better control of the polymerization. Alkoxides based on low electropositive metals, such as: yttrium alkoxides, lanthanum alkoxides, etc, can prevent these reactions. [15] [32]

2.3.4. Cationic ROP

Cationic ring-opening polymerization is difficult to control. The initiator and catalyst can be divided in: alkylating agents ($CF_3SO_3CH_3$, $BF_4^{(-)}$, $Et_3O^{(+)}$), acylating agents ($CH_3CO^{(+)}$), Lewis acids ($AlCl_3$, BF_3, $FeCl_2$, $ZnCl_2$, etc.) and protonic acids (HCl, RCO_2H, RSO_3H).

Scheme 7 shows the mechanism proposed for the cationic ROP. The cation reacts with the exocyclic oxygen, to form the dialkoxycarbocationic species, followed by the cleavage of the alkyl-oxygen bond when reacting with a second molecule of monomer. [47] [48]

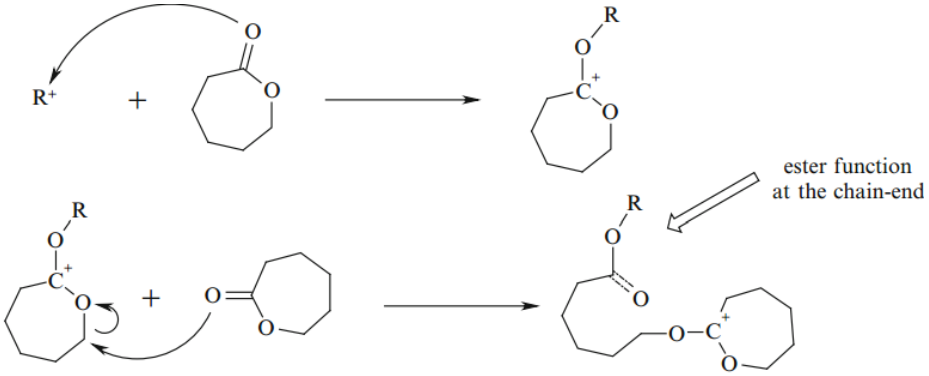

Scheme 7 - Mechanism proposed for cationic ROP initiated by an alkylating agent (R).

In Scheme 8 it is shown another way for the cationic polymerization to proceed. In this cationic ROP the initiator can be an alcohol or an amine, and a Brönsted acid is used as catalyst. The initiation mechanism entails the activation of the monomer, which is made by the protonation of the exocyclic oxygen, and consequently there is a nucleophilic attack of the alcohol and the cleavage of the oxygen-acyl bond. Subsequently, the propagation mechanism is analogous except that the hydroxyl function at the chain-end is the nucleophilic species. The activation monomer mechanism is favorable compared with the mechanism shown in Scheme 8 because the nucleophilicity of the exocyclic oxygen of lactones is lower than that of alcohols. [32]

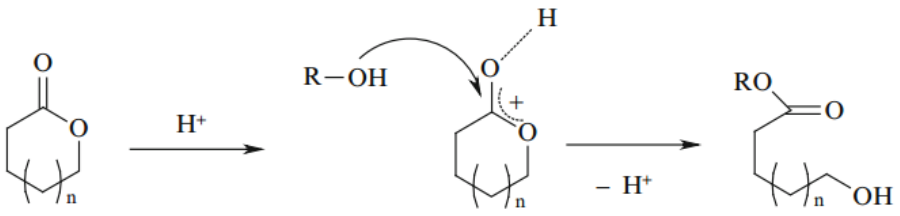

Scheme 8 - Monomer activation mechanism for the ROP of lactones catalysed by Brönsted acids and initiated by nucleophilic alcohols.

Though this polymerization route is difficult to control, many studies with different catalysts and initiators to obtain interesting polyesters were described. [2] Organocatalysts have also proven to be able to perform the polymerization of lactones via cationic polymerization. [49]

Endo *et al.* [50] in the beginning of 2000s, studied the first cationic ROP of Ɛ-CL and δ-VL in the presence of an alcohol as an initiator and $HCl.Et_2O$ as the catalyst. More recently, the cationic ROP of Ɛ-CL was performed with the help of trifluoromethanesulfonic acid as the catalyst, giving polymers with molar masses up to 20 000 g/mol. [51] Later, the catalyst was substituted by methanesulfonic acid. [52]

2.4. (Co)Polymerization of γ-lactones

As mentioned before, 5-membered lactones, like γ-butyrolactone, are commonly referred as being non-polymerizable due to its low strain energy. [53] [54] Nevertheless, several studies described in the literature succeeded to (co)polymerize γ-lactones. As an example, Tadokoro *et al.* [55] investigated the polymerization of spirocyclic γ-butyrolactone. This polymerization proceeded with success at room temperature, in tetrahydrofuran (THF) as the solvent and tert-butoxide (t-BuOK) or methyllithium (MeLi) as the initiator.

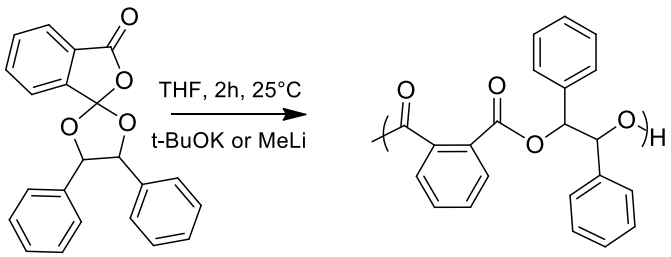

Scheme 9 – Anionic ROP of a spirocyclic γ-butyrolactone, with THF as a solvent and t-BuOK or MeLi as initiator, at room temperature, for two hours.

The conversion was complete in both cases. However, when using MeLi as the initiator, the polymer obtained presented a molar mass of 10^4 g/mol and a narrow molar mass distribution, with a dispersity value of 1.14, which is much lower than the one for t-BuOK, with a value of 1.57. MeLi is a better initiator because it is a stronger nucleophile compared to t-BuOK, i.e., the lithium cation may suppress the transfer reaction in a greater extent than the potassium cation.

Other systems have also been described in the literature to polymerize γ-BL, these include the use of zeolites and enzymes. *Hong and Chen* [56] investigated the polymerization of γ-butyrolactone, with phosphazene as the catalyst and an alcohol as the initiator. They developed the first organopolymerization of γ-BL, that operates in THF and at low temperature (-40ºC). The conversion obtained in the presence of the alcohol reached 90% while in its absence it reached only 59%. When the temperature increased, the conversion dropped, reaching 0% at ambient temperature. The strong base *tert*-Bu-P_4 can directly engage the ROP by deprotonation of the γ-BL to produce an enolate.

However, the most effective ROP system is based on a prior deprotonation of an alcohol then, the activated alcohol will attack the carbonyl carbon, allowing the opening of the cycle. By using *tert*-Bu-P_4 high conversions of the monomers were achieved, and therefore poly(γ-BL)s with molar masses between 9000 and 27 000 g/mol were obtained.

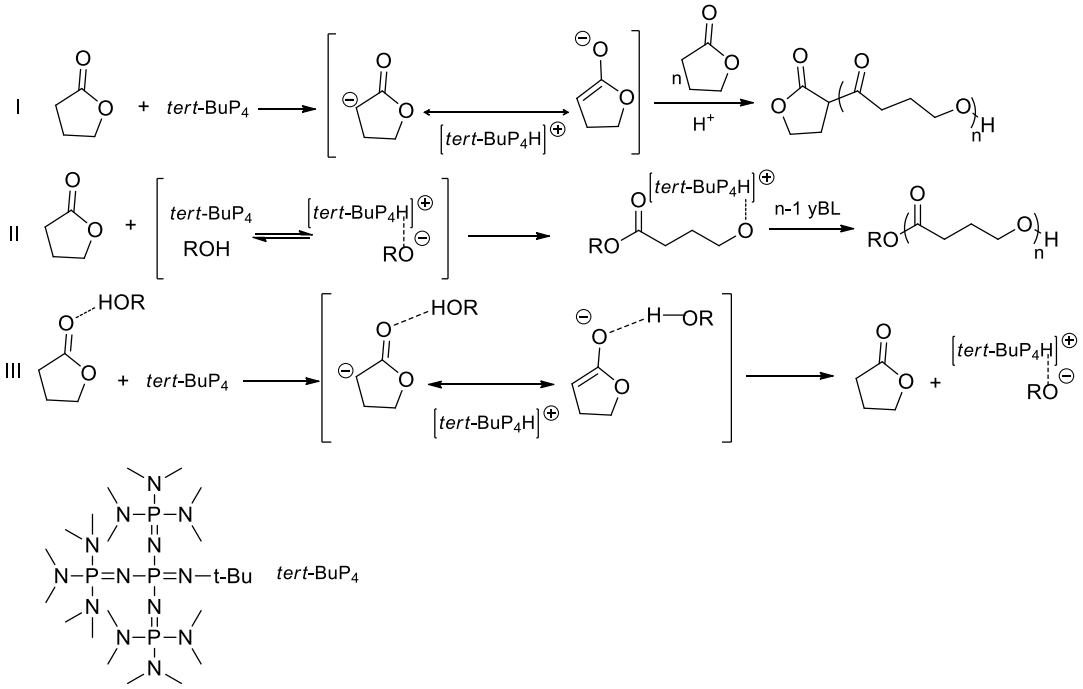

Scheme 10 - Three different ROP mechanisms of γ-BL.

In another study, these two researchers investigated the ROP of ɣ-butyrolactone using lanthanides as the catalyst. More specifically, the system used is $La[N(SiMe_3)_2]_3$ associated with an alcohol such as BnOH or Ph_2CHCH_2OH. All polymerizations were carried out at -40 ° C as there was no polymer formation at higher temperatures. [57] When the alcohol used with the lanthanide catalyst is benzyl alcohol, the polyester synthesized will be rather linear whereas with Ph_2CHCH_2OH the polyester obtained will have a cyclic structure. The use of lanthanide alone to produce the ROP gives only 3.1% conversion to γBL after 32 hours, but with the presence of an alcohol, the conversion of γ-BL reaches 67%. Other rare earth metals are also used in this publication, the best conversion (90%) is obtained with yttrium at -40 ° C. The synthesis methodology developed demonstrates an effective chemical synthesis of poly(γ-BL) by ROP of γ-BL with polymers having a molar mass between 5 000 and 30 000 g/mol. This work also proved the complete recyclability of the cyclic or linear poly(γ-BL) which were converted back into the monomer.

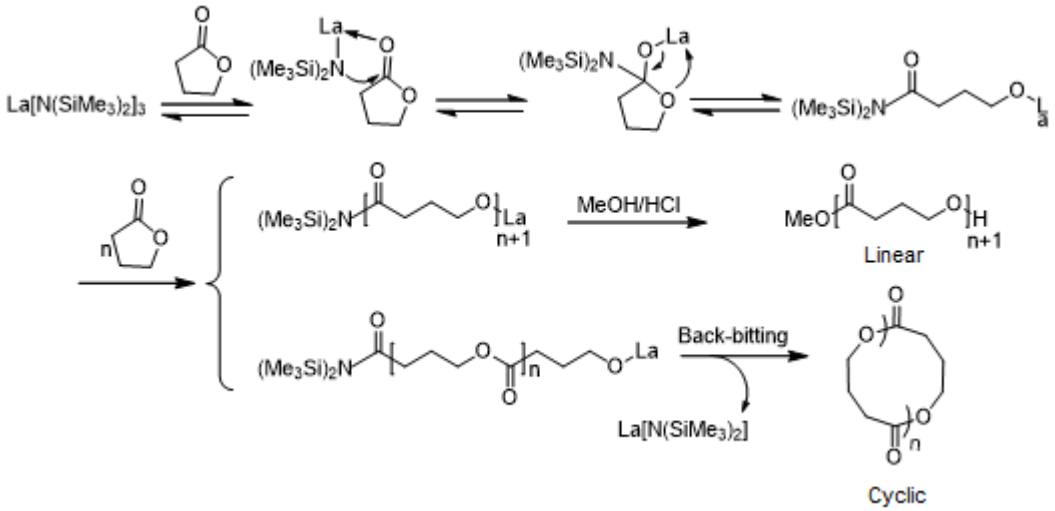

Scheme 11 – ROP of ɣ-BL with lanthanide as catalyst.

Hong and Chen [58] have also described the first ring-opening copolymerization based on the coordination-insertion mechanism of α-methylene-γ-butyrolactone (MBL) and ε-CL. The catalyst used for these copolymerization is $La[N(SiMe_3)_2]_3$ and this reaction exclusively produce an unsaturated PMBL-co-PCL copolyester, with an incorporation up to 40% of MBL and without any formation of homoPMBL. Additionally, when the polymerization was carried out at -20ºC, in a low polar solvent (toluene), the ring opening of the MBL was favoured and there was no formation of vinyl double bond compound. In Scheme 12, it is shown the mechanism of this copolymerization.

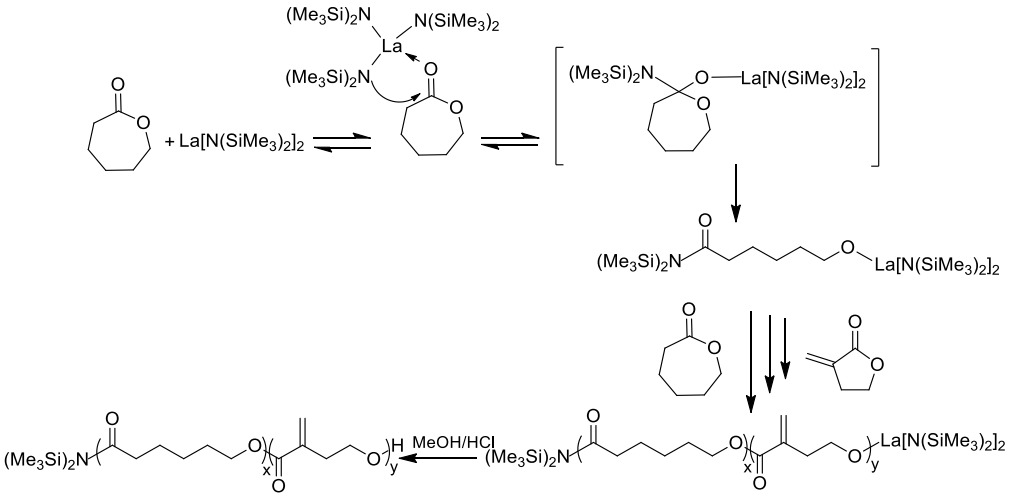

Scheme 12 – Coordination-insertion mechanism of α-methylene-γ-butyrolactone (MBL) and ε-CL, using $La[N(SiMe_3)_2]_3$ as a catalyst.

Gagliardi et al. [59] reported the copolymerization of Ɛ-CL and ɣ-VL, by ROP using methoxy polyethyleneglycol (mPEG) as the initiator. It was shown that the reaction can occur in a controlled way in the temperature range from 120 °C to 180 °C. The low reactivity of ɣ-VL five membered ring affected the copolymerization decreasing the molar mass obtained, when compared to the theoretical ones. At lower temperatures, the results were better. In this case, the reaction is being favored by increasing the

reactivity of ɣ-VL. This copolymerization, carried out at 120ºC with $Sn(Oct)_2$ as a catalyst and at short reaction times (5 hours) was shown to provide a good strategy to synthesize biodegradable polymers, with an incorporation of ɣ-VL up to 16%. In Scheme 13, it is shown the schematic representation of this copolymerization reaction.

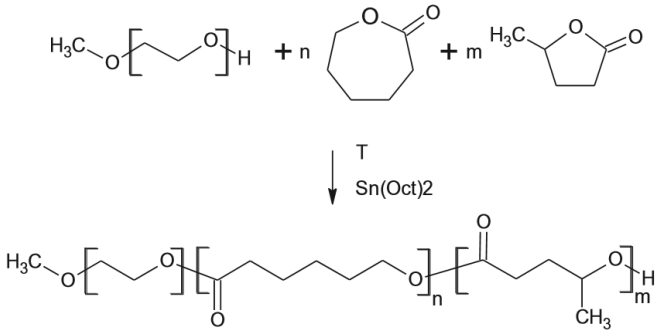

Scheme 13 – Ring-Opening Polymerization for selected monomers and obtained copolymer.

Lee *et al.* [60] investigated the copolymerization of ɣ-VL with β-butyrolactone (Scheme 14), in bulk conditions with $BF_3.OEt_2$ as the catalyst, at room temperature. The amount of 4HV (4-hydroxyvalerate) in the polymer increases with the proportion of γ-VL in the initial monomer mixture, until it reaches a percentage of 33%, for a proportion of 50% in γ-VL. Moreover, the yield decreases progressively with the increase in the proportion of γ-VL. Thus, despite the small amount of γ-VL in the copolymer, well-controlled polyesters with molar masses between 1000 and 4000 g/mol and a dispersity ranging from 1.3 to 1.7, can be synthesized. The system is therefore effective to polymerize a 5-membered lactone with a 4-membered lactone, but the co-monomer could also be a lactone with a large ring such as ε-caprolactone.

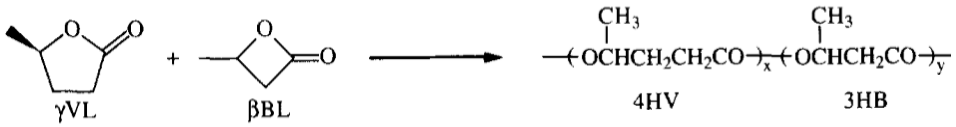

Scheme 14 - General reaction of ɣ-VL with β-butyrolactone to obtain poly(3-hydroxybutyrate-co-4-hydroxyvalerate).

Very recently, Undin *et al.* [61] have demonstrated that by using an organic catalyst, diphenyl phosphate (DPP), a conversion close to 100% is obtained for α-bromo-γ-butyrolactone (α-Br-γBL) whatever the co-monomer (TMC, AOMEC (2-allyloxymethyl-2- ethyl-trimethylene carbonate), ε-CL). These copolymers are also well controlled, exhibiting molar masses varying from 10,000 to 30,000 g/mol, which are close to the theoretical molar masses. Moreover, the dispersity is about 1.10 for all copolymers, this is attributed to the high activity and high selectivity of the DPP organocatalyst. The good control of the copolymerization makes it possible to construct a much more complex polymer structure such as, for example, a multifunctional triblock composed of AOMEC for the central block surrounded by a random copolymer consisting of ε-CL and αBrγBL.

2.5. Conclusion

This literature review helped to put forward several recommendations on the way to perform ROP of lactones and to identify specific issues on which complete and accurate data are not yet available. As it is shown in the literature review, 5-membered lactones are very difficult to polymerize, so due to this fact, the main scope of this work is to be able to polymerize these types of lactones by homopolymerization or by linking these monomers to another monomer that is easier to polymerize. Research already carried out on the polymerization of γ-butyrolactone has shown that it is difficult but possible to circumvent the unfavorable thermodynamics of this lactone and hence to open its cycle. The bibliographic study thus made it possible to better understand the subject and to approach the course under the best conditions.

In the following chapter, it will be investigated the ROP of γ-butyrolactone over an acid catalyst, based on Campos et al. [62] [63] work. This way, several experiments will be performed under different conditions (temperature, monomer concentration, comonomer molar ratio and catalyst used).The effect of these parameters on conversion and on the molar masses, and dispersity of the produced polyesters will be analyzed, by NMR and SEC techniques. The experimental values will be compared with theoretical ones and discussed.

3. Experimental part

3.1. Apparatus

All the reactions and manipulations were performed under an inert atmosphere of nitrogen. A Schlenk line is used to perform the reactions, since the compounds are air-sensitive. These Schlenk-line is shown in Figure 5 and it can be described by an inert gas line with nitrogen and a vacuum line. The inert gas could be directly fed into a gas manifold (A), or it can pass through a drying column first (B). The nitrogen supply comes from the run off from the main in-house liquid nitrogen tank (C). The gas can exit the manifold through a bubbler, which provides a pressure release system for the line, and monitories the general flow of gas. The vacuum line is composed by the same manifold (B), but while this line is open, the inert gas line must be closed. Between the manifold and the pump (F) should be placed a cold trap (D). The trap prevents volatile or corrosive solvent vapors to enter in the pump and to degrade its oil. The trap is submerged in a Dewar flask (E) containing liquid nitrogen, which cools the trap and forces the vapors and gases from the Schlenk line to condense. After the setup of the lines, it is possible to link the flask with a magnetic stir bar inside, to the manifold. The flask with the magnetic agitator is sealed with grease, ground-glass stopper and under vacuum, then dried with a burner. The process is repeated several times, to ensure the elimination of the undesired compounds. Next, the inert gas line was turned on to begin the addition of the reactants. [64]

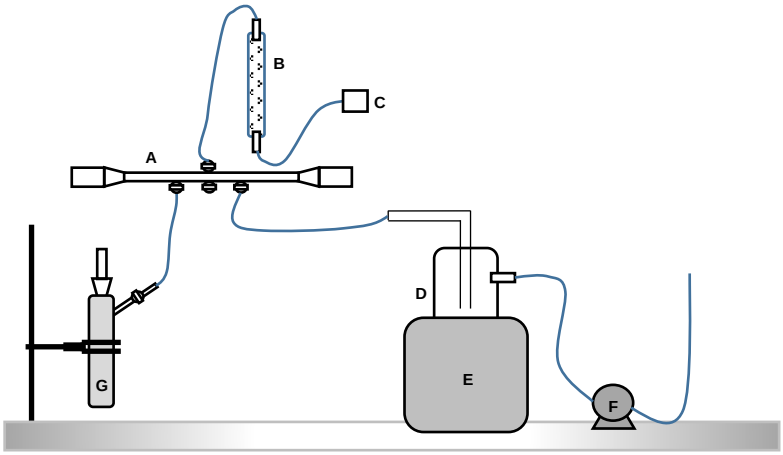

Figure 5 – Scheme of the assembly used to the polymerization.

When the reactions were performed at high temperature it was added to the setup an oil bath and in the situation of low temperature, the flask was placed in an aluminum reservoir with a mixture of liquid nitrogen and ethanol. This mixture allows that the reaction undergoes the necessary temperature. In this situation, the addition of liquid nitrogen should be carefully done for preventing the solidification. On both cases, a thermostat connected to a magnetic agitator is used to control the temperature.

3.1.1. Materials

Toluene (XiLab, 99%) and dichloromethane (Sigma Aldrich, 99%) were dried and cryodistilled just before use. ε-caprolactone (ε-CL, Alfa Aesar, 99%), γ-Butyrolactone (γ-BL, Alfa Aesar, 99%) and γ-Valerolactone (γ-VL, Alfa Aesar, 98%) were stirred with CaH_2 for 2 days, cryodistilled and stored under nitrogen. Biphenyl-4-methanol (BPM, Alfa Aesar, 98%) was recrystallized from dichloromethane. Methanesulfonic Acid (MSA, Aldrich, 99,5%) and Trifluoromethanesulfonic Acid (TfOH, Aldrich, 99%) were bubbled for some hours with nitrogen, prior to use, then stored in a flask under this gas. N,N-diisopropylethylamine (DIPEA, Aldrich, 99%) was used as received.

3.1.2. General Polymerization Procedure

A typical polymerization procedure is as follows: ε-CL (2.5 mL, 20 mmol) and dried toluene (43 mL) were taken from burettes and introduced into a 100mL round-bottom flask with a stirrer, under nitrogen. This flask was immersed in a thermostated bath. After the homogenization of the mixture, BPM (50 mg, 0.258 mmol) was added. A catalyst solution of MSA (17 µL, 0.258 mmol, 1 equivalent / initiator) was finally added with a micro syringe. Small aliquots (2 mL) were taken from the reaction and quenched with DIPEA (Hünig's base) to quench the MSA and stop the polymerization. The analysis of the sample was made to check the conversion of the monomer by ^{1}H NMR spectroscopy. The sample is precipitated in cold methanol, dried under vacuum and washed several times with cold methanol. After this procedure, the sample was analyzed by SEC analysis.

The procedure was further repeated for the copolymers with $[\varepsilon\text{-CL}]_0/[\gamma\text{-BL}]_0$ ratios at 1:2, 1:4 and 4:1. The copolymerization was performed with $[\varepsilon\text{-CL}]_0+[\gamma\text{-BL}]_0=10M$ and using biphenyl-4-methanol as initiator. Monomer conversions were again surveyed by ^{1}H NMR spectroscopy in deuterated solvent containing DIPEA. The product was recovered as described above, and characterized by ^{1}H NMR and SEC. [63]

3.2. Characterization - Instrumental Analysis

3.2.1. Nuclear Magnetic Resonance Spectroscopy (NMR)

Nuclear magnetic resonance spectroscopy (NMR) was used to analyze the progress of the reaction, the composition of the polymer formed and the average-number molar mass. ^{1}H NMR (400.13 MHz) and ^{13}C NMR (100.62 MHz) spectra were recorded with a Bruker Avance 400 spectrometer at 298 K. For the measurements, either 10 mg (^{1}H NMR) or 100 mg (^{13}C NMR) of the polymer was dissolved in 0.8 mL of $CDCl_3$ in a sample tube that has 5 mm in diameter. The spectra were calibrated using the residual proton of the solvent signal (i.e., 7.26 ppm (^{1}H NMR) and 77.0 ppm (^{13}C NMR) for $CDCl_3$).

3.2.2. Size Exclusion Chromatography (SEC)

Size exclusion chromatography (SEC) was used to evaluate the molar mass. The number-average molar mass (Mn) and dispersity (*Đ*) of the polymers during and after polymerization were determined using a Polymer Laboratories PL-GPC 50 Plus chromatograph equipped with RI and UV detectors, with one Tosoh HXL-L guard column and three Tosoh G4000HXL, G3000HXL and G2000XL columns, calibrated with polystyrene standards. Tetrahydrofuran (THF) was used as the eluent with a flow rate of 1.0 $mL.min^{-1}$, with trichlorobenzene as flow marker. For the measurements, 5 mg of polymer was dissolved in 1 mL of THF in a flask with a stirrer, and left for 24 hours in a magnetic agitator. After the complete homogenization of the solution, 1 mL was taken from the flask, filtered at 0.45 µm and analyzed in SEC.

THIS PAGE WAS INTENTIONALLY LEFT BLANK

4. Results and Discussion

4.1 Synthesis of homopolyesters

Before performing copolymerization reactions Ɛ-CL, ɣ-BL and ɣ-VL were first homopolymerized to evaluate the best reaction conditions. In this chapter, it will thus be discussed the influence of several reaction parameters.

The study will be made in the presence of biphenyl-4-methanol (BPM) as the initiator and an organic acid, methanesulfonic acid (MSA) or trifluoromethanesulfonic acid (TfOH) as the catalyst. Toluene was used as the solvent.

The cationic homopolymerization of Ɛ-CL is shown in Scheme 15.

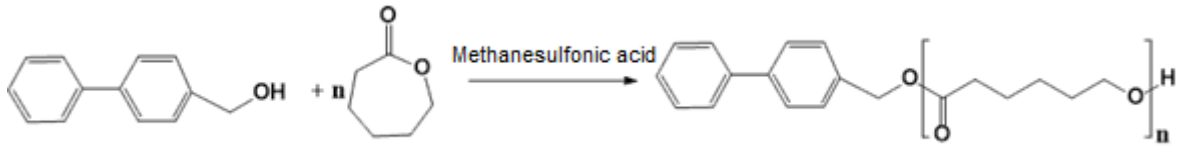

Scheme 15 – General procedure for ROP of Ɛ-CL with MSA as a catalyst.

In Table 2 are gathered the experimental conditions used in a first set of homopolymerizations and the corresponding information on monomer conversion, degree of polymerization and theoretical and experimental molar masses, determined from ^{1}H NMR and SEC data of either unpurified samples obtained during the polymerization or end-polymerization purified samples.

The ^{1}H NMR spectrum of the monomer, together with a typical spectrum of a brute and of a purified polymerization sample is shown in Figure 6. Data show that the white solid obtained after precipitation is indeed polycaprolactone.

The monomer conversion of Ɛ-CL was calculated by the ^{1}H NMR of the unpurified sample using the peak areas of the monomer (CH_2, δ=2.48 ppm, number 1), with the peak area for the signal of the polymer (CH_2, δ=2.30 ppm, number 1'). Equation 1 is used to calculate the conversion of Ɛ-CL, with the signals acquired from the ^{1}H NMR spectrum.

$$x_{\varepsilon-CL}(\%) = \frac{(I_{peak_{1'}})/2}{\frac{I_{peak_{1'}}}{2} + \frac{I_{peak_1}}{2}} \times 100 \quad (1)$$

The molar masses can be calculated through Equation 5, using the average of DP of the three peaks of the polymeric chain in the ^{1}H NMR of polycaprolactone purified: at 3.6 ppm, the signal corresponds to the final CH_2OH (Equation 2); at 5.2ppm the signal corresponds to the Ph-$PhCH_2O$ (Equation 3); In the range 7.1-7.5 ppm the signal corresponds to the aromatic protons of the initiator (Equation 4).

$$DP\ (3.6ppm) = \frac{I_{peak_{1'}}/2}{I_{peak_{7'}}/2} \quad (2)$$

$$DP\ (5.2ppm) = \frac{I_{peak_1},/2}{I_{peak_6},/2} \quad (3)$$

$$DP\ (7.3ppm) = \frac{I_{peak_1},/2}{I_{peak_{aromatics}}/9} \quad (4)$$

$$Mn_{Poly(\varepsilon-CL)}(g/mol) = \overline{DP} \times M_{\varepsilon-CL} + M_{BPM} \quad (5)$$

$$\overline{Mn}\,th = \frac{[\varepsilon - CL]_0}{[BPM]_0} \times M_{\varepsilon-CL} \times x_{\varepsilon-CL} + M_{BPM} \quad (6)$$

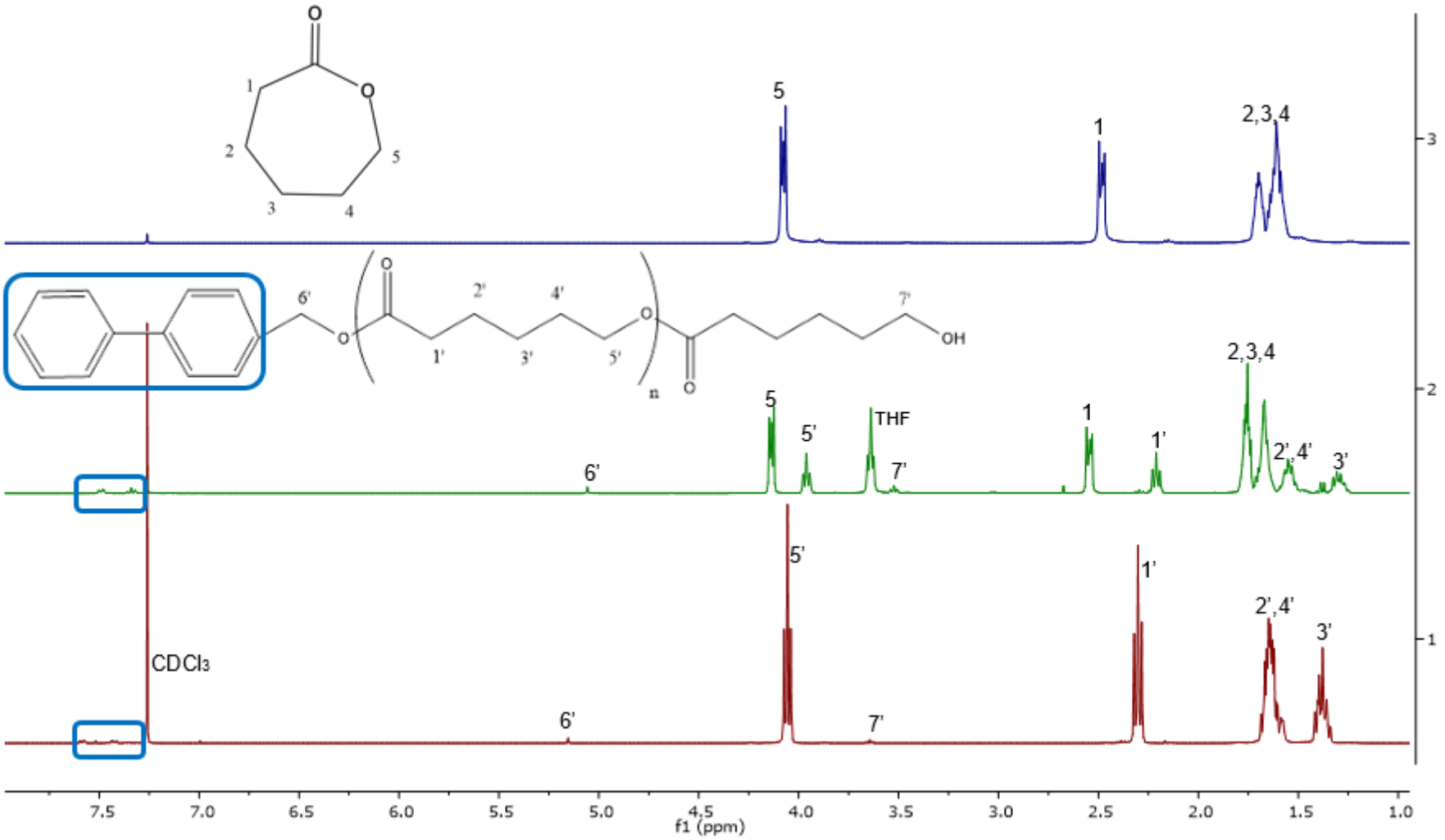

Figure 6 - ^{1}H NMR spectrum in $CDCl_3$ zoomed between 1.00 ppm and 8.00 ppm. The blue spectrum refers to the monomer Ɛ-CL, the green spectrum to unpurified polycaprolactone sample of Run 3 and the red spectrum to purified polycaprolactone of Run 5, of Table 2.

The main results of the polymerization of caprolactone are summarized in Table 2, varying the temperature and the monomer concentration.

Table 2 – Polymerization of Ɛ-CL in toluene with MSA as the catalyst in Runs 1-5 and TfOH in Run 6.

Run	*[ε-CL]$_0$ (mol/L)*	*t (h)*	*T (°C)*	$x_{\varepsilon-CL}$ *a)* *(%)*	$\overline{Mn}$ *th b)* *(g/mol)*	*DP c) (g/mol)*			$\overline{Mn}$ ***NMR d) (g/mol)***	$\overline{Mn}$ *SEC d) (g/mol)*	$\frac{M_w}{M_n}$ *e)*
						3.6-3.7 ppm	*5.1-5.2 ppm*	*7.1-7.5 ppm*			
1	1	5	-40	0	-	-	-	-	-	-	-
2	5	4	-20	0	-	-	-	-	-	-	-
3	5	8	-10	32	3 400	-	-	-	-	-	-
4	5	7	0	48	5 050	-	-	-	-	-	-
5	0.5	5	30	100	10 230	88	87	85	10 070	8 250	1.16
6(*)	9	1	50	100	10 230	-	89	90	10 400	15 620	1.44

[ε-CL]/[BPM]=88/1 ; [BPM]/[MSA]=1/1.

a) Conversions calculated by ^{1}H NMR spectroscopy of the crude sample.
b) Theoretical number-average molar mass $\overline{Mn}$ th calculated by Equation 6.
c) DP calculated by ^{1}H NMR spectroscopy of the precipitate sample, calculated by Equations 2, 3 and 4.
d) Number average molar mass calculated by Equation 5.
e) Number-average molar mass measured by SEC in THF versus PS calibration.
f) Molar mass dispersities estimated from SEC data.
(*) The reaction 6 was performed in bulk (no toluene was used).

From Table 2 it can be noticed that below -10ºC, no polymerization occurred. It is important to note that the concentration had to be less than 5M at negative temperatures, because caprolactone in larger concentrations is not fully soluble.

It is also seen that the conversion increases with the temperature for MSA catalyst, reaching 100% at 30ºC and 5 hours reaction. Fully conversion is also obtained for the TfOH catalyst under the tested experimental conditions (run 6).

An important aspect to notice is that the degree of polymerization, calculated for both chain ends and based on the integration of different peaks, are quite similar (run 5). This is indicative of a good polymerization control with no side initiation. This behavior is also corroborated by the good agreement between the theoretical molar masses and the experimental ones, especially those based on NMR data. Calibration issues can account for a higher difference when dealing with SEC data.

Despite the similarity on monomer conversion and on the molar masses of PCL obtained from MSA and TfOH catalysts, a higher dispersity is observed in the latter case. This may be related to a more efficient polymerization control when using MSA under the experimental conditions of run 5.

The polymerization of ɣ-butyrolactone was performed under a range of experimental conditions which are presented in Table 3. Most of the experiments were made with MSA catalyst.

Table 3- Homopolymerization of ɣ-BL in toluene with methanesulfonic acid as the catalyst.

Run	*$[\gamma\text{-BL}]_0$ (mol/L)*	*T (°C)*	*Reaction Time (h)*
1(*)	5	-40	7
2	10	-40	4
3	5	0	7
4	1	25	24
5	10	25	24
6	10	25	120

[ɣ-BL]/[BPM]=100/1 ; [BPM]/[MSA]=1/1 .

*) The reaction 1 was performed with trifluoromethanesulfonic acid as a catalyst.

As already pointed out, the homopolymerization of butyrolactone is difficult to occur due to its low strain energy and the experiments done at several temperatures confirmed that precisely. MSA and TfOH were used as catalysts, the temperature varied between -40ºC and 25ºC and the reaction time varied too. However, no polymerization occurred whatever the conditions.

The last homopolymerization performed was the polymerization of ɣ-valerolactone. In Table 4 are presented the different polymerization conditions tested. Again, like for ɣ-BL, no polymerization occurred, whatever the conditions.

Table 4 - Homopolymerization of ɣ-VL in toluene with methanesulfonic acid as the catalyst.

Run	***$[\gamma\text{-VL}]_0$ (mol/L)***	***T (°C)***	***Reaction Time (h)***
1	3	-30	2
2(*)	3	-30	6
3	3	0	7
4	0.5	40	3
5	0.5	40	24
6	0.5	40	48

[ɣ-VL]/[BPM]=100/1 ; [BPM]/[MSA]=1/1 ; Solvent : Toluene

*) The reaction 2 was performed under trifluoromethanesulfonic acid as a catalyst.

4.2 Synthesis of copolymers: Ɛ-Caprolactone with ɣ-Butyrolactone

Several copolymerizations were performed at different temperatures in the presence of the same initiator and catalysts as before. A molar ratio of 1:1 between the catalyst and the alcohol initiator was used and the molar proportion of the monomers was varied: 50/50, 25/75 and 75/25. In Scheme 16, it is shown the expected structure for the copolymer obtained.

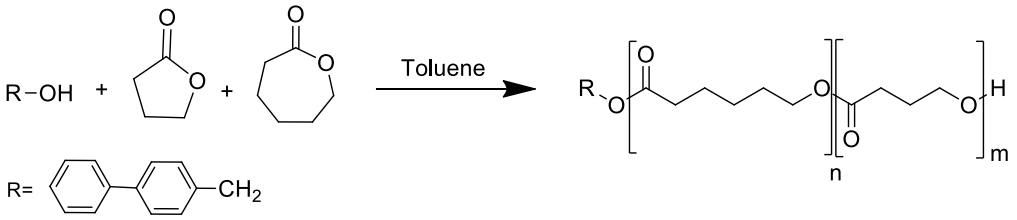

Scheme 16 – Copolymerization of Ɛ-CL with ɣ-BL in the presence of BPM, with MSA or TfOH as a catalyst.

The conversion of poly-ɣ-butyrolactone is calculated with the spectrum of the unpurified sample (Figure 7) making the integration of the peak (8) of the monomer, at 4.35 ppm, and the polymer peak at 1.95 ppm, peak (7'), as it is shown in Equation 7. On the other hand, the conversion of Ɛ-caprolactone can be calculated through the integration of the monomer peak (5) at 4.20 ppm (in Figure 7 this peak is not visible because the conversion of ε-caprolactone is 100%) and the polymer peak (3') at 1.35 ppm, as shown Equation 8.

$$x_{\gamma-BL}(\%) = \frac{(I_{peak_{7'}})/2}{\frac{I_{peak_{7'}}}{2} + \frac{I_{peak_8}}{2}} \times 100 \quad (7)$$

$$x_{\varepsilon-CL}(\%) = \frac{(I_{peak_{3'}})/2}{\frac{I_{peak_{3'}}}{2} + \frac{I_{peak_5}}{2}} \times 100 \quad (8)$$

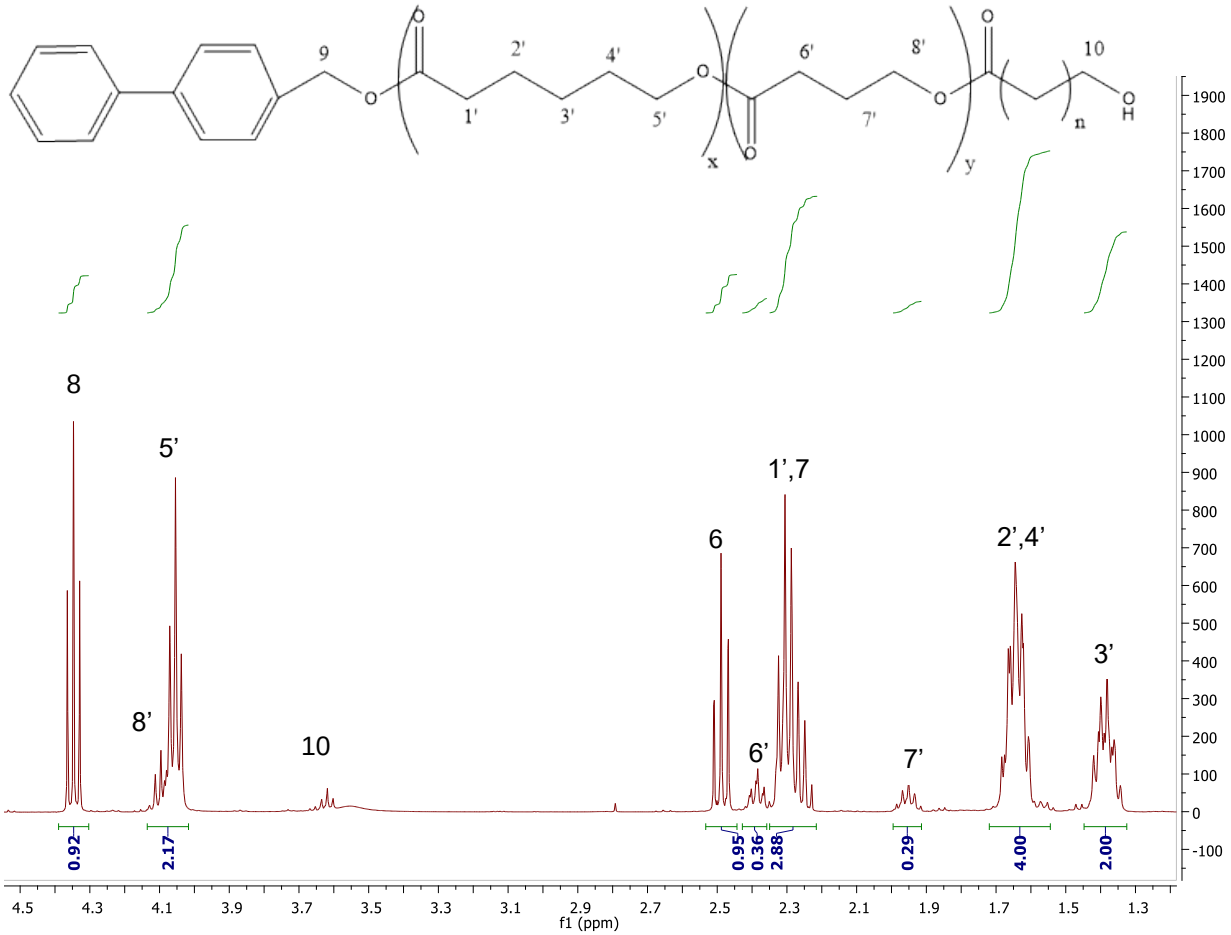

Figure 7 - ^{1}H NMR spectrum in $CDCl_3$ zoomed between 1.00 ppm and 4.5.00 ppm. This figure refers to non-purified copolymer of Run 2, Table 5.

An unexpected feature observed in the^{1} H NMR spectrum (Figure 8) is that the signals of the polymers and of the monomers shifted slightly when the two species are in the copolymer compared to the peaks of the monomers alone or of the homopolymers. This shift is likely due to a change in chemical environment during the synthesis of the copolymer.

In Figure 8 it is shown the ^{1}H NMR spectrum of each one of the monomers along with the spectrum of a mixture of the monomers. Again, a shift in the peak position is observed when the two monomers are mixed, relatively to the individual components.

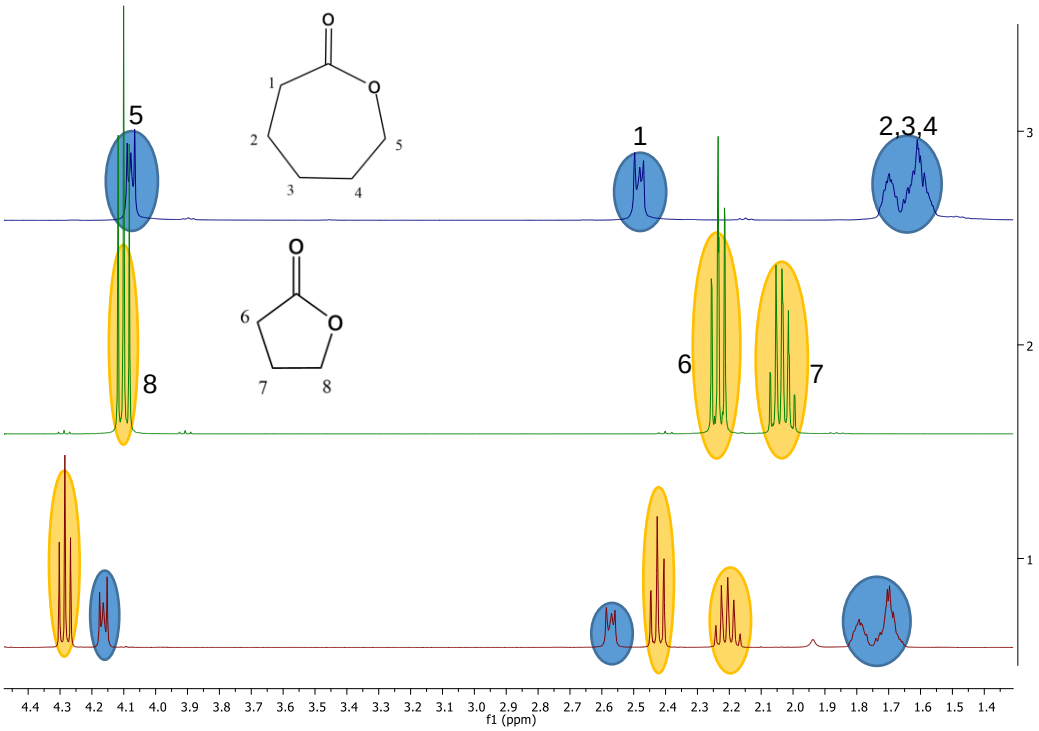

Figure 8 – ^{1}H NMR spectrum between 1.4 ppm and 4.4 ppm in $CDCl_3$. The blue spectrum is related to Ɛ-caprolactone, the green spectrum is from ɣ-butyrolactone and the red spectrum is from the mixture of both monomers.

From the ^{1}H NMR spectrum of the purified copolymers it is also possible to calculate its molar composition in ɣ-butyrolactone and Ɛ-caprolactone, through Equations 9 and 10 respectively. The peaks corresponding to two protons of poly-caprolactone and polybutyrolactone, at 1.35 ppm (3') and 1.9 ppm (7') respectively, were used.

$$Molar\ proportion_{\gamma-BL}(\%) = \frac{(I_{peak_{7'}})/2}{\frac{I_{peak_{7'}}}{2} + \frac{I_{peak_{3'}}}{2}} \times 100 \quad (9)$$

$$Molar\ proportion_{\varepsilon-CL}(\%) = \frac{(I_{peak_{3'}})/2}{\frac{I_{peak_{7'}}}{2} + \frac{I_{peak_{3'}}}{2}} \times 100 \quad (10)$$

Then, the molar masses of the copolymers can be calculated by the three peaks of the polymer chain, like it was referred in the case of polycaprolactone, through Equation 6. In an analogous way, like what was referred for polycaprolactone the DP and the molar masses of the copolymers can be calculated by the following equations:

$$\mathrm{DP}_{\gamma-\mathrm{BL}}\ (3.6\mathrm{ppm}) = \frac{\mathrm{I}_{\mathrm{peak}_{7'}}/2}{\mathrm{I}_{\mathrm{peak}_{10'}}/2} \quad (11)$$

$$\mathrm{DP}_{\gamma-\mathrm{BL}}\ (5.2\mathrm{ppm}) = \frac{\mathrm{I}_{\mathrm{peak}_{7'}}/2}{\mathrm{I}_{\mathrm{peak}_{9'}}/2} \quad (12)$$

$$DP_{\gamma-BL}\ (7.3ppm) = \frac{I_{peak_7,}/2}{I_{peak_{aromatics}}/9} \quad (13)$$

$$\overline{Mn}\,th = \frac{[\varepsilon - CL]_0}{[BPM]_0} \times M_{\varepsilon-CL} \times x_{\varepsilon-CL} + \frac{[\gamma - BL]_0}{[BPM]_0} \times M_{\gamma-BL} \times x_{\gamma-BL} + M_{BPM} \quad (14)$$

$$Mn\ (g/mol) = \overline{DP}_{\varepsilon-CL} \times M_{\varepsilon-CL} + \overline{DP}_{\gamma-BL} \times M_{\gamma-BL} + M_{BPM} \quad (15)$$

Figure 9 displays the ^{1}H NMR spectrum for a representative 50/50 copolymer of Ɛ-CL and ɣ-BL sample (Run 2, table 5).

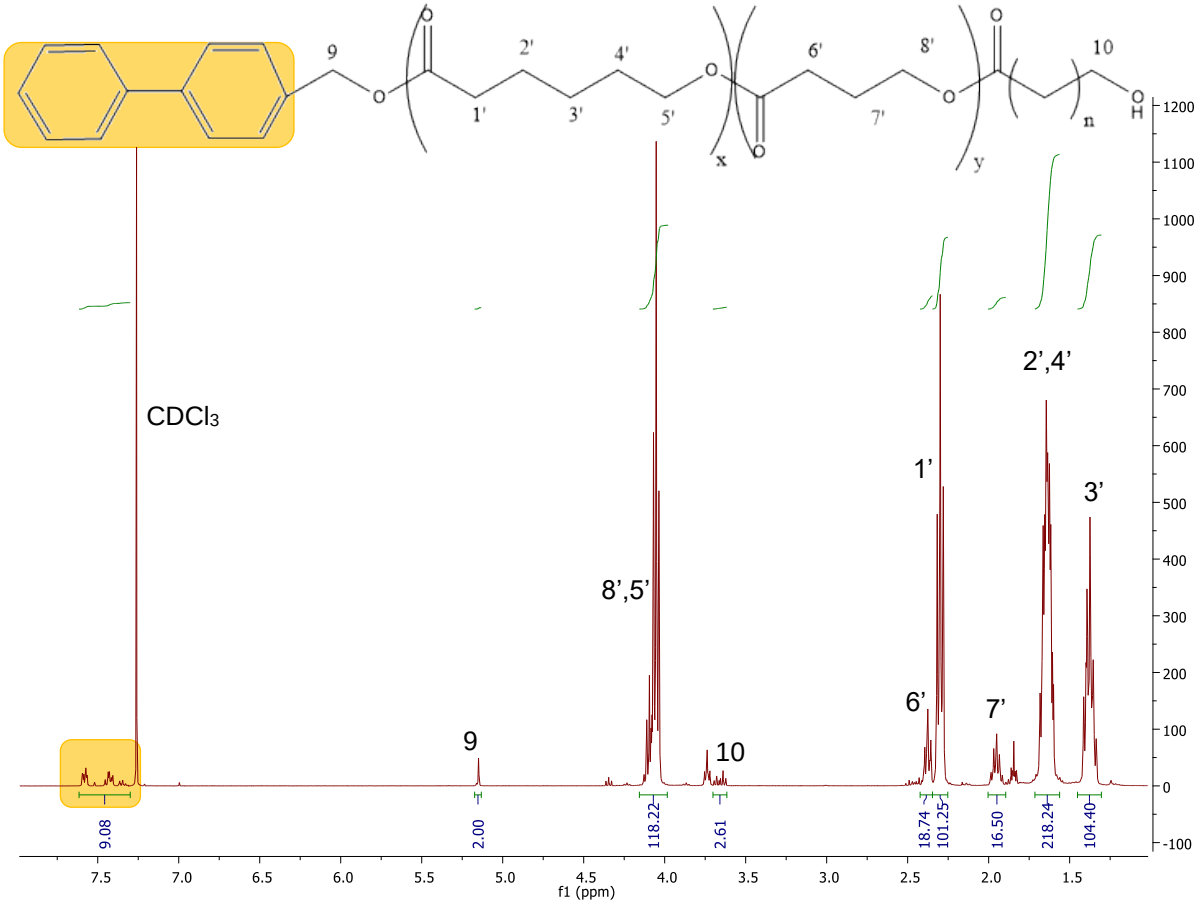

Figure 9 – ^{1}H NMR spectrum of the copolymer Ɛ-CL with ɣ-BL of the precipitated sample (Run 2, Table 5), indicating the peaks of the copolymer.

The two singlet peaks at 5.1 ppm and 5.2 ppm in Figure 10, can be recognized as the benzylic protons present in the BPM initiator. These two peaks demonstrate that the initiation can be made by two different attacks, either the alcohol initiates polymerization by attacking Ɛ-caprolactone or by attacking γ-butyrolactone. In the spectrum of Figure 10, the signal corresponding to the attack of Ɛ-caprolactone is more intense than the signal corresponding to the attack of γ -butyrolactone. The one at lower chemical shift is attributed to structures where Ɛ-CL is the first monomer linked to the CH_2OH group of the initiator while the other signal at higher chemical shift represents a similar structure but with

ɣ-BL as first monomer. It should be noticed that in this region of the spectrum, there are no neighbouring peaks which indicates that there were no free benzylic groups remaining.

The two multiplet peaks at 3.64 ppm and 3.68 ppm in Figure 11, represent the terminal methylene protons located at the chain ends. The one at higher chemical shift is ascribed to ɣ-BL and the other one to Ɛ-CL. The intensity of the peaks indicates that the monomer which is preferentially located at the chain end is Ɛ-CL.

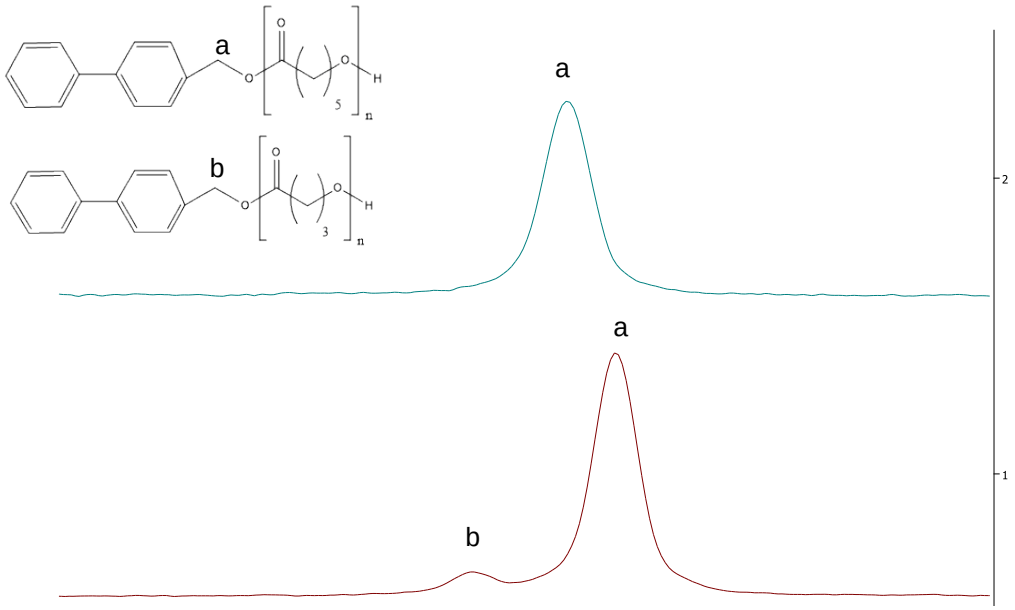

Figure 10 - Zoom of spectrum (5.10-5.20 ppm) ^{1}H NMR in $CDCl_3$ showing CH_2OH group. In blue, the spectrum of homocaprolactone (Run 5, Table 2) and in red the spectrum of the copolymer (Run 2, Table 5).

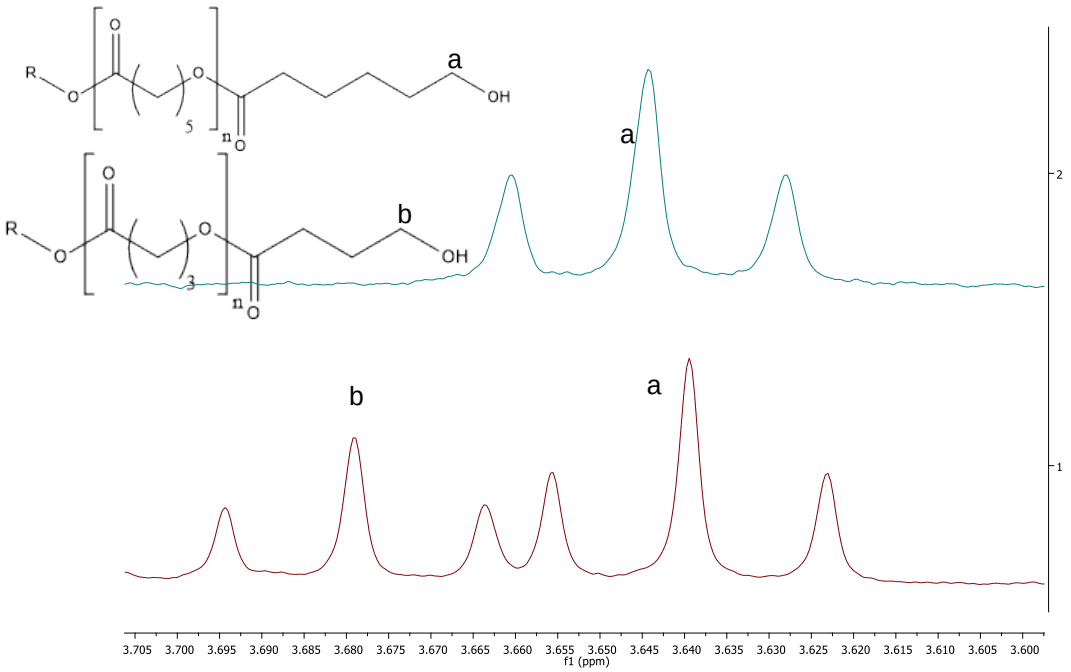

Figure 11 - Zoom of spectrum (3.60-3.70 ppm) ^{1}H NMR in $CDCl_3$ showing CH_2OH group. In blue, the spectrum of homocaprolactone (Run 5, Table 2) and in red the spectrum of the copolymer (Run 2, Table 5).

The first copolymers were synthesized at room temperature with an initial molar ratio of 50/50, varying the reaction time. The results are shown in Table 5.

Table 5 – Copolymerization of Ɛ-CL with ɣ-BL at 25ºC, with a molar ratio of 50/50 in the presence of MSA as a catalyst.

Run	*Time (h)*	$x_{\varepsilon-CL}$ *a)* *(%)*	$x_{\gamma-BL}$ *a)* *(%)*	$\overline{Mn}$ *th b)* *(g/mol)*	***Proportion c)* *(ɣ-BL)/(Ɛ-CL)***	$\overline{Mn}$ *d)* *(g/mol)*	$\overline{Mn}$ *SEC e)* *(g/mol)*	$\frac{M_w}{M_n}$ *f)*
1	10	100	13	6400	16/84	6 200	-	-
2	24	100	24	6900	14/86	6 730	8240	1.17

[ε-CL-ɣ-BL]/[BPM]=100/1 ; [BPM]/[MSA]=1/1.

a) Conversions calculated by ^{1}H NMR spectroscopy of the brute sample, by Equations 7 and 8.
b) Theoretical number-average molar mass $\overline{Mn}$ th calculated by Equation 14.
c) Composition of the recovered polymer (molar fraction), as determined by ^{1}H NMR with Equations 9 and 10.
d) Number average molar mass calculated by Equation 15.
e) Number-average molar mass measured by SEC in THF versus PS calibration.
f) Molar mass dispersities estimated from SEC data.

With an initial molar proportion of 50/50 between the monomers, the increasing of the reaction time doesn't affect the conversion of caprolactone since this monomer, has already attained fully conversion after 10 hours. The increase of reaction time, increases however the conversion of ɣ-BL. After 24 hours, the conversion of ɣ-BL attains 24%. Although the homopolymerization of butyrolactone at the same temperature with the same catalyst did not work, in copolymerization conditions, ɣ-BL is successfully incorporated in the copolymer.

Due to the difference in the reactivity of the two monomers the final composition of the copolymer is different from the theoretical one, 50% ɣ-butyrolactone and 50% Ɛ-caprolactone. Under the tested conditions an incorporation of 16% in butyrolactone is attained after 10 hours.

The molar masses calculated by NMR and SEC are close to the theoretical ones, indicating a controlled polymerization. Moreover, the dispersity is quite good, corroborating the control of the polymerization.

Another set of polymerizations were performed under different molar proportions of Ɛ-Caprolactone and ɣ-Butyrolactone of 25/75 and 75/25. The results are shown in Tables 6 and 7, respectively.

Table 6 - Copolymerization of Ɛ-CL with ɣ-BL at 25ºC and with a molar proportion of 25/75.

Run	Time (h)	$\mathbf{x_{\varepsilon-CL}}$ a) (%)	$\mathbf{x_{\gamma-BL}}$ a) (%)	$\overline{\mathbf{Mn}}$ th b) (g/mol)	**Proportion c) (ɣ-BL)/(Ɛ-CL)**	$\overline{\mathbf{Mn}}$ **NMR d) (g/mol)**	$\overline{\mathbf{Mn}}$ SEC e) (g/mol)	$\frac{\mathbf{M_w}}{\mathbf{M_n}}$ f)
1	24	99	12	4040	-	-	-	-
1.1	144	99	13	4140	25/75	4420(*)	5500	1.27
2	24	98	10	3860	-	-	-	-
2.1	168	99	16	4360	-	-	-	-

[ε-CL-ɣ-BL]/[BPM]=107/1 ; [BPM]/[MSA]=1/1.

a) Conversions calculated by ^{1}H NMR spectroscopy of the brute sample, by Equations 7 and 8.
b) Theoretical number-average molar mass $\overline{Mn}$ th calculated by Equation 14.
c) Composition of the recovered polymer (molar fraction), as determined by ^{1}H NMR with Equations 9 and 10.
d) Number average molar mass calculated by Equation 15.

e) Number-average molar mass measured by SEC in THF versus PS calibration.
f) Molar mass dispersities estimated from SEC data
(*) Number average molar mass calculated by Equation 15, with the DP only corresponding to 3.6 ppm peak.

Table 7 - Copolymerization of Ɛ-CL with ɣ-BL at 25ºC and with a molar proportion of 75/25.

Run	*Time (h)*	$x_{\varepsilon-CL}$ [a] *(%)*	$x_{\gamma-BL}$ [a] *(%)*	$\overline{Mn}$ *th* [b] *(g/mol)*	***Proportion*** [c] ***(ɣ-BL)/(Ɛ-CL)***	$\overline{Mn}$ *NMR* [d] ***(g/mol)***	$\overline{Mn}$ *SEC* [e] *(g/mol)*	$\frac{M_w}{M_n}$ [f]
1	5	-	-	-	8/92	10180	8500	1.28
2	24	99	37	8810	7/93	10790	9500	1.32

[ε-CL-ɣ-BL]/[BPM]=93/1 ; [BPM]/[MSA]=1/1.
a) Conversions calculated by ^{1}H NMR spectroscopy of the brute sample, by Equations 7 and 8.
b) Theoretical number-average molar mass $\overline{Mn}$ th calculated by Equation 14.
c) Composition of the recovered polymer (molar fraction), as determined by ^{1}H NMR with Equations 9 and 10.
d) Number average molar mass calculated by Equation 15.
e) Number-average molar mass measured by SEC in THF versus PS calibration.
f) Molar mass dispersities estimated from SEC data.

Despite the increase of the proportion of *ɣ-BL* in the polymerization media from 50/50 to 25/75 there's only a marginal increase of the *ɣ*-BL content in the copolymer from around 14% up to 25%. This is a consequence of the low reactivity of *ɣ*-BL and of the rather low values obtained for the butyrolactone conversion even at 144 h polymerization time. Results in table 6, also show A good agreement between the molar masses obtained from NMR and SEC analysis, along with a low value of 1.27 for dispersity.

For the copolymerizations of Ɛ-CL with ɣ-BL with a molar proportion of 75/25 (results in Table 7) it can be observed tha the conversion of butyrolactone is 37% and the final content of butyrolactone in the copolymer is 8%. The molar masses calculated are in a good agreement, like for the previous experiments, with a polydispersity in the same range of values (1.28-1.32).

The SEC chromatograms for copolymerization of Ɛ-CL with ɣ-BL at molar proportion of 50/50, 25/75 and 75/25 (Run 2, Table 5, Run 1.1, Table 6, Runs 1 and 2, Table 7 respectively) are shown in Figure 12.

In this Figure 12, it is possible to verify the existence of two populations in the blue line, which corresponds to the copolymerization of Ɛ-CL and ɣ-BL with a molar proportion of 75/25. The observation of these two peaks, represents the occurrence of side reactions in this polymerization, generating additional chains with higher molar mass.

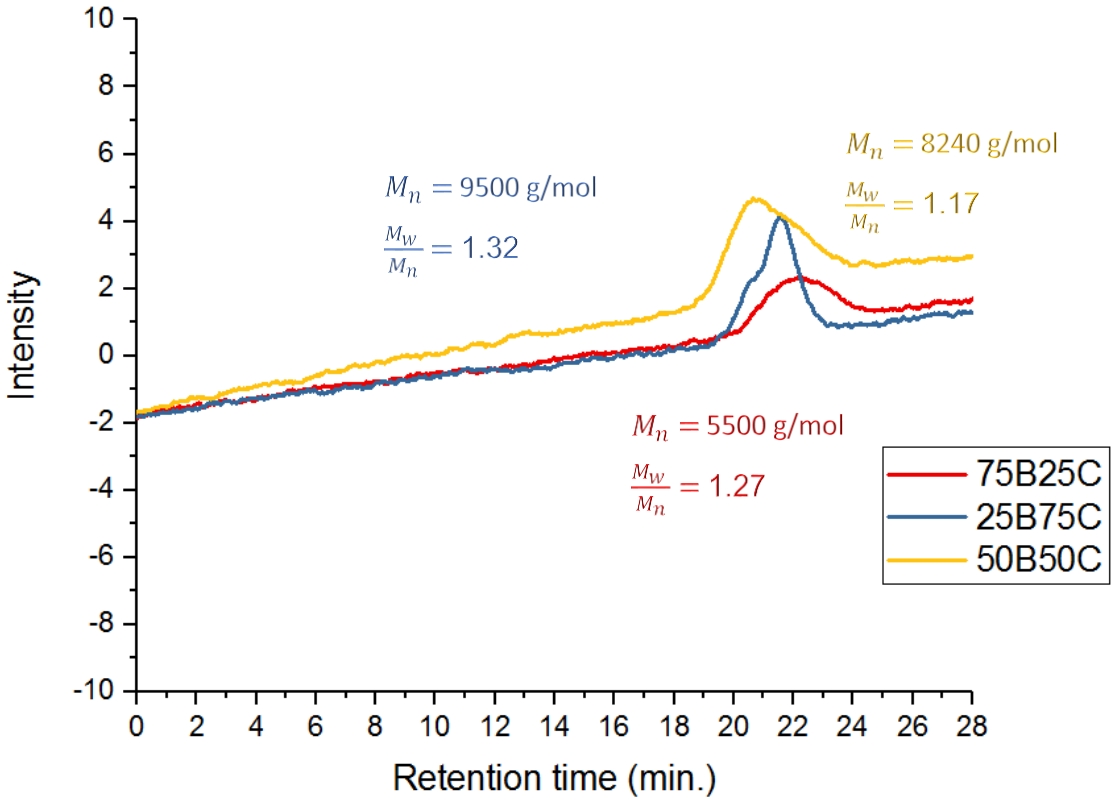

Figure 12 - SEC chromatograms of the poly (ɣ-butyrolactone-co-ε-caprolactone) copolymers obtained at 25ºC in different molar ratios (THF with polystyrene calibration at 40 ° C).

Based on the previous results, demonstrating the successful homopolymerization of Ɛ-caprolactone at 0 ºC, the copolymerization Ɛ-CL with ɣ-BL at this temperature was also performed. Table 8 shows the experiments made in different conditions and the corresponding results. TfOH was used as catalyst and the tested molar proportion Ɛ-CL/ɣ-BL was 50/50.

Table 8 - Copolymerization of Ɛ-CL with ɣ-BL at 0ºC and with a molar ratio of 50/50. The catalyst used in these experiments is TfOH and the solvent is DCM.

Run	*Time (h)*	$x_{\varepsilon-CL}$ [a] *(%)*	$x_{\gamma-BL}$ [a] *(%)*	$\overline{Mn}$ *th* [b] *(g/mol)*	***Proportion*** [c] ***(ɣ-BL)/(Ɛ-CL)***	$\overline{Mn}$ ***NMR*** [d] ***(g/mol)***	$\overline{Mn}$ *SEC* [e] *(g/mol)*	$\frac{M_w}{M_n}$ [f]
1	7	100	10	6300	-	-	-	-
1.1	24	100	12	6400	16/84	7460	7170	1.32

[ε-CL-ɣ-BL]/[BPM]=100/1 ; [BPM]/[TfOH]=1/1.

a) Conversions calculated by ^{1}H NMR spectroscopy of the brute sample, by Equations 7 and 8.
b) Theoretical number-average molar mass $\overline{Mn}$ th calculated by Equation 14.
c) Composition of the recovered polymer (molar fraction), as determined by ^{1}H NMR with Equations 9 and 10.
d) Number average molar mass calculated by Equation 15.
e) Number-average molar mass measured by SEC in THF versus PS calibration.
f) Molar mass dispersities estimated from SEC data.

The conversion of butyrolactone does not exceed the 12%, which is a lower conversion than the one obtained for the experiments at room temperature. However, due to superposition of some NMR peaks, it is very difficult to provide a good evaluation of the incorporation of ɣ-BL in the copolymer. On the otherhand, the theoretical mass is in a good agreement with the molar mass calculated by NMR and

SEC, indicating that this system has a good control. In Figure 13 it can be verified the SEC chromatograms of the Run 1.1 of Table 8.

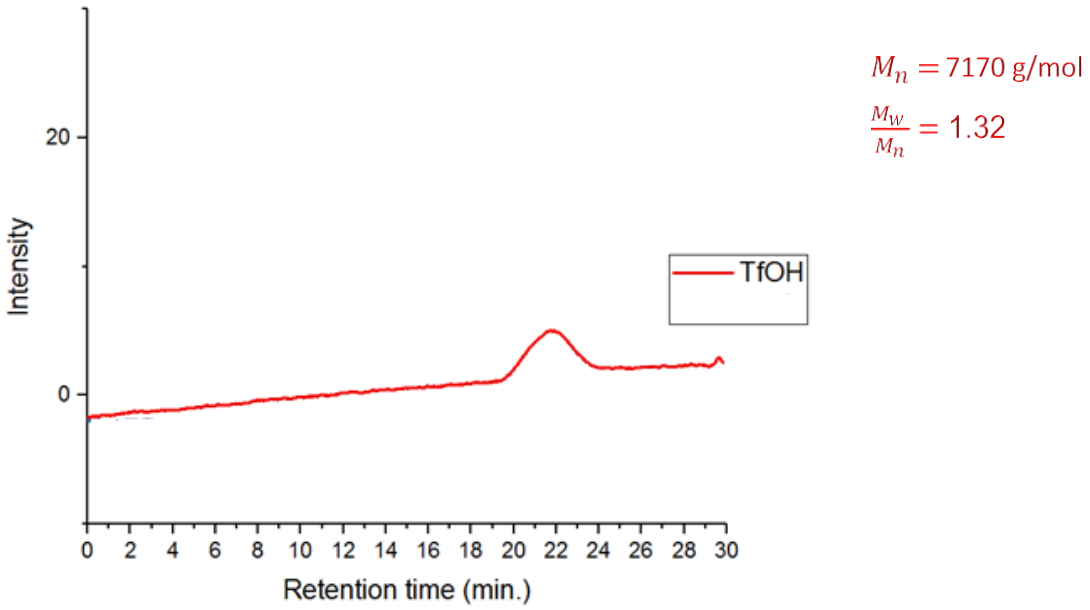

Figure 13 - SEC chromatogram of the poly (ɣ-butyrolactone-co-ε-caprolactone) copolymers obtained at 0ºC for Run 1.1 of Table 8 (THF with polystyrene calibration at 40 ° C).

Another set of experiments were made in bulk, without any solvent at 50 ºC. The results for the 50/50 molar proportion using TfOH or MSA as the catalyst are given in Tables 9 and 10 respectively.

Table 9 - Copolymerization of Ɛ-CL with ɣ-BL at 50ºC in bulk with a molar ratio 50/50 and TfOH as the catalyst.

Run	*Time (h)*	$x_{ɣ-BL}$ [a] *(%)*	$x_{ε-CL}$ [a] *(%)*	$\overline{Mn}$ *th* [c] *(g/mol)*	***Proportion*** [b] ***(ɣ-BL) / (Ɛ-CL)***	$\overline{Mn}$ *NMR* [d] ***(g/mol)***	$\overline{Mn}$ *SEC* [e] *(g/mol)*	$\frac{M_w}{M_n}$ [f]
1	1	15%	97%	6350	14/86	10 560	-	-
2	48	31%	100%	7200	15/85	14 625(*)	5 940	1.54

[ε-CL-ɣ-BL]/[BPM]=100/1 ; [BPM]/[TfOH]=1/1.

a) Conversions calculated by ^{1}H NMR spectroscopy of the brute sample, by Equations 7 and 8.
b) Theoretical number-average molar mass $\overline{Mn}$ th calculated by Equation 14.
c) Composition of the recovered polymer (molar fraction), as determined by ^{1}H NMR with Equations 9 and 10.
d) Number average molar mass calculated by Equation 15.
e) Number-average molar mass measured by SEC in THF versus PS calibration.
f) Molar mass dispersities estimated from SEC data.
(*) Number average molar mass calculated by Equation 15, with the DP only corresponding to 3.6 ppm peak.

In Table 9, it is possible to notice that after 1 h the conversion for Ɛ-caprolactone is almost complete while the conversion of ɣ-butyrolactone is about 31% after 48h. On the other hand, the proportion of ɣ-BL reaches 15% after 2 days of polymerization. A beneficial effect from the point of view of the conversion and the incorporation of ɣ-butyrolactone on the copolymer can be observed when comparing these values with those attained at 0ºC.

However, the molar mass obtained by NMR is much higher than the theoretical molar masses and the dispersity given by SEC analysis is quite high, 1.54. This indicates a loss of polymerization control under the tested experimental conditions.

In these experiments, a change of color appeared from rose to violet, as it is shown in Figure 14, but the reason for that was not completely identified. One possibility is the occurrence of side reactions such as cyclization.

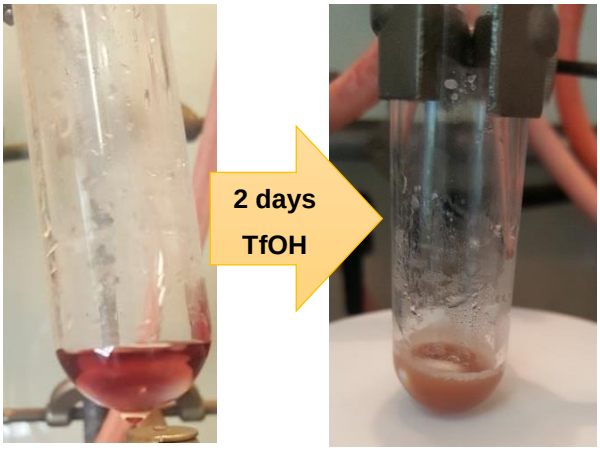

Figure 14 – Sample from run 2 in Table 9, after 1 hour (crude sample) and 2 days (brute sample), with triflic acid.

Table 10 - Copolymerization of Ɛ-CL with ɣ-BL at 50ºC in bulk with a molar ratio 50/50 and MSA as the catalyst.

Run	*Time (h)*	$x_{\varepsilon-CL}$ [a] *(%)*	$x_{\gamma-BL}$ [a] *(%)*	$\overline{Mn}$ *th* [b] *(g/mol)*	***Proportion*** [c] ***(ɣ-BL)/(Ɛ-CL)***	$\overline{Mn}$ [d] *(g/mol)*	$\overline{Mn}$ *SEC* [e] *(g/mol)*	$\frac{M_w}{M_n}$ [f]
1	1	99	16	6500	10/90	8030(*)	6150	1.20
2	48	99	25	6920	18/82	6000	9220	1.50
3	72	100	23	6860	15/85	5850	11885	1.48

[ε-CL-ɣ-BL]/[BPM]=100/1 ; [BPM]/[TfOH]=1/1.

a) Conversions calculated by ^{1}H NMR spectroscopy of the brute sample, by Equations 7 and 8.
b) Theoretical number-average molar mass $\overline{Mn}$ th calculated by Equation 14.
c) Composition of the recovered polymer (molar fraction), as determined by ^{1}H NMR with Equations 9 and 10.
d) Number average molar mass calculated by Equation 15.
e) Number-average molar mass measured by SEC in THF versus PS calibration.
f) Molar mass dispersities estimated from SEC data.
(*) Number average molar mass calculated by Equation 15, with the DP only corresponding to 3.6 ppm peak.

In Table 10, it is possible to notice that the conversion of butyrolactone is around 24% after two days, which is slightly higher than the one for TfOH catalyst. The molar proportion of ɣ-BL/Ɛ-CL in the copolymer after three days is 15/85. In what concerns molar masses, the theoretical values are not very far from those determined by NMR. However, the corresponding values determined by SEC analysis, are much higher and the dispersities also show relatively high values, particularly for the long polymerization times. Therefore, a loss of polymerization control together with the presence of side reactions seems to occur in these conditions.

Figure 15 - Sample corresponding to Sample 1 in Table 10, after 1 hour (crude sample) with methanesulfonic acid.

5. Conclusions

The aim of this work was to develop an effective system for the (co)polymerization of 5-membered lactones, caprolactone and butyrolactone, by ROP with an acidic catalyst.

The investigation performed has shown that the homopolymerization of caprolactone can be done and is more effective at room temperature than in other conditions of temperature. On the contrary, the homopolymerization of the other two lactones (γ-butyrolactone and γ-valerolactone) wasn't successful under the same conditions.

Since the homopolymerization of γ-butyrolactone was not effective, the possibility to link this monomer to Ɛ-caprolactone, which is able to polymerize at any temperature in the conditions referred, was investigated. It has been shown that the synthesis of novel γ-butyrolactone/Ɛ-caprolactone copolymers is an effective alternative to polymerize γ-butyrolactone units at room temperature. NMR and SEC analyses show a good control of (co) polymerization with the formation of random copolyesters, at room temperature.

The copolymers obtained in bulk conditions and at 50 ºC show high molar masses but also a high polydispersit, which suggests the presence of some side reactions.

In this investigation -butyrolactones not derived from renewable resources were successfully copolymerized by ROP. In a future work, it would be advantageous, to use this system to polymerize bio-sourced γ-butyrolactone.

6. References

[1] "Plastics," *Plastics Europe- Association of plastics manufacturers,* pp. 1-30, 2015.

[2] K. Stridsberg, M. Ryner and A.-C. Albertsson, "Controlled Ring-Opening Polymerization: Polymers with designed Macromolecular Architecture," *Polymer Science,* vol. 157, pp. 41-65, 2002.

[3] U. Lucknow, "A Theoretic Study of degradable polymers," *European Journal of Academic Essays,* vol. 2, no. 2, pp. 7-10, 2015.

[4] H.-T. Liao and C.-S. Wu, "Preparation and characterization of ternary blends composed of polylactide, poly(e-caprolactone) and starch," *Materials Science Engineering,* vol. A 515, pp. 207-214, 2009.

[5] N. Ljundegberg and B. Wesslén, *J. Appl. Polym. Sci.,* vol. 86, pp. 1227-1234, 2002.

[6] N. Ljungberg, T. Andersson and B. Wesslén, *J. Appl. Polym. Sci. ,* vol. 88, pp. 3239-3247, 2003.

[7] O. Martin and L. Avérous, *Polymer,* vol. 42, pp. 6209-6219, 2001.

[8] T. Ke and X. Sun, *J. Appl. Polym. Sci.,* vol. 88, pp. 2947-2955, 2003.

[9] T. Takayama and M. Todo, *J. Mater. Sci,* vol. 41, pp. 4989-4992, 2006.

[10] A. Hoffman, *Adv. Drug Deliv. Rev.,* vol. 54, pp. 3-12, 2002.

[11] M. Woodruff and D. Hutmacher, "The return of a forgotten polymer- Polycaprolactone in the 21st century," *Progress in Polymer Science,* vol. 35, pp. 1217-1256, 2010.

[12] E. Wissler, *Ring-opening polymerization of lactones and lactides: An organic chemistry lab synthesis,* College of Saint Benedict/Saint John's University, paper 23, 2014.

[13] I. Engelberg and J. Kohn, "Physico-mechanical properties of degradable polymers used in medical applications: a comparative study," *Biomaterials,* vol. 12, pp. 292-304, 1991.

[14] E. Frazza and E. Schmitt, "A new absorbable suture," *J. Biomed. Mat. Res. Symp.,* vol. 1, pp. 43-58, 1971.

[15] Ann.-C. Albertsson and I. Varma, "Recent Developments in Ring Opening Polymerization of Lactones for Biomedical Applications," *Biomacromolecules,* vol. 4, pp. 1466-1486, 2003.

[16] P. Ólsen, K. Odelius and A.-C. Albertsson, "Thermodynamic Presynthetic Considerations for Ring-Opening Polymerization," *Biomacromolecules,* vol. 17, no. 3, pp. 699-709, 2016.

[17] "http://polymerdatabase.com/polymer%20chemistry/Condensation%20Polymerization.html," [Online]. [Accessed 13/ 11/ 2016].

[18] W. Carothers and J. Arvin, *Am. Chem. Soc. ,* vol. 51, p. 2560, 1929.

[19] "http://polymerdatabase.com/polymer%20chemistry/Chain%20versus%20Step%20Growth.html," [Online]. [Accessed 13 11 2016].

[20] C. Jêrome and P. Lecomte, "Recent advances in the synthesis of aliphatic polyesters by ring-opening polymerization," *Advanced Drug Delivery Reviews ,* vol. 60, pp. 1056-1076, 2008.

[21] H. Leuchs, "Glycine-carbonic acid," *Ber. Dtsch. Chem.,* vol. 39, 1906.

[22] O. Pask and D. Stephen, *Polymers,* no. 5, pp. 361-403, 2013.

[23] J. E. McGrath, Ed., Ring-Opening Polymerization, vol. 286, American Chemical Society, 1985.

[24] S. Sosnowski, M. Gadzinowski and S. Slomkowski, "Poly (L,L-lactide) microspheres by ring-opening polymerization," *Macromolecules,* vol. 29, p. 4556, 1996.

[25] M. Gadzenowski, S. Sosnowski and S. Slomkowski, "Kinetics of the dispersion ring-opening polymerization of e-caprolactone initiated with diethylaluminum ethoxide," *Macromolecules,* vol. 29, p. 6404, 1996.

[26] P. Dubois (Editor), O. Coulembier (Editor) and J.-M. Raquez (Editor), Handbook of Ring Opening Polymerization, 2009, p. 1.

[27] R. Snow and F. Frey, *J. Am. Chem. Soc.,* vol. 65, p. 2417, 1943.

[28] F. Dainton and K. Irvin, *J. Nature,* vol. 162, p. 705, 1948.

[29] F. Dainton and K. Irvin, *J. Proc. R. Soc. London,* vol. 212, pp. 96, 207, 1952.

[30] M. Save, M. Schappacher and A. Soum, *Macromol. Chem. Phys.,* vol. 203, p. 889, 2002.

[31] A. Duda and A. Kowalski, Handbook of Ring-Opening Polymerization, 2009, pp. 1-51.

[32] P. Lecomte and C. Jérôme, "Recent Developments in Ring-Opening Polymerization of Lactones," *Adv. Polym. Sci.,* vol. 245, pp. 173-218, 2012.

[33] H. Schenck, M. Ryner, A.-C. Albertsson and M. Svensson, "Ring-Opening Polymerization of Lactones and Lactides with Sn(IV) and Al (III) initiators," *Macromolecules,* vol. 35, pp. 1556-1562, 2002.

[34] P. Lecomte and C. Jérôme, "Recent advances in the synthesis of aliphatic polyesters by ring-opening polymerization," *Advanced Drug delivery review,* vol. 60, pp. 1056-1076, 2008.

[35] H. Kricheldorf, A. Stricker and D. Langanke, "Polylactones, 50. Reactivity cyclic and noncyclic dibutylin bisalkoxides as initiator in the polymerization of lactones.," *Macromol. Chem. Phys.,* vol. 202, pp. 2525-2534, 2001.

[36] H. Kricheldorf and S. Eggerstedt, "Macrocycles 2. Living macrocyclic polymerization of e-caprolactone with 2,2-dibutyl-2-stanna-1,3-dioexepane as initiator," *Macromol. Chem. Phys.,* vol. 199, pp. 283-290, 1998.

[37] H. Kricheldorf, "Biodegradable polymers with variable architectures via ring-expansion polymerization," *J. Polym. Sci. A. Polym. Chem.,* vol. 42, pp. 4723-4742, 2004.

[38] M. Benvenuti and R. Lenz , "Polymerization and copolymerization of b-butyrolactone and benzyl-beta-malolactonate by aluminoxane catalyst.," *J Polym Sci Polym Chem Ed,* vol. 29, no. 6, pp. 793-805, 1991.

[39] O. Coulembiera, L. James, P. Dubois and P. Degée, "From controlled ring-opening polymerization to biodegradable aliphatic polyester: Especially poly(b-malic acid) derivatives," *Prog. Polym. Sci.,* vol. 31, p. 723–747, 2006.

[40] A. Kowalski, J. Libiszowski, T. Biela, M. Cypryk, A. Duda and S. Penczek, "Kinetics and mechanism of cyclic esters polymerization initiated with tin(II) octoate. polymerization of e-caprolactone and L,L-lactide co-initiated with primary amines.," *Macromolecules,* vol. 38, pp. 8170-8176, 2005.

[41] Z. Jedlinski, P. Kurock and M. Kowalczuk, *Macromolecules,* vol. 18, p. 20679, 1985.

[42] Z. Jedlinski, P. Kurock and M. Kowalczuk, *Macromolecules,* vol. 24, p. 1218, 1991.

[43] Z. Jedlinski and M. Kowalczuk, *Macromolecules,* vol. 22, p. 3242, 1989.

[44] Z. Jedlinski, P. Kurock, W. Walach, H. Janeczek and Radecka, *Macromolecules Chem.,* vol. 194, p. 1681, 1993.

[45] P. Kurock, S. Penczek, J. Franek and Z. Jedlinski, "2285," *Macromolecules,* vol. 25, 1992.

[46] P. Kurock, M. Kowalczuk, K. Hennek and Z. Jedlinski, *Macromolecules,* vol. 25, p. 2017, 1992.

[47] A. Hoffman, R. Szymanski, S. Slowkowski and S. Penczek, "Structure of species in the cationic polymerization of b-propiolactone ad e-caprolactone," *Makromol. Chem.,* vol. 185, pp. 655-667, 1984.

[48] H. Kricheldorf, J. Jonte and R. Dunsing, "Polylactones 7. The mechanism of cationic polymerization of b-propionolactone and e-caprolactone," *Makromol. Chem.,* vol. 187, pp. 771-785, 1986.

[49] N. Hadjichristidis, K. Ratkanthwar, J. Zhao, H. Zhang and J. Mays, "Anionic Polymerization," *Springer Japan ,* 2015.

[50] Y. Shibasiki, H. Sanada, M. Yokoi, F. Sanda and T. Endo, "Activated monomer cationic polymerization of lactones and the application to well defined block copolymer synthesis with seven-membered cyclic carbonate," *Macromolecules,* vol. 33, pp. 4316-4320, 2000.

[51] M. Basko and P. Kubisa, "Cationic copolymerization of e-caprolactone and L,L-lactide by an activated monomer mechanism.," *J. Polym Sci A Polym Chem,* vol. 44, pp. 7071-7081, 2006.

[52] S. Gazeau-Bureau, D. Delcroix, B. Martin-Vaca, D. Bourissou, C. Navarro and S. Magnet, "Organo-catalyzed ROP of e-caprolactone: methane sulfonic acid competes with trifluoromethanesulfonic acid," *Macromolecules,* vol. 41, pp. 3782-3784, 2008.

[53] D. Johns, R. Lenz and A. Luick, "Ring-Opening Polymerization," *Elsevier Applied Science Publishers,* vol. 1, p. 461, 1984.

[54] R. Jerome and P. Teyssie, "Comprehensive Polymer Science," *Pergamon Press,* vol. 3, p. 501, 1989.

[55] A. Tadokoro, T. Takata and T. Endo, *Macromolecules,* vol. 26, pp. 2388-2389, 1993.

[56] M. Hong and E. Chen, *Angew. Chemie - Int Ed.,* vol. 55, pp. 4188-4193, 2016.

[57] M. H. a. E. Y.-X. Chen, "Completely recyclable biopolymers with linear and cyclic topologies via ring-opening polymerization of γ-butyrolactone," *Nature Chemistry,* pp. 1-8, 2015.

[58] M. Hong and . E. Y. X. Chen, *Macromolecules,* vol. 11, p. 3614–3624, 2014.

[59] M. Gagliardi, F. Di Michele, B. Mazzolai and A. Bifone, "Chemical synthesis of a biodegradable PEGylated copolymer from e-caprolactone and gamma-valerolactone: evaluation of reaction and functional properties," *J. Polym. Res.,* vol. 22, no. 17, 2015.

[60] C. Lee, R. Urakawa and Y. Kimura, "Copolymerization of gamma-valerolactone and beta-butyrolactone," *Eur. Polym. J.,* vol. 34, pp. 117-122, 1998.

[61] J. Undin, P. Ólsen, J. Godfrey, K. Odelius and A.-C. Albertsson, "Controlled Copolymerization of the functional 5-membered lactone monomer, alfa-bromo-gamma-butyrolactone, via selective organocatalysis," *Polymer,* no. 87, pp. 17-25, 2016.

[62] J. Campos, M. Ribeiro, M. Ribeiro, A. Deffieux and F. Peruch, "A new insight into the mechanism of the ring-opening polymerization of trimethylene carbonate catalyzed by methanesulfonic acid," *Macrom. Chem. Phys.,* vol. 214, pp. 85-93, 2013.

[63] J. Campos, M. Ribeiro, M. Ribeiro, A. Deffieux and F. Peruch, "Copoolimerisation of e-caprolactone and trimethylene carbonate catalysed by methanesulfonic acid," *European Polymer Journal,* vol. 49, pp. 4025-4034, 2013.

[64] "http://www.chemistryviews.org/details/education/3728881/Tips_and_Tricks_for_the_Lab_Air-Sensitive_Techniques_1.html," [Online]. [Accessed 14 November 2016].

Appendix A

^{1}H NMR SPECTRA

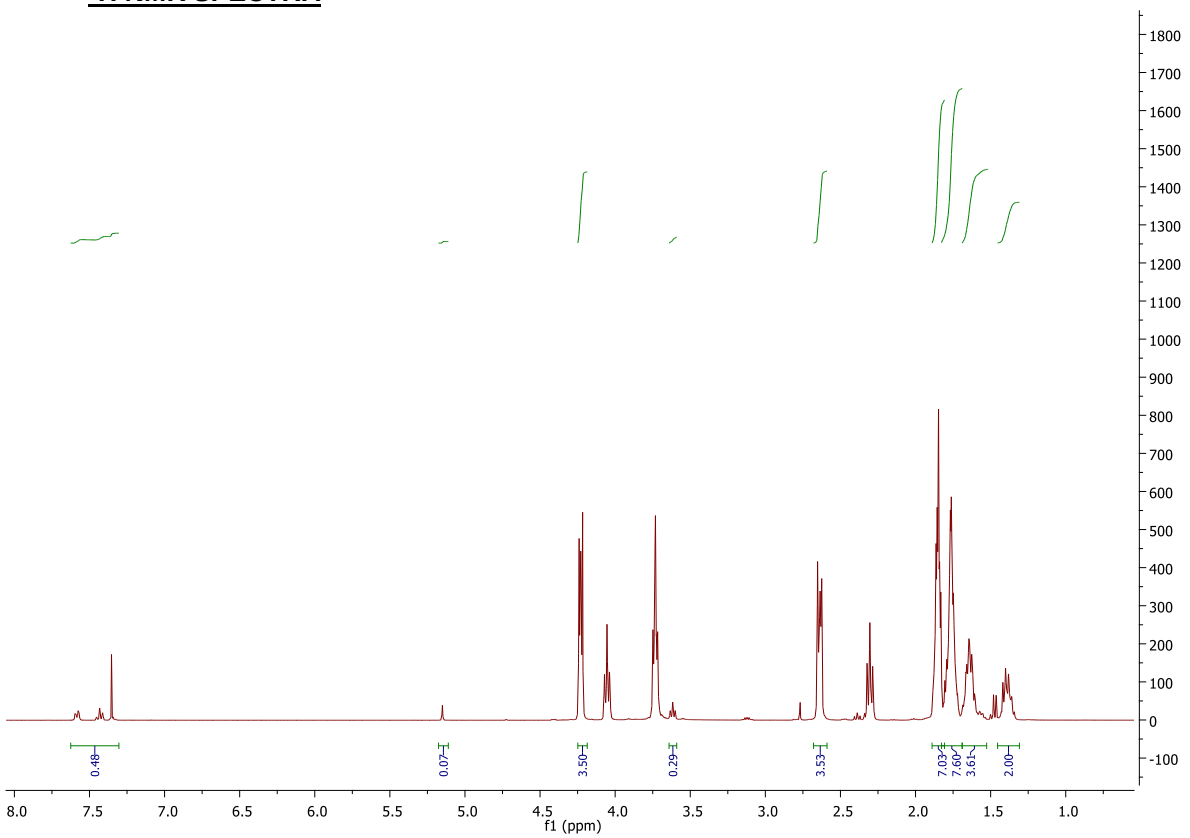

Figure A. 1 - ^{1}H NMR spectrum of the poly Ɛ-CL of the crude sample (Run 3, Table 2), with integration peaks.

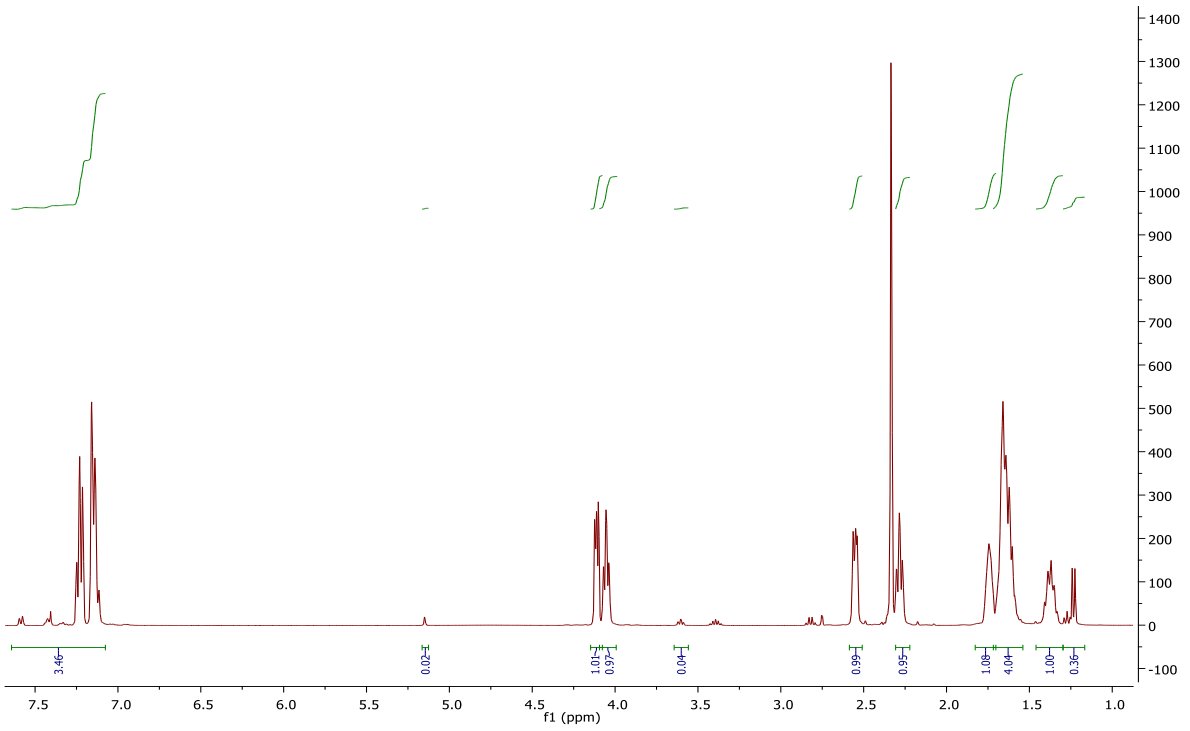

Figure A. 2 - ^{1}H NMR spectrum of the poly Ɛ-CL of the crude sample (Run 4, Table 2), with integration peaks.

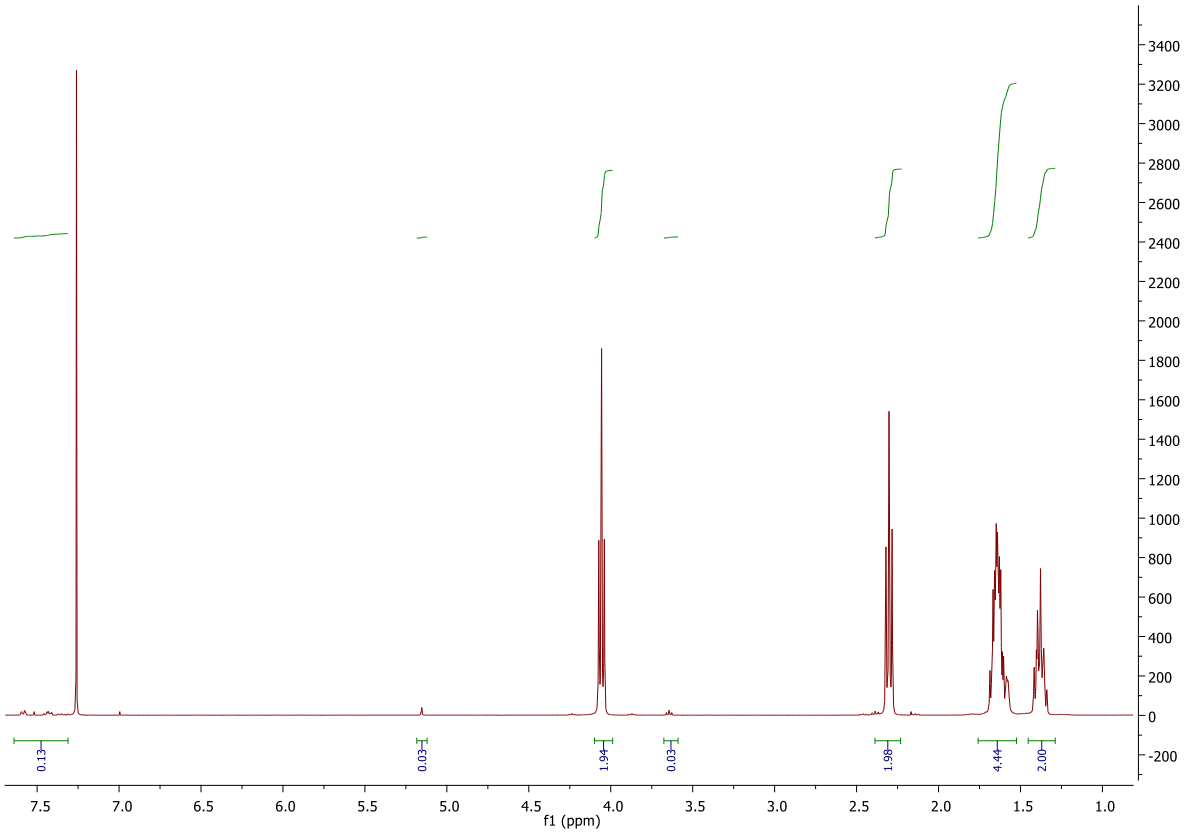

Figure A. 3 - ^{1}H NMR spectrum of the poly Ɛ-CL of the pure sample (Run 5, Table 2), with integration peaks.

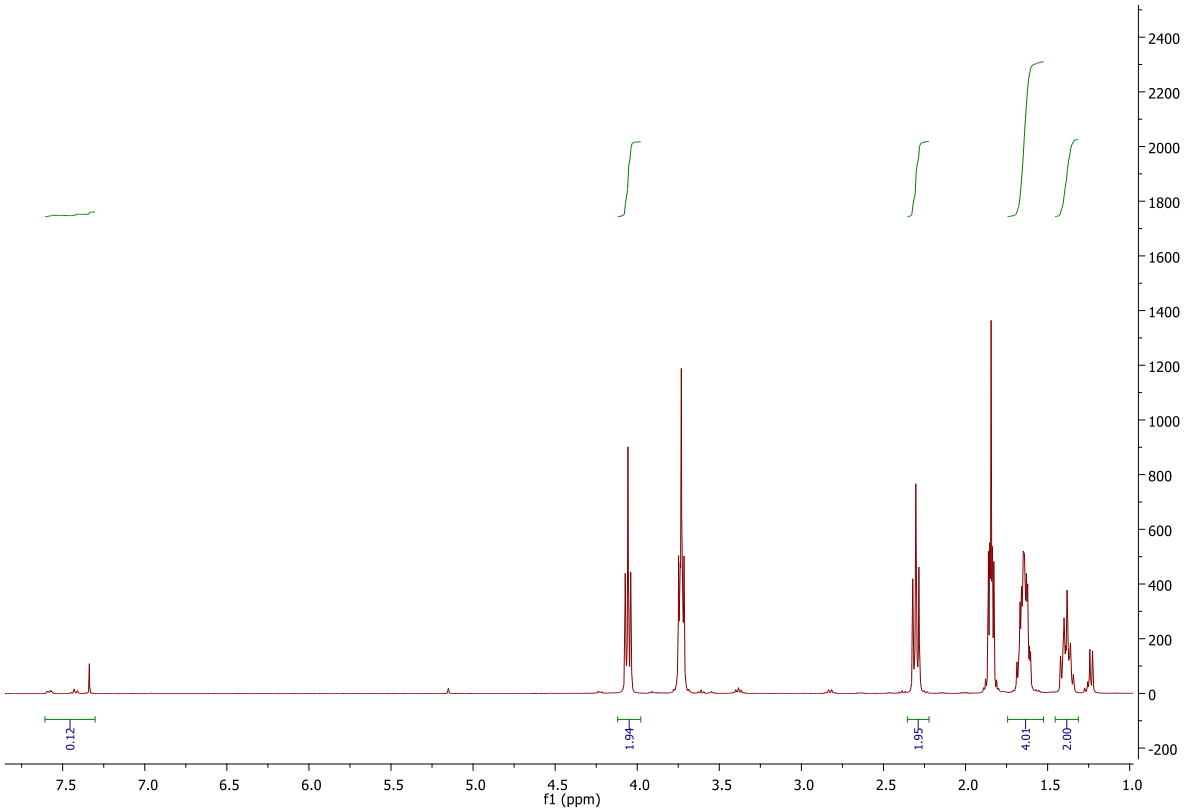

Figure A. 4 - ^{1}H NMR spectrum of the poly Ɛ-CL of the crude sample (Run 6, Table 2), with integration peaks.

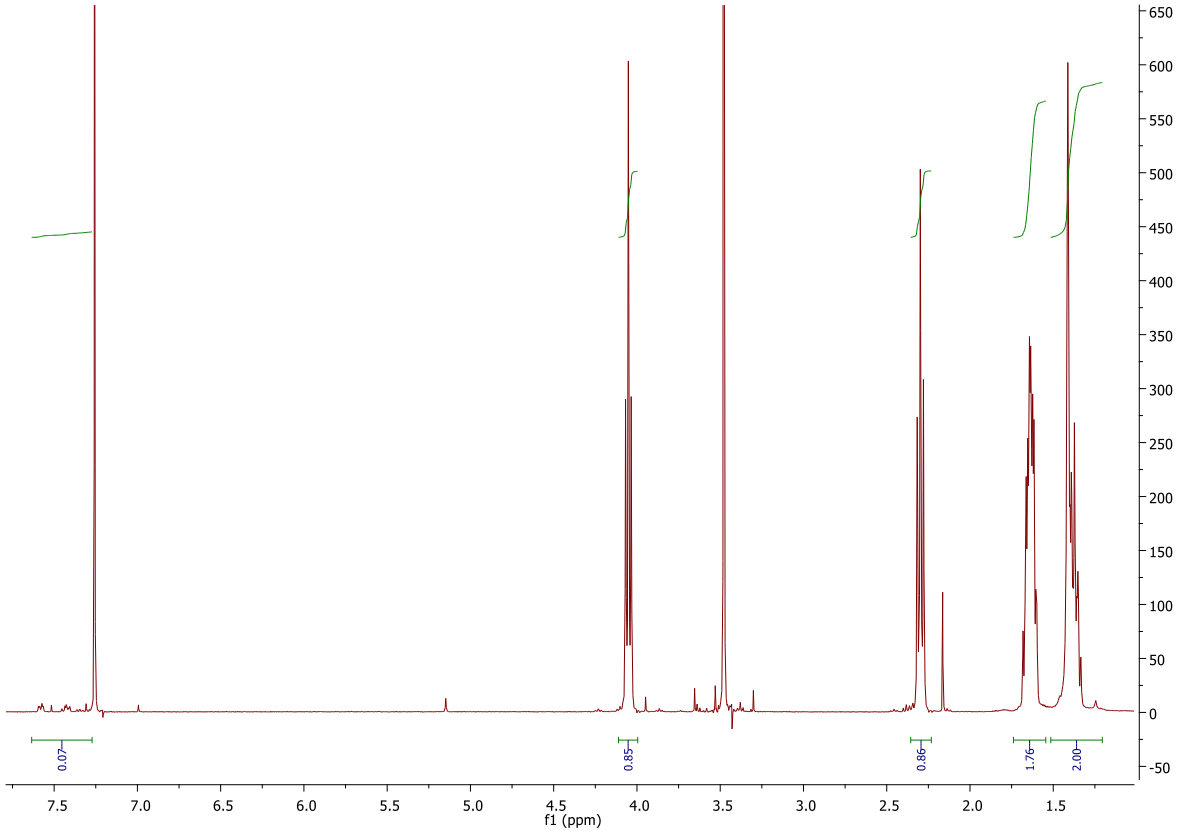

Figure A. 5 - ^{1}H NMR spectrum of the poly Ɛ-CL of the pure sample (Run 6, Table 2), with integration peaks.

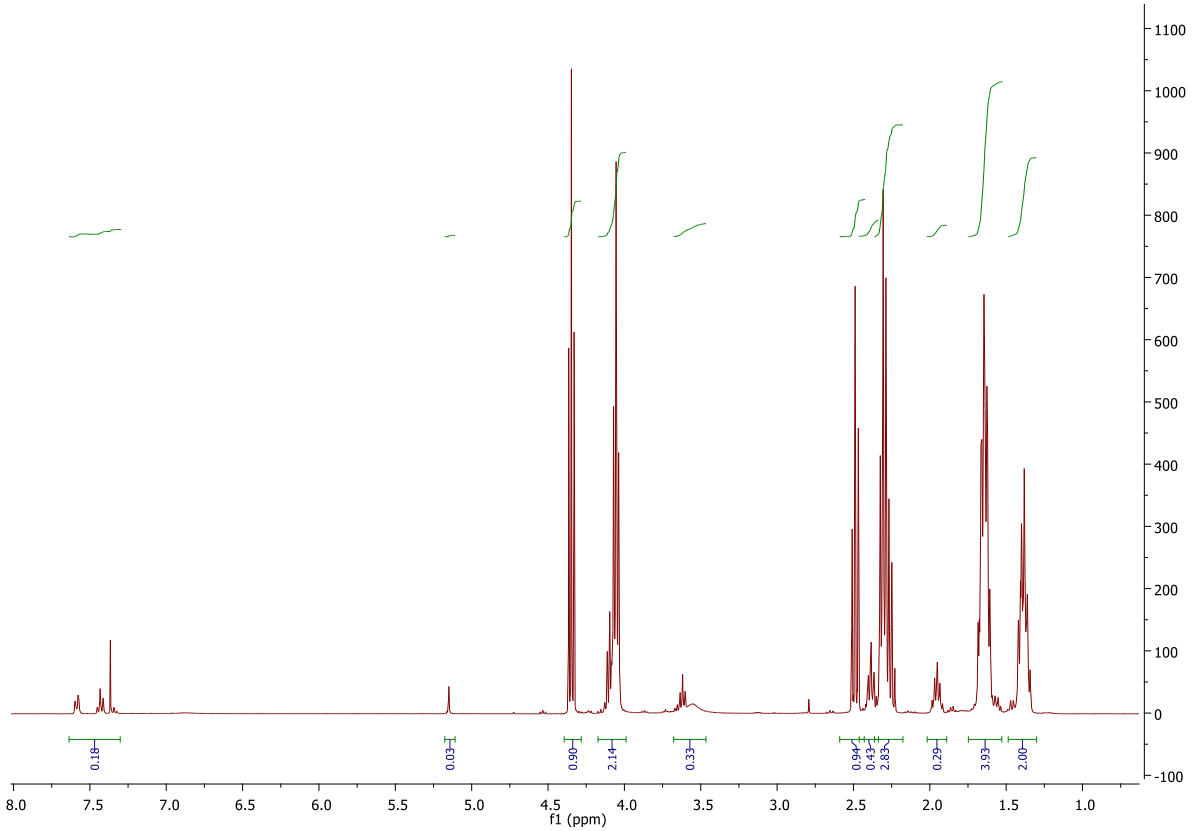

Figure A. 6 - ^{1}H NMR spectrum of the copolymer Ɛ-CL and ɣ-BL of the crude sample (Run 2, Table 3), with integration peaks.

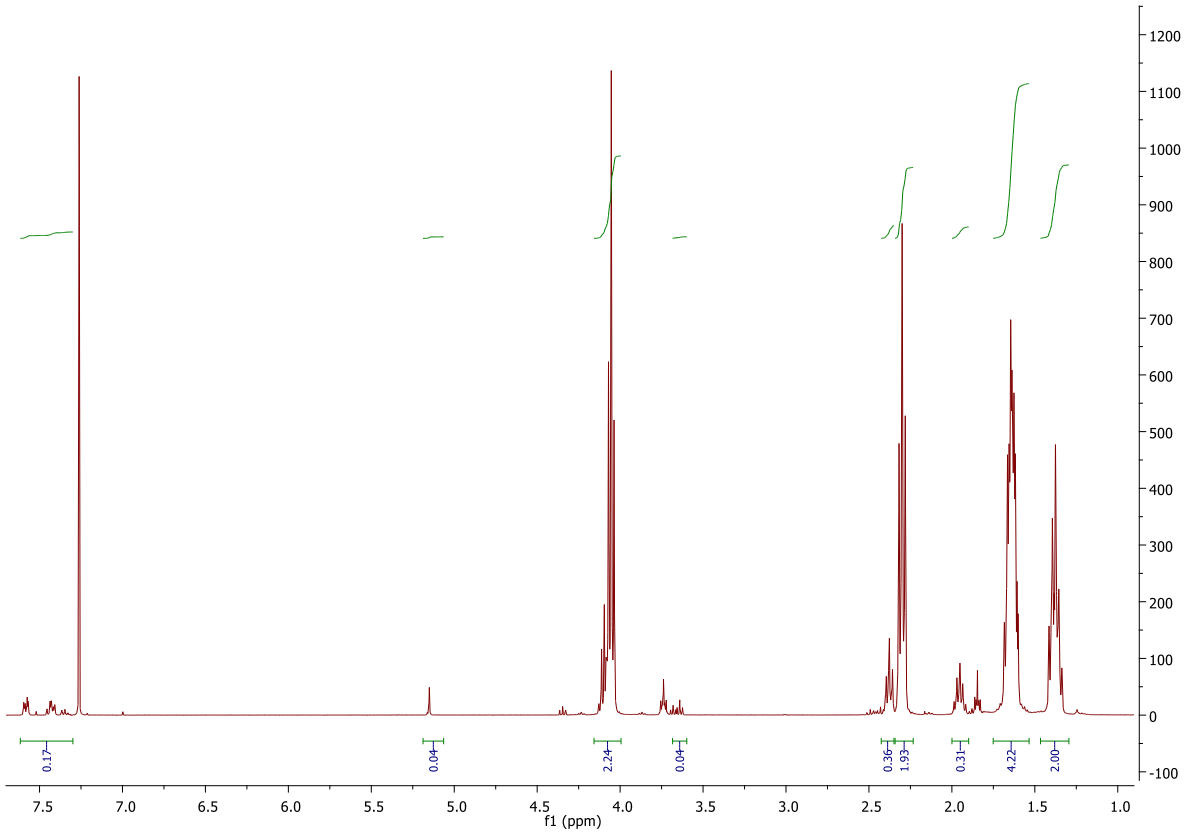

Figure A. 7 - ^{1}H NMR spectrum of the copolymer Ɛ-CL and ɣ-BL of the pure sample (Run 2, Table 3), with integration peaks.

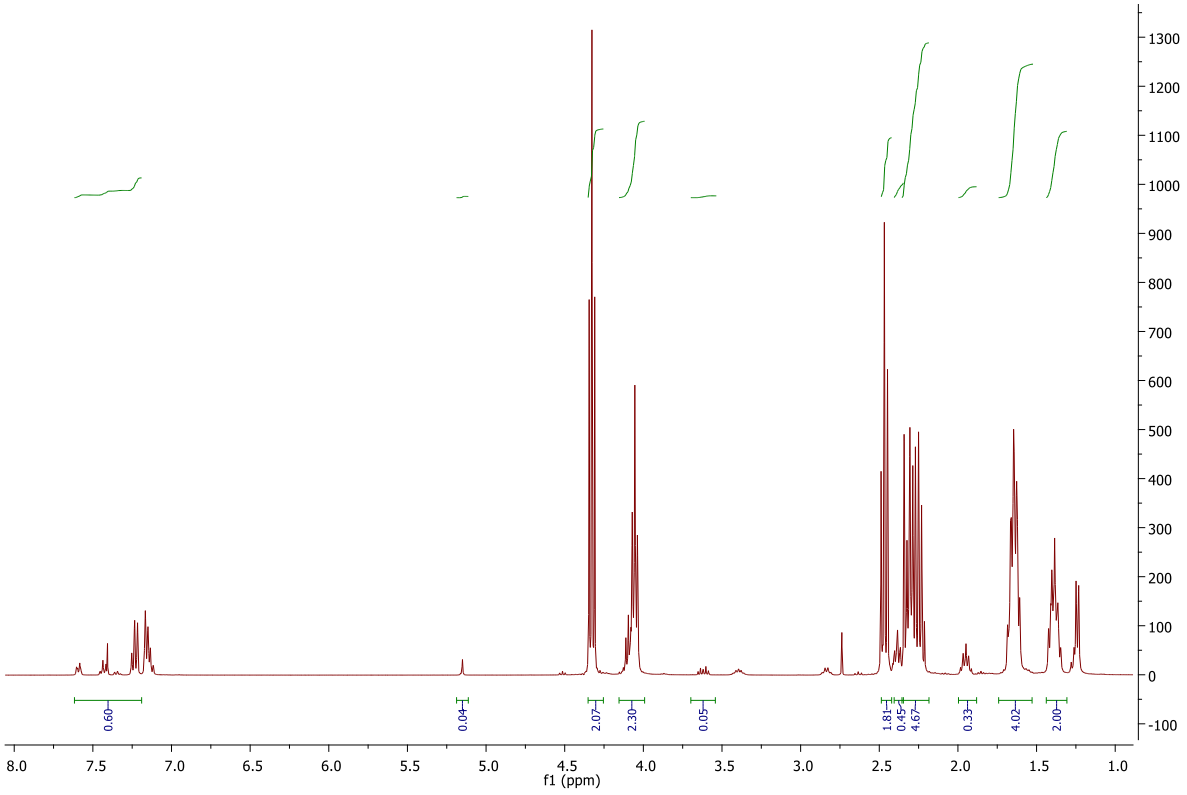

Figure A. 8 - ^{1}H NMR spectrum of the copolymer Ɛ-CL and ɣ-BL of the crude sample (Run 1, Table 3), with integration peaks.

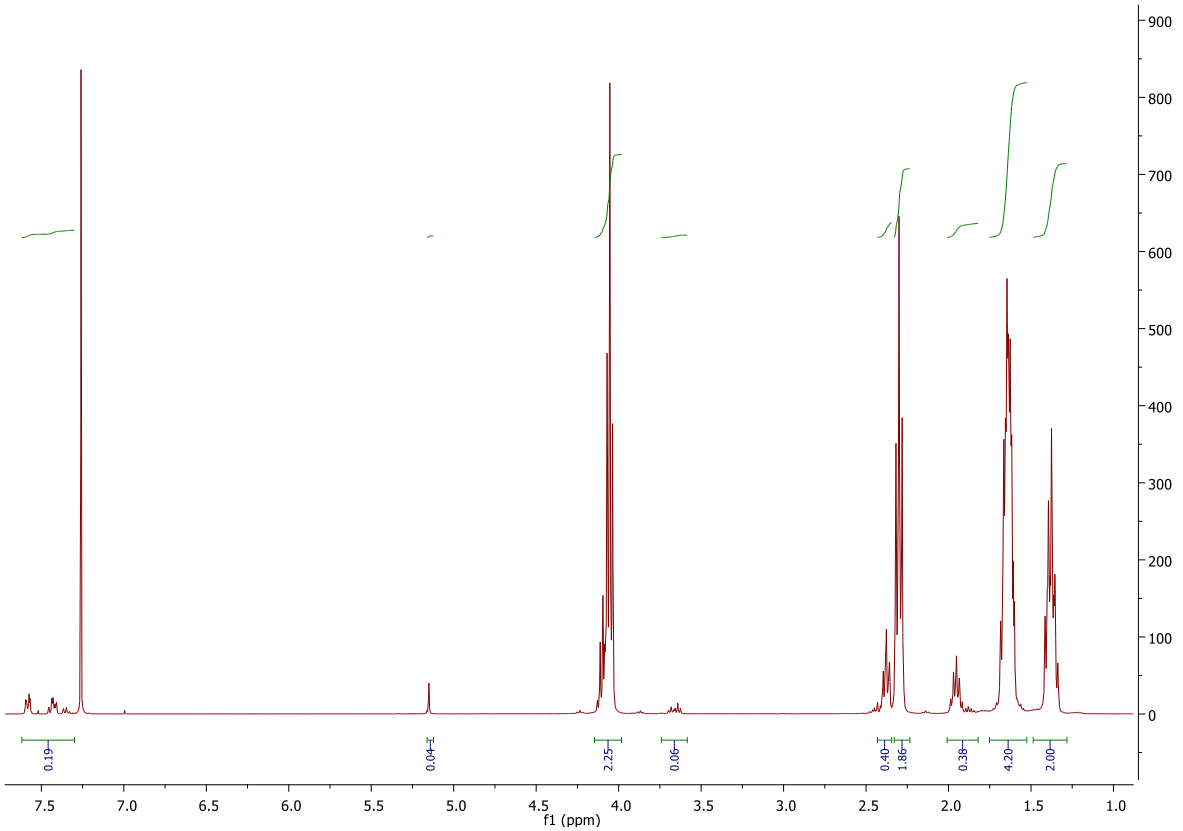

Figure A. 9 - ^{1}H NMR spectrum of the copolymer Ɛ-CL and ɣ-BL of the pure sample (Run 1, Table 3), with integration peaks.

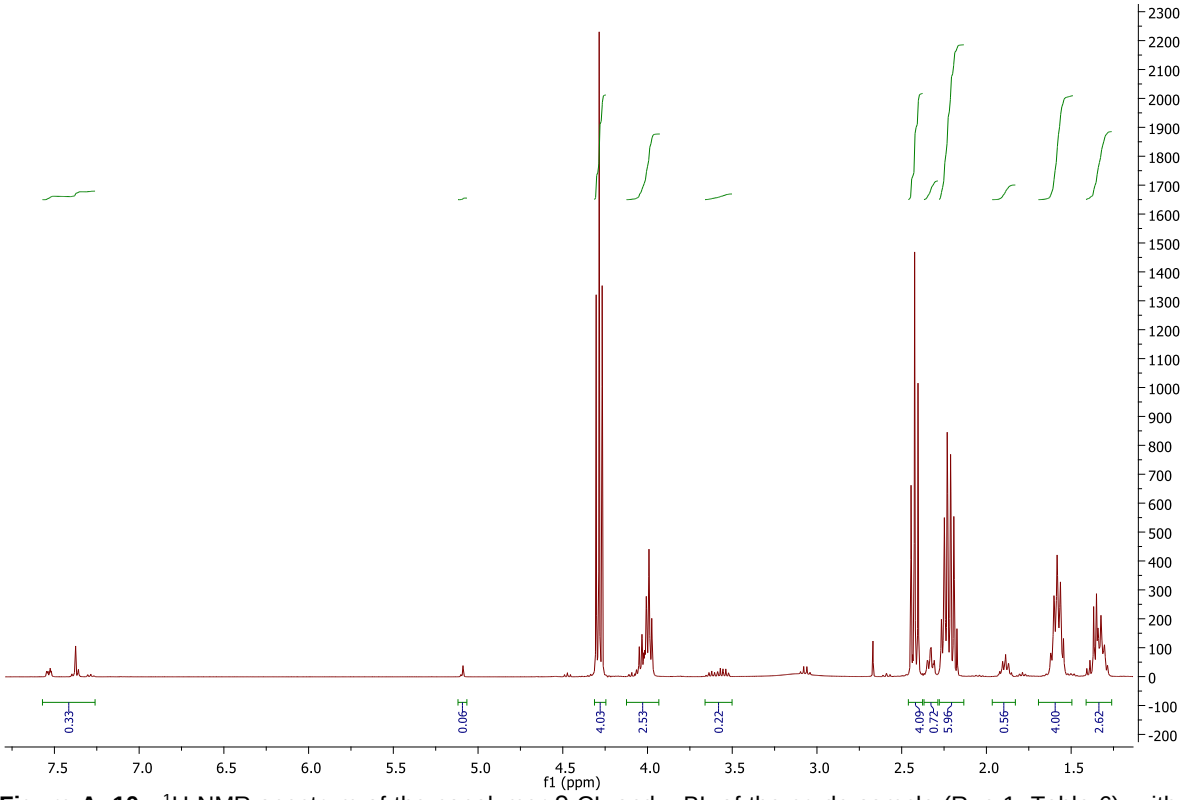

Figure A. 10 - ^{1}H NMR spectrum of the copolymer Ɛ-CL and ɣ-BL of the crude sample (Run 1, Table 6), with integration peaks.

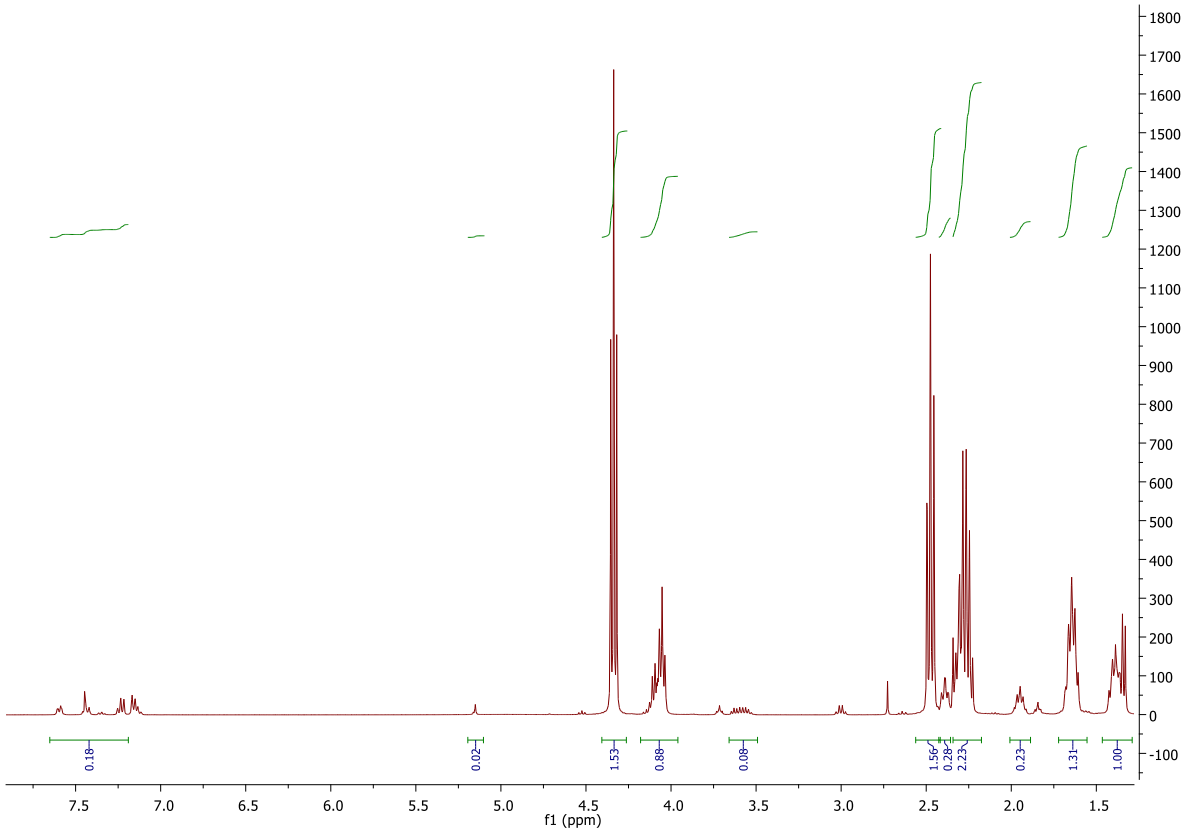

Figure A. 11 - ^{1}H NMR spectrum of the copolymer Ɛ-CL and ɣ-BL of the crude sample (Run 1.1, Table 6), with integration peaks.

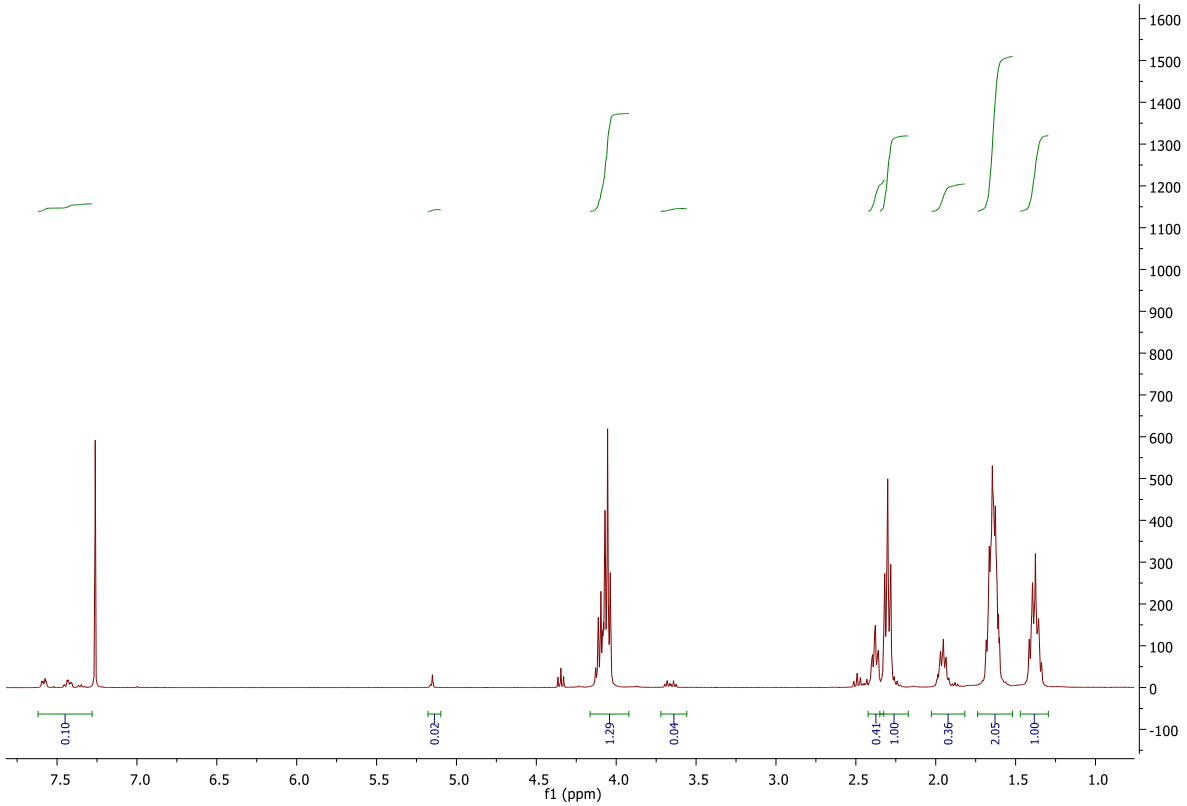

Figure A. 12 - ^{1}H NMR spectrum of the copolymer Ɛ-CL and ɣ-BL of the pure sample (Run 1.1, Table 6), with integration peaks.

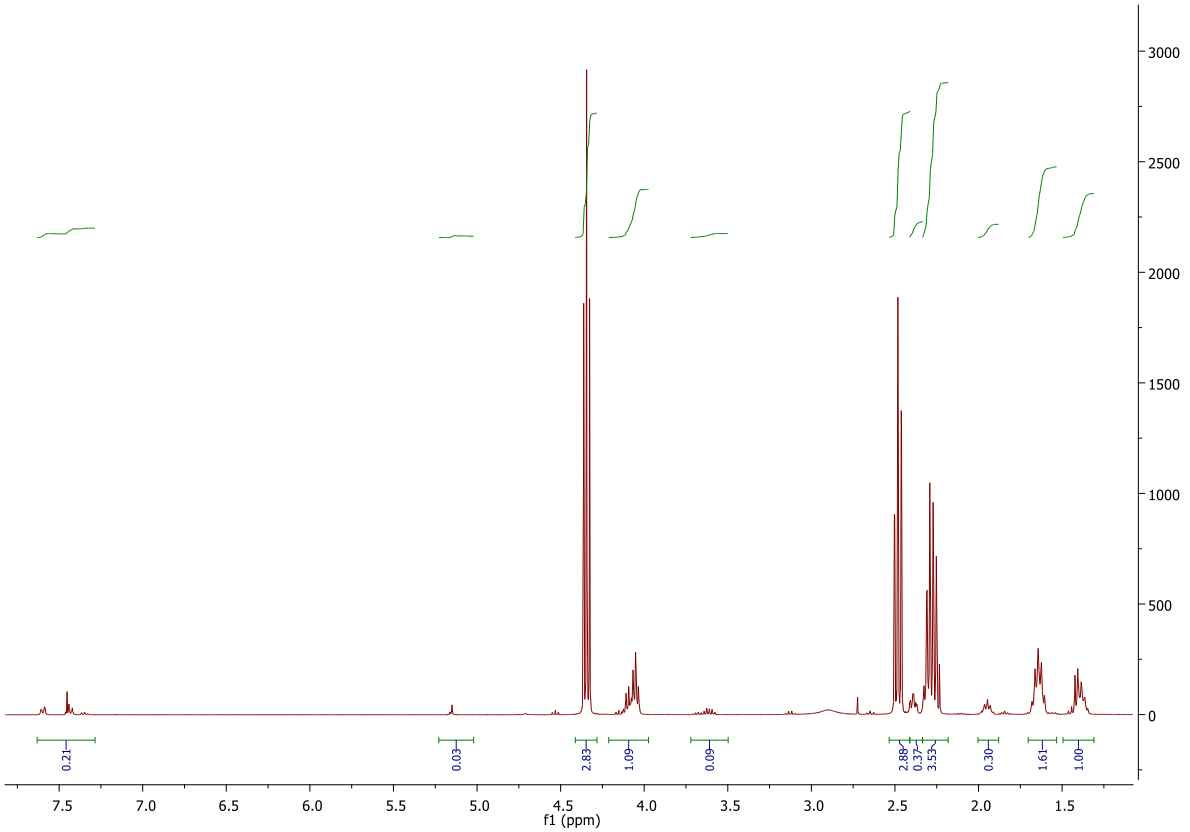

Figure A. 13 - ^{1}H NMR spectrum of the copolymer Ɛ-CL and ɣ-BL of the crude sample (Run 2, Table 6), with integration peaks.

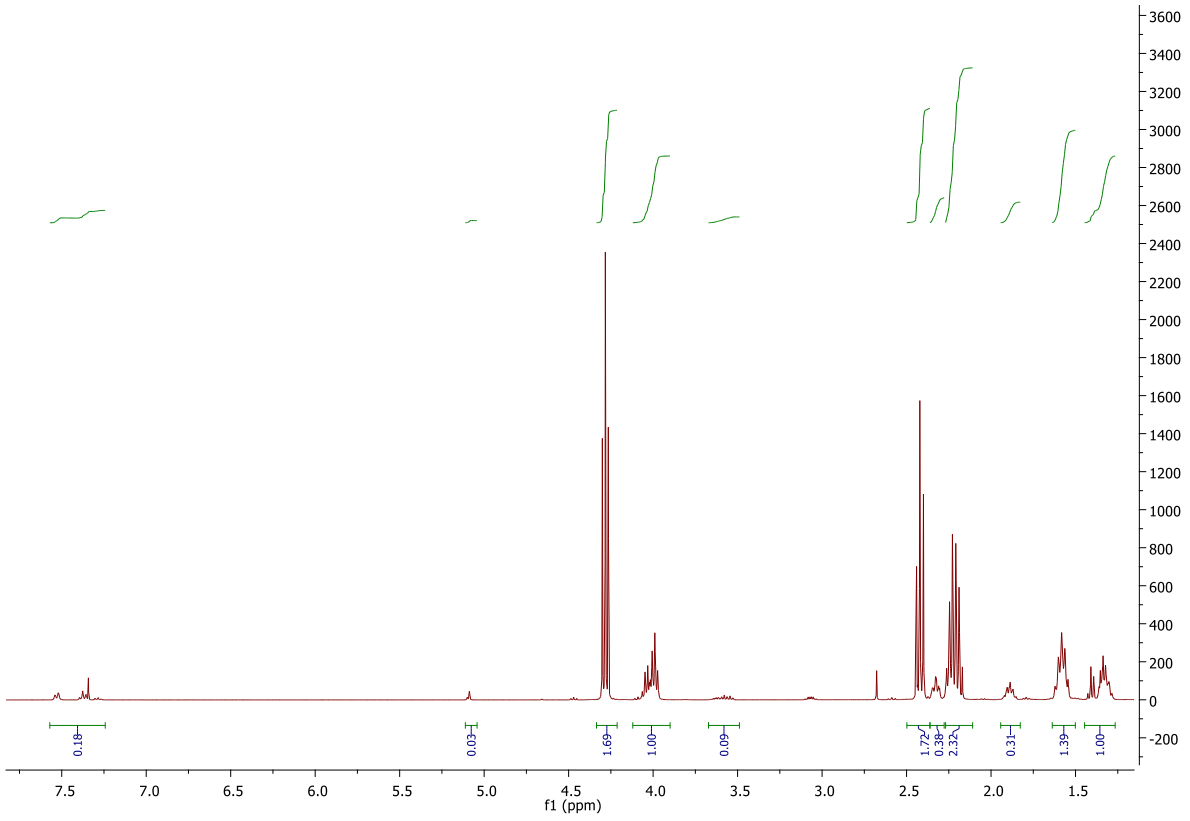

Figure A. 14 - ^{1}H NMR spectrum of the copolymer Ɛ-CL and ɣ-BL of the pure sample (Run 2.1, Table 6), with integration peaks.

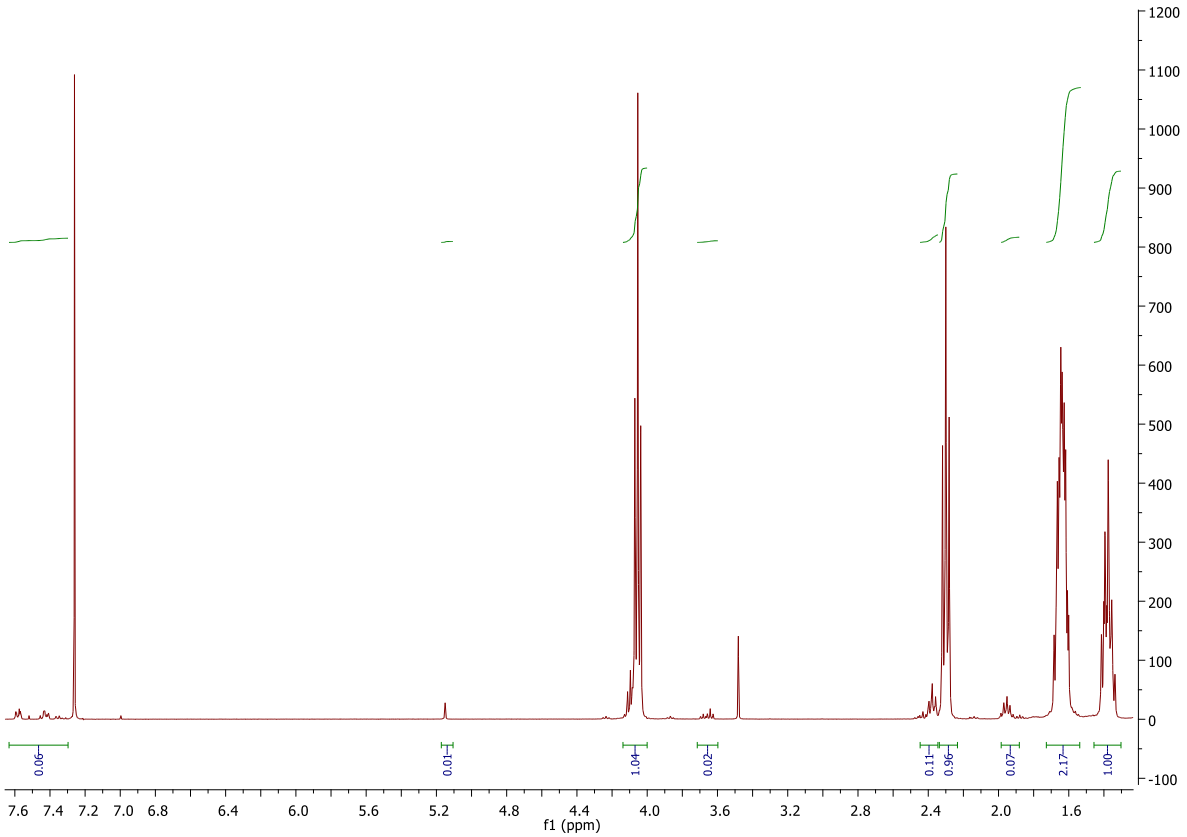

Figure A. 15 - ^{1}H NMR spectrum of the copolymer Ɛ-CL and ɣ-BL of the crude sample (Run 1, Table 7), with integration peaks.

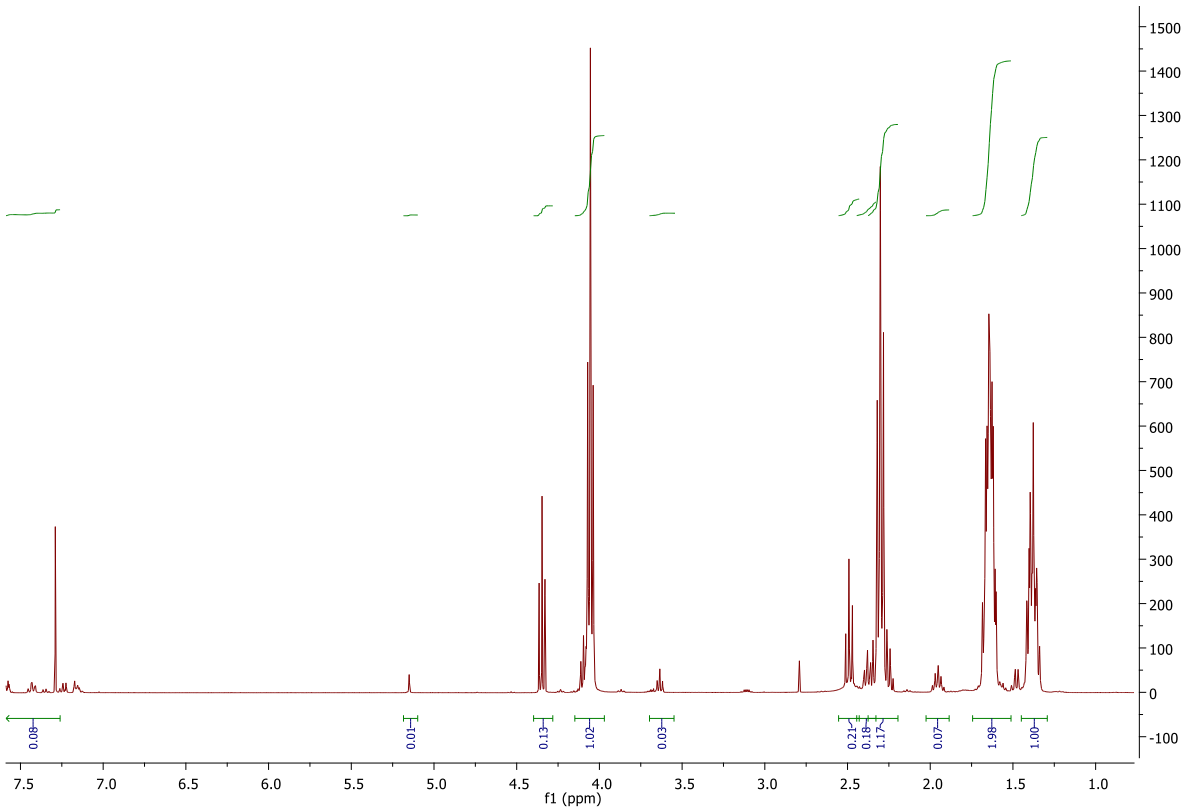

Figure A. 16 - ^{1}H NMR spectrum of the copolymer Ɛ-CL and ɣ-BL of the crude sample (Run 2, Table 7), with integration peaks.

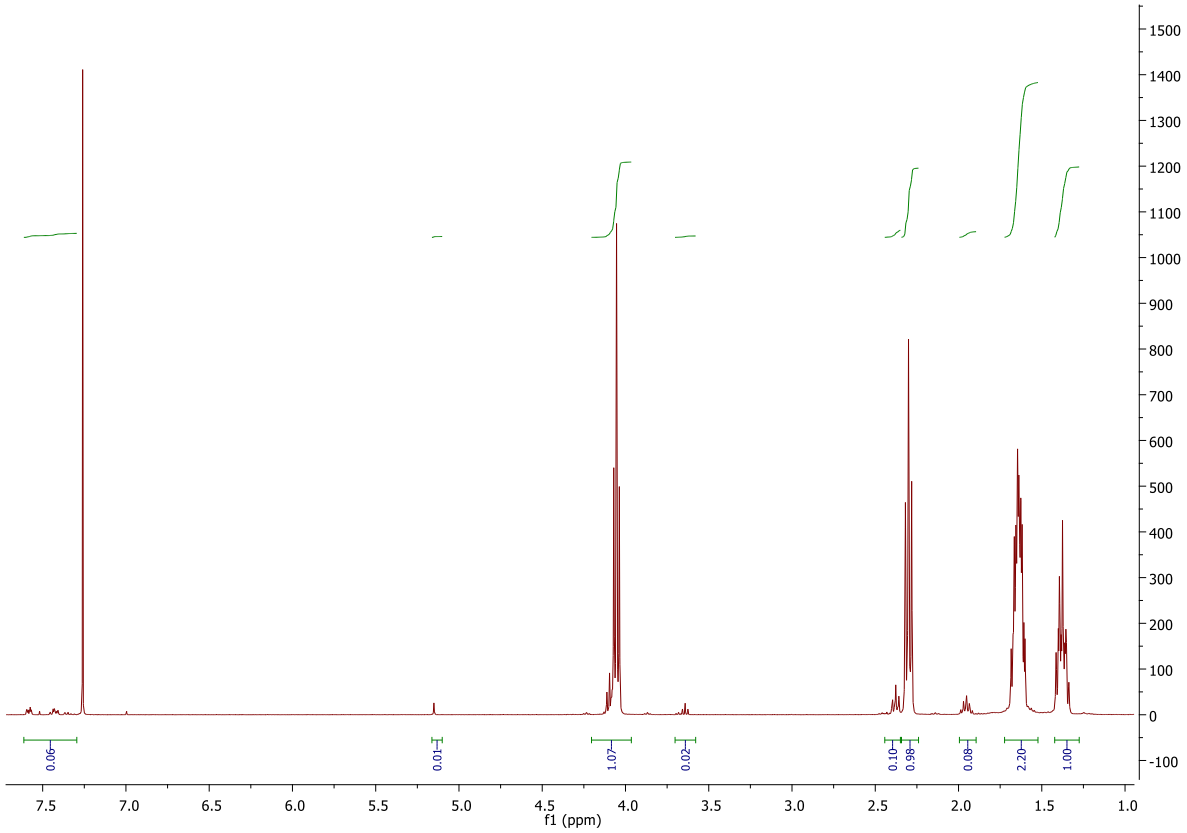

Figure A. 17 - ^{1}H NMR spectrum of the copolymer Ɛ-CL and ɣ-BL of the pure sample (Run 2, Table 7), with integration peaks.

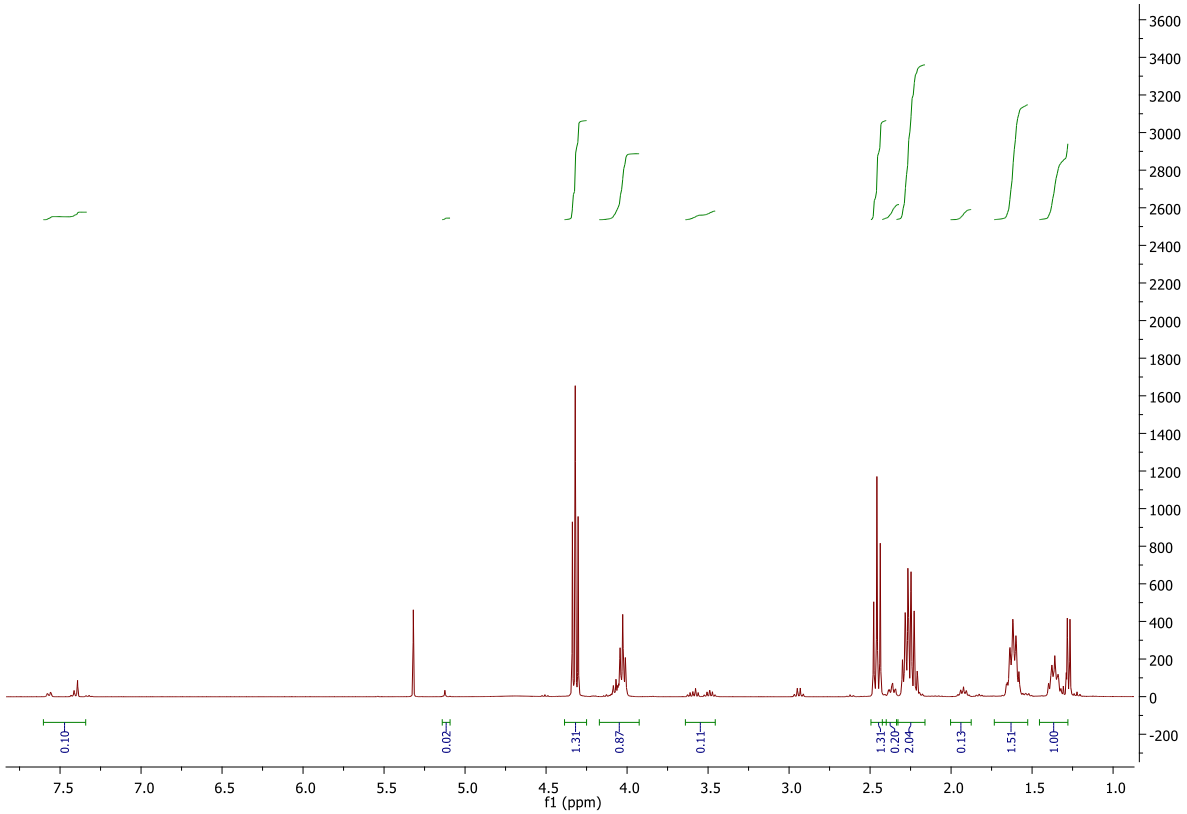

Figure A. 18 - ^{1}H NMR spectrum of the copolymer Ɛ-CL and ɣ-BL of the crude sample (Run 1, Table 8), with integration peaks.

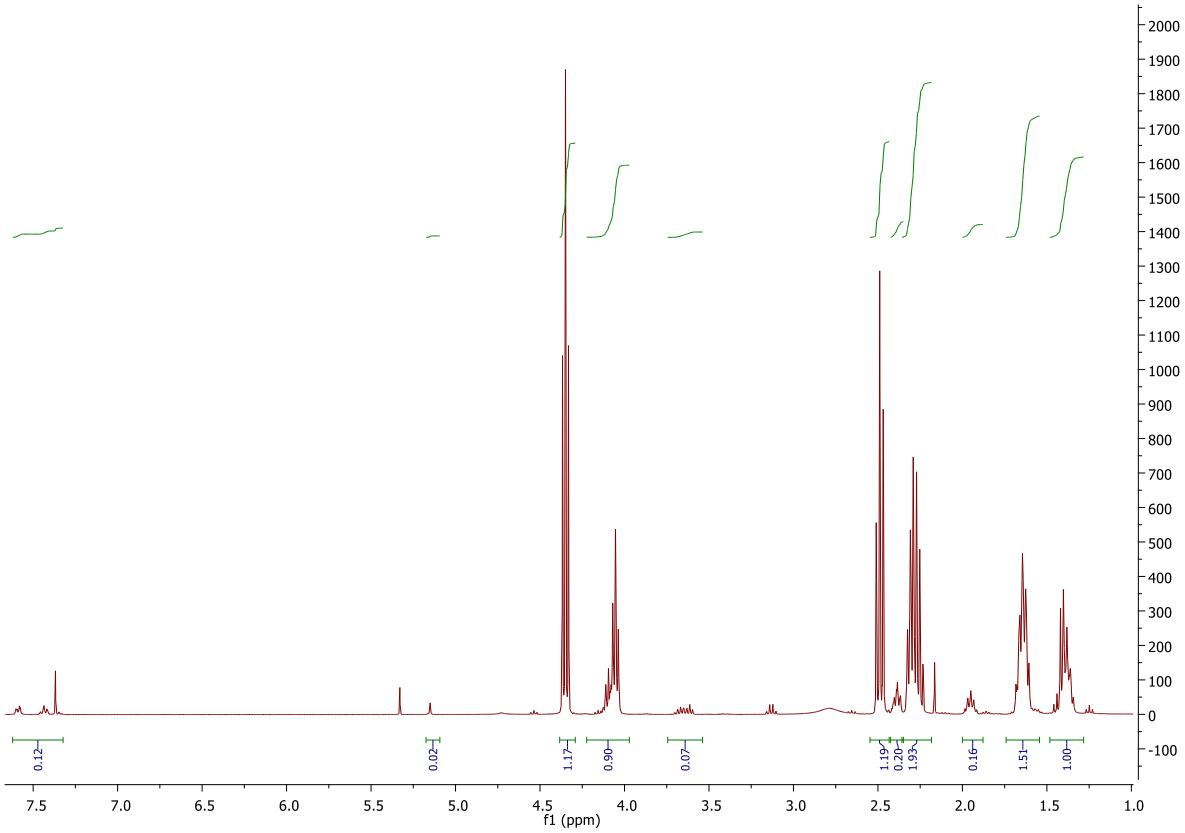

Figure A. 20 - ^{1}H NMR spectrum of the copolymer Ɛ-CL and ɣ-BL of the crude sample (Run 2, Table 8), with integration peaks.

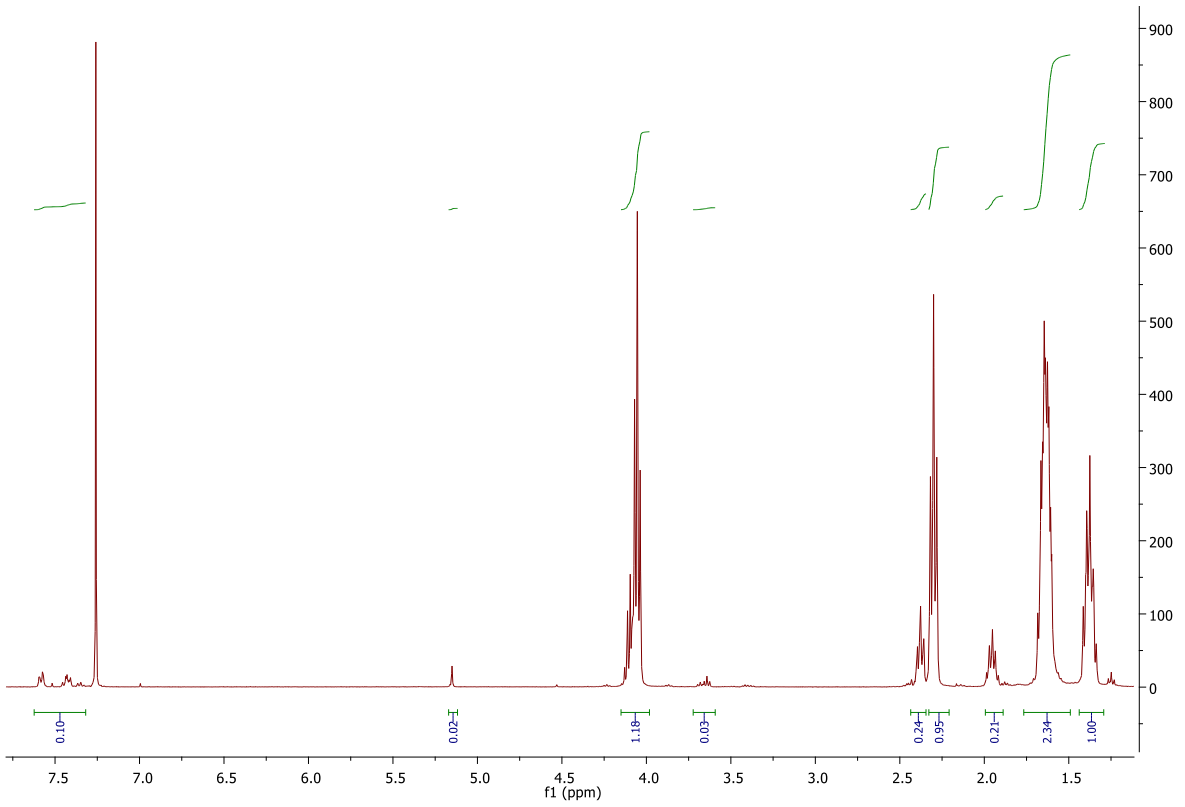

Figure A. 19 - ^{1}H NMR spectrum of the copolymer Ɛ-CL and ɣ-BL of the crude sample (Run 2, Table 8), with integration peaks.

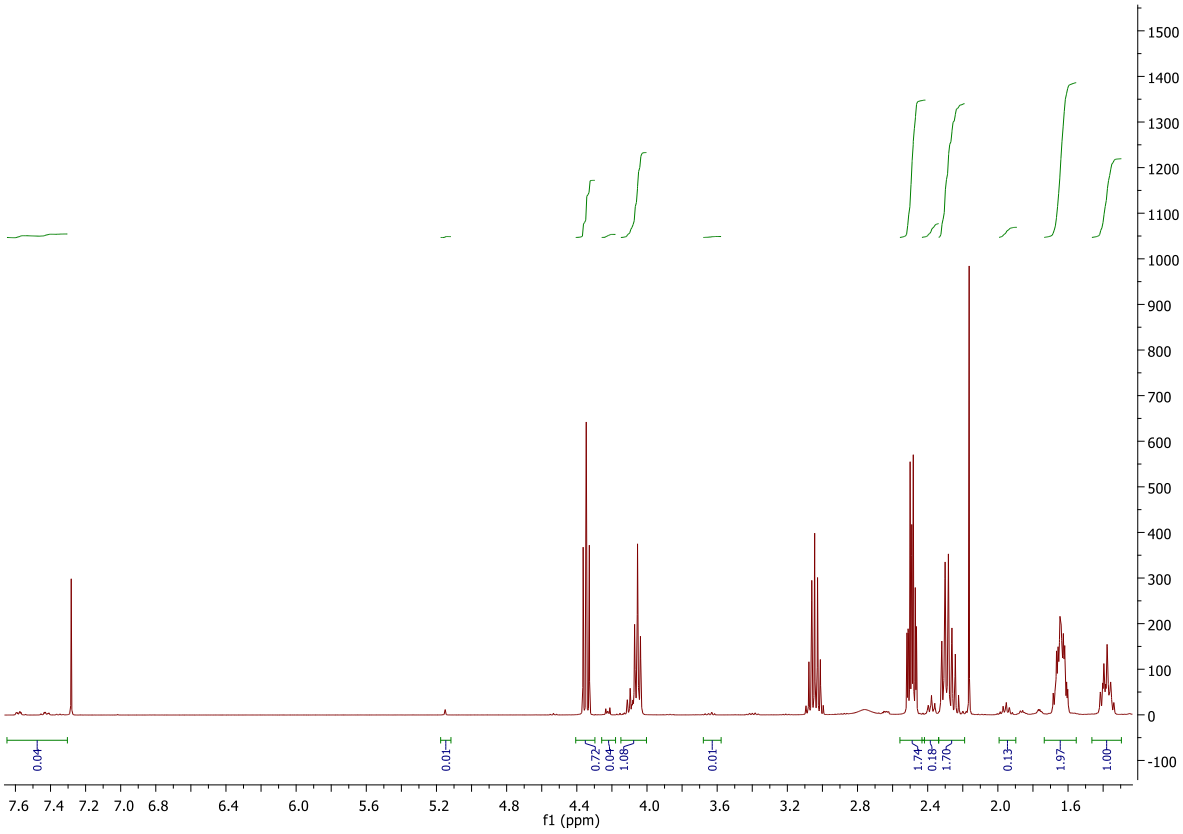

Figure A. 21 - ^{1}H NMR spectrum of the copolymer Ɛ-CL and ɣ-BL of the crude sample (Run 1, Table 9), with integration peaks.

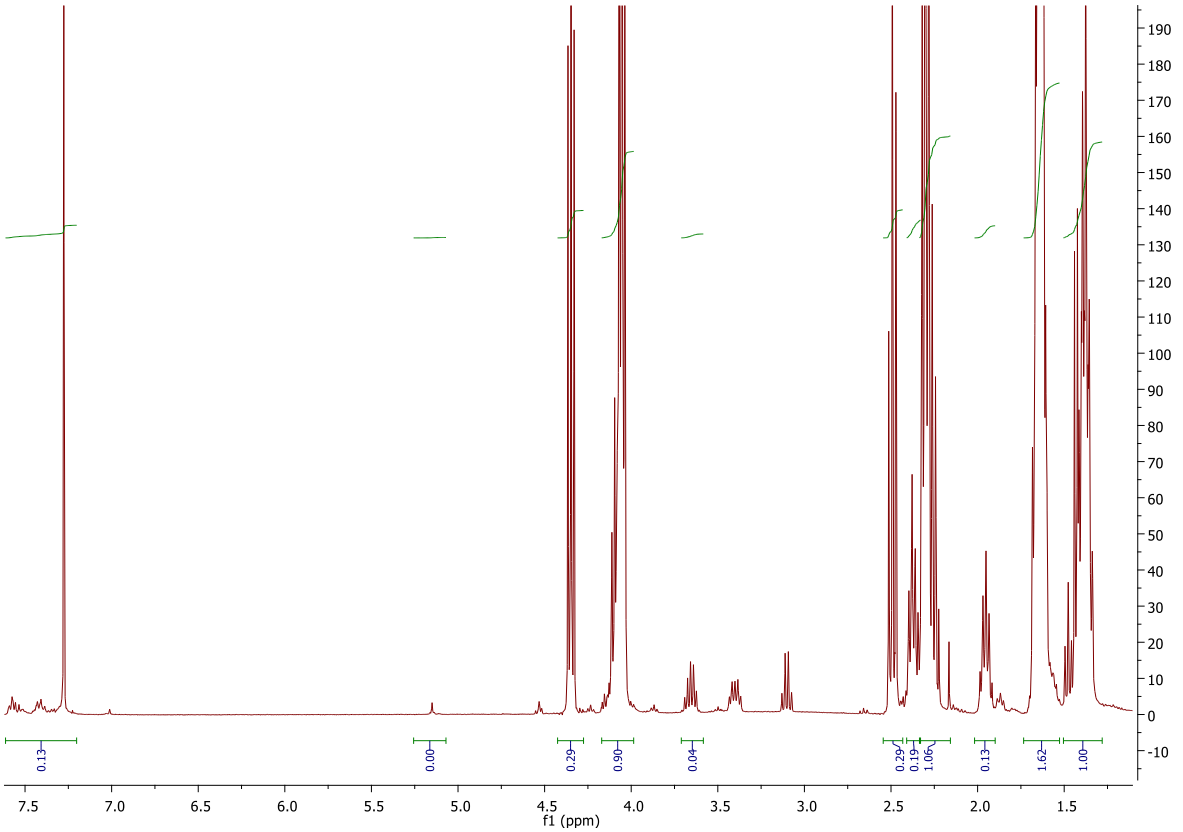

Figure A. 22 - ^{1}H NMR spectrum of the copolymer Ɛ-CL and ɣ-BL of the crude sample (Run 2, Table 9), with integration peaks.

k

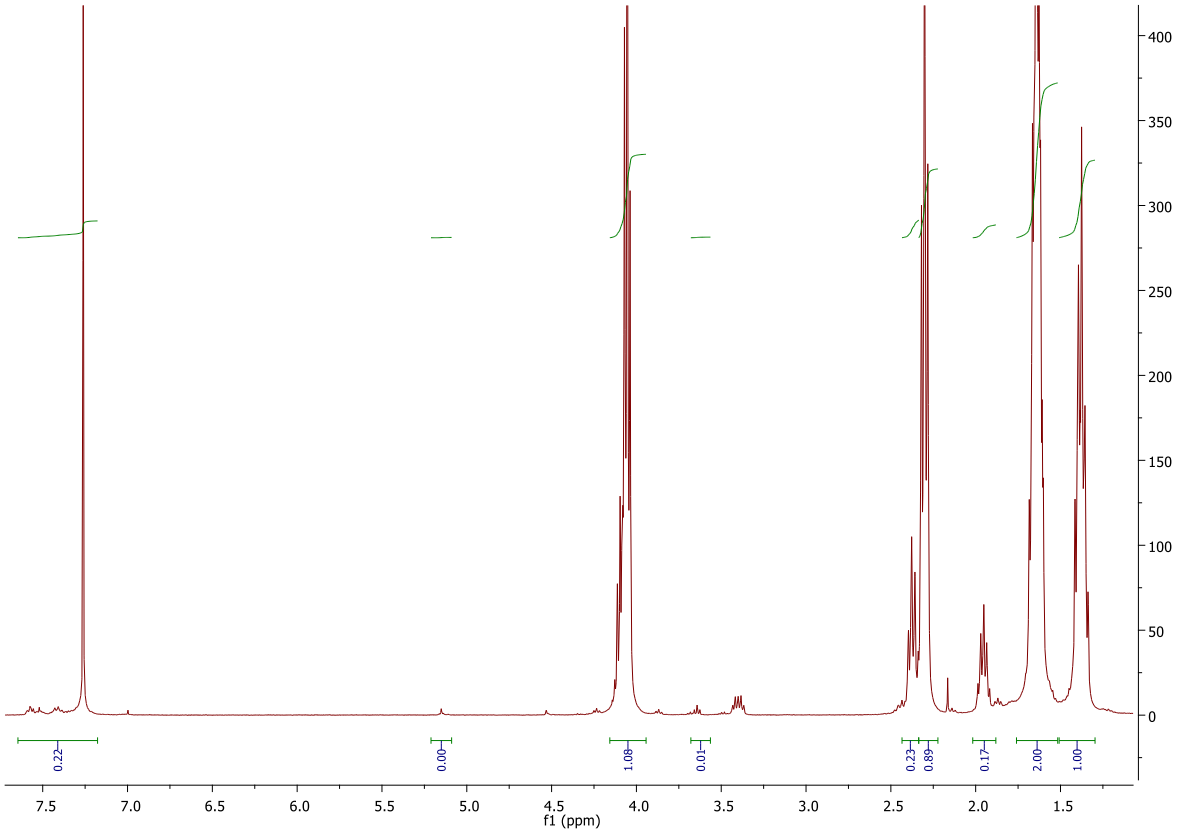

Figure A. 23 - ^{1}H NMR spectrum of the copolymer Ɛ-CL and ɣ-BL of the pure sample (Run 2, Table 9), with integration peaks.

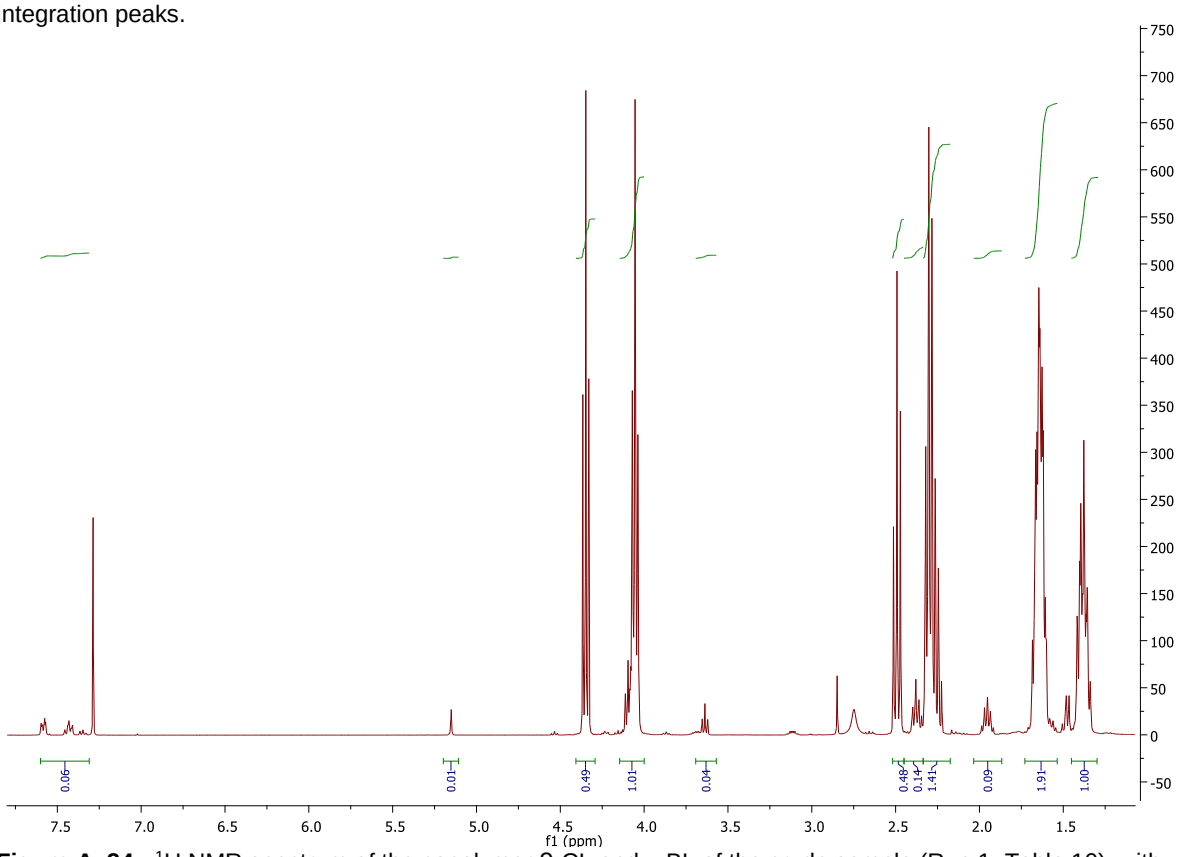

Figure A. 24 - ^{1}H NMR spectrum of the copolymer Ɛ-CL and ɣ-BL of the crude sample (Run 1, Table 10), with integration peaks.

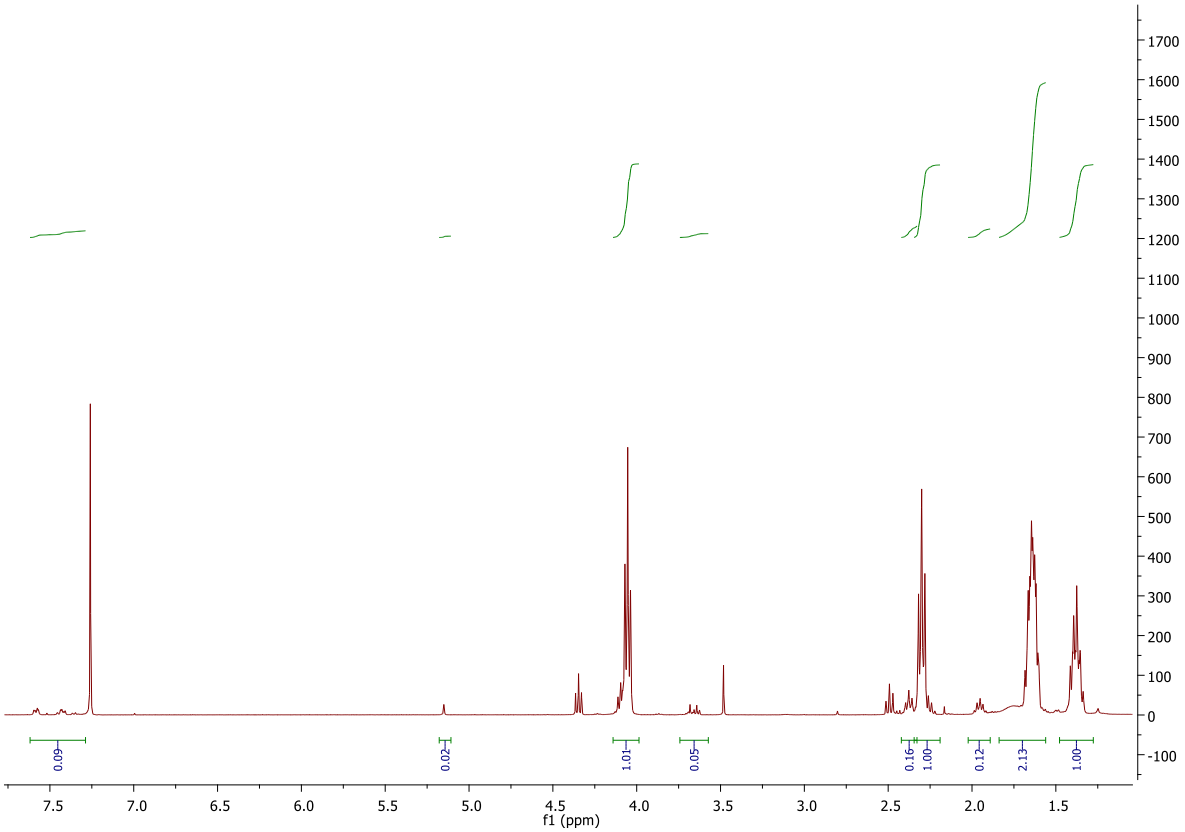

Figure A. 25 - ^{1}H NMR spectrum of the copolymer Ɛ-CL and ɣ-BL of the pure sample (Run 1, Table 10), with integration peaks.

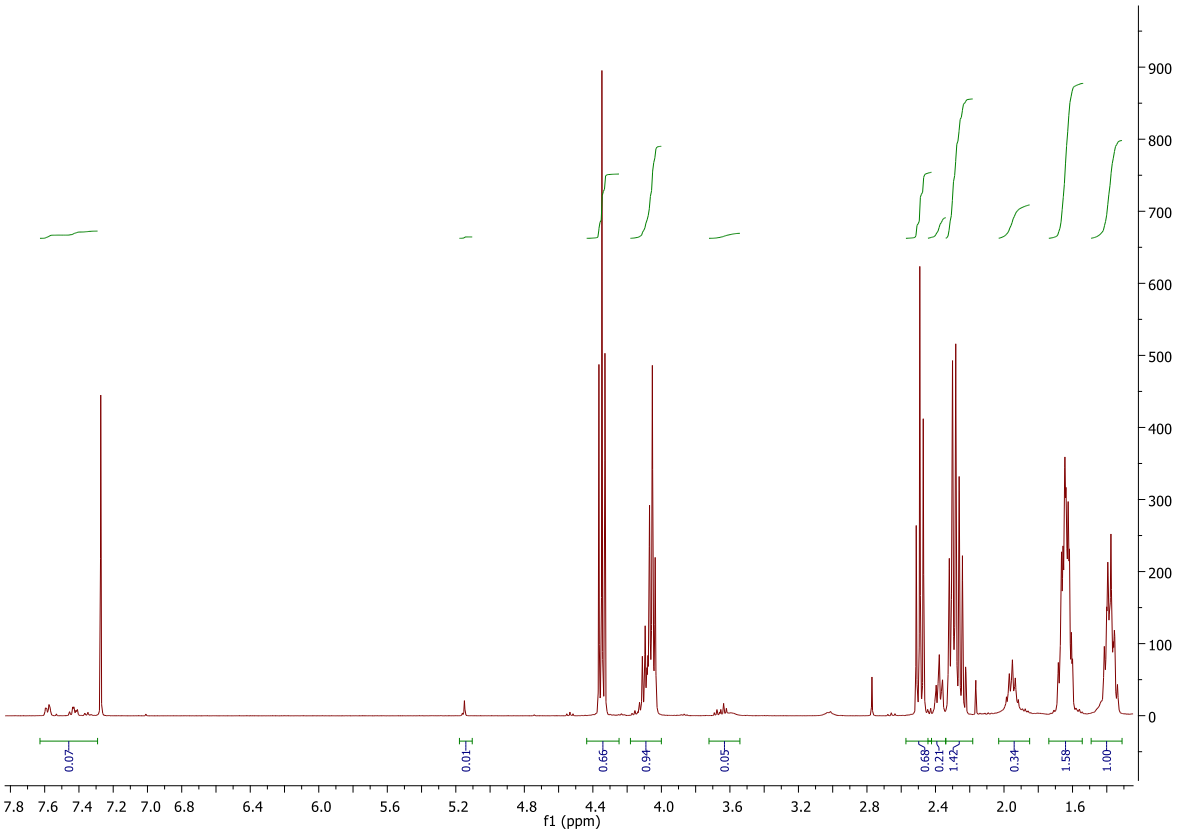

Figure A. 26 - ^{1}H NMR spectrum of the copolymer Ɛ-CL and ɣ-BL of the crude sample (Run 2, Table 10), with integration peaks.

m

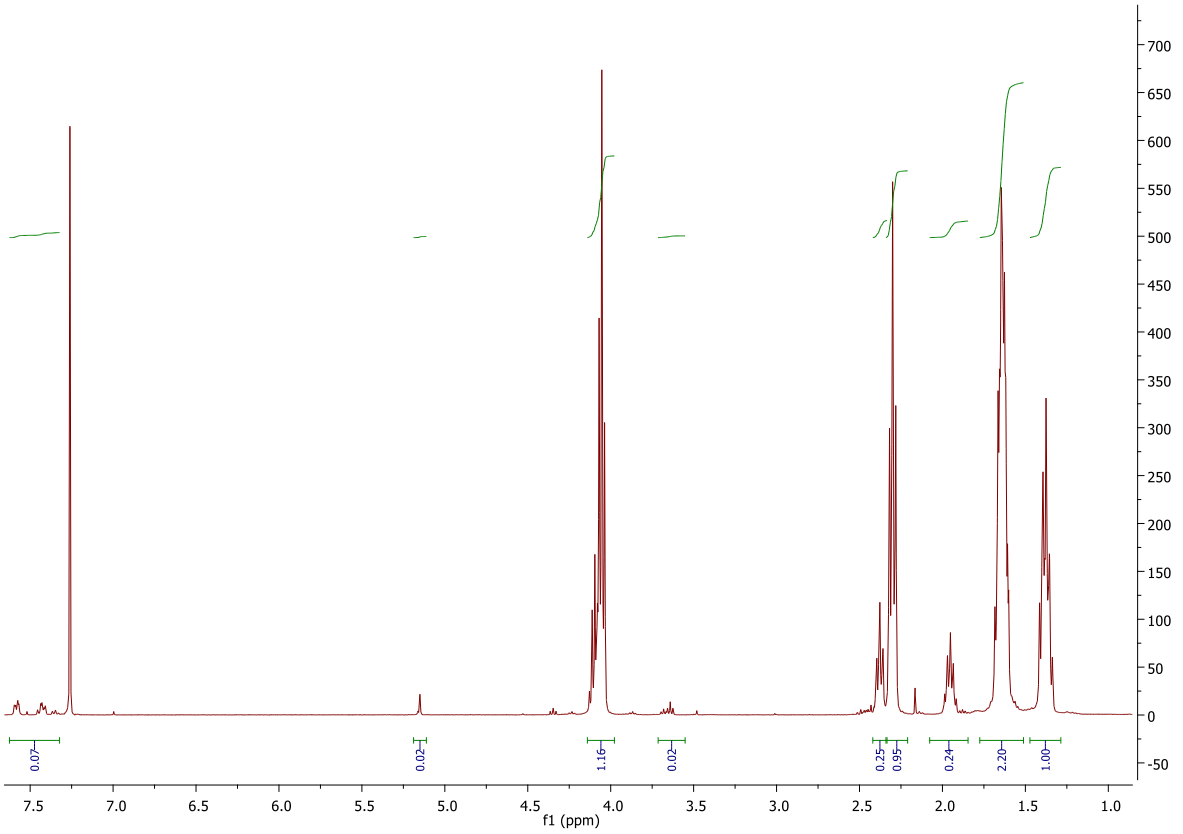

Figure A. 28 - ^{1}H NMR spectrum of the copolymer Ɛ-CL and ɣ-BL of the pure sample (Run 2, Table 10), with integration peaks.

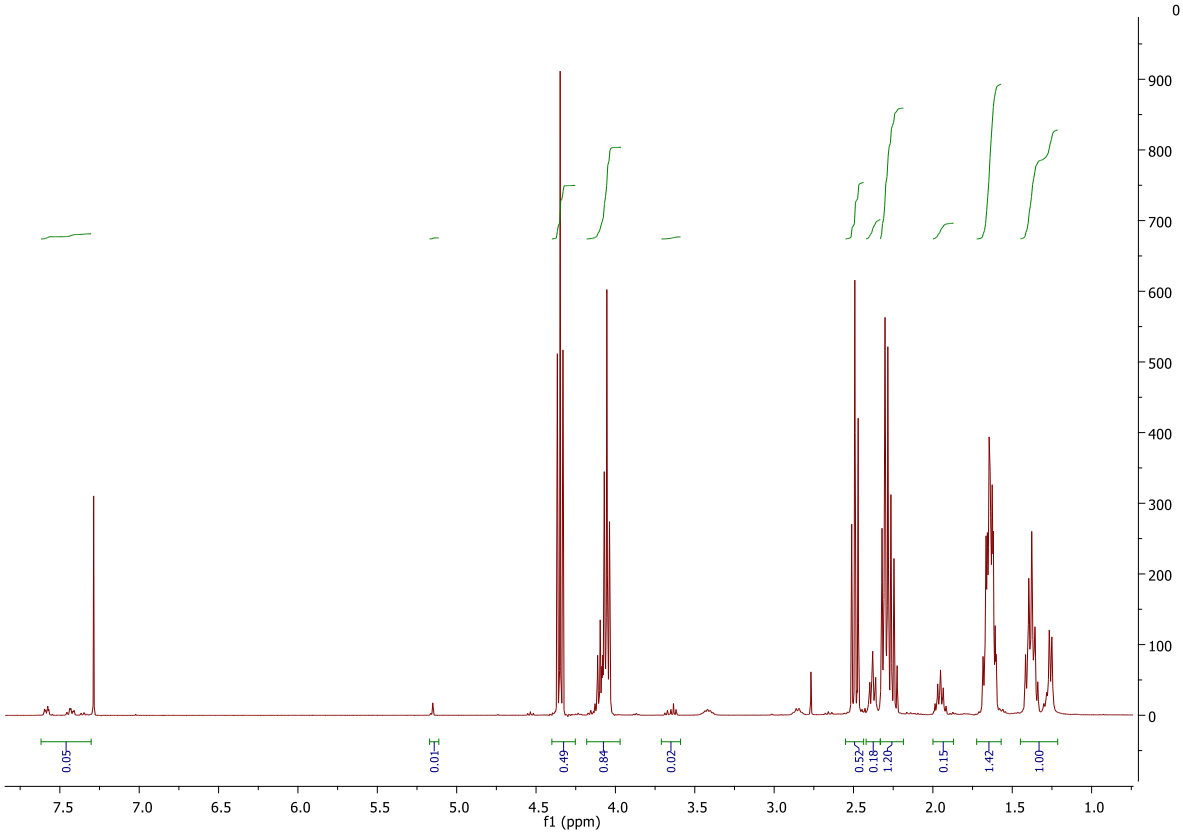

Figure A. 27 - ^{1}H NMR spectrum of the copolymer Ɛ-CL and ɣ-BL of the crude sample (Run 3, Table 10), with integration peaks.

n

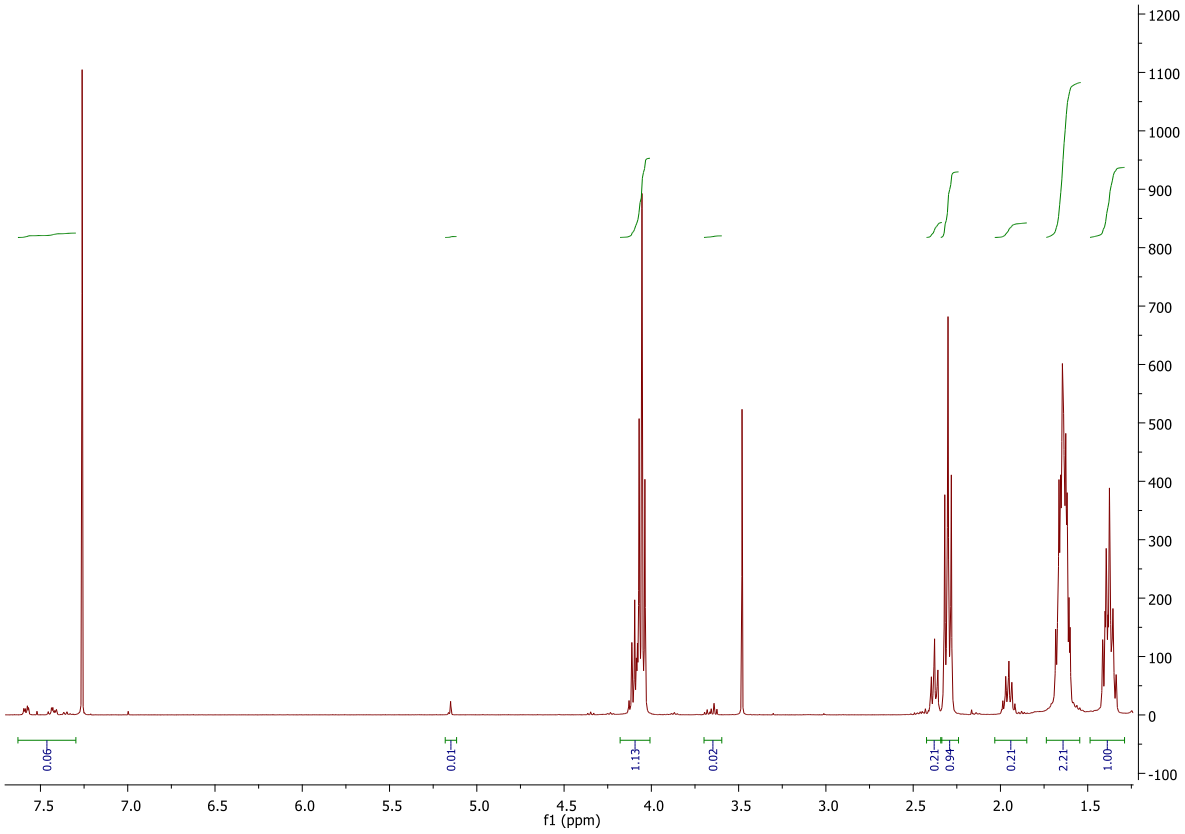

Figure A. 29 - ^{1}H NMR spectrum of the copolymer Ɛ-CL and ɣ-BL of the pure sample (Run 3, Table 10), with integration peaks.

SEC

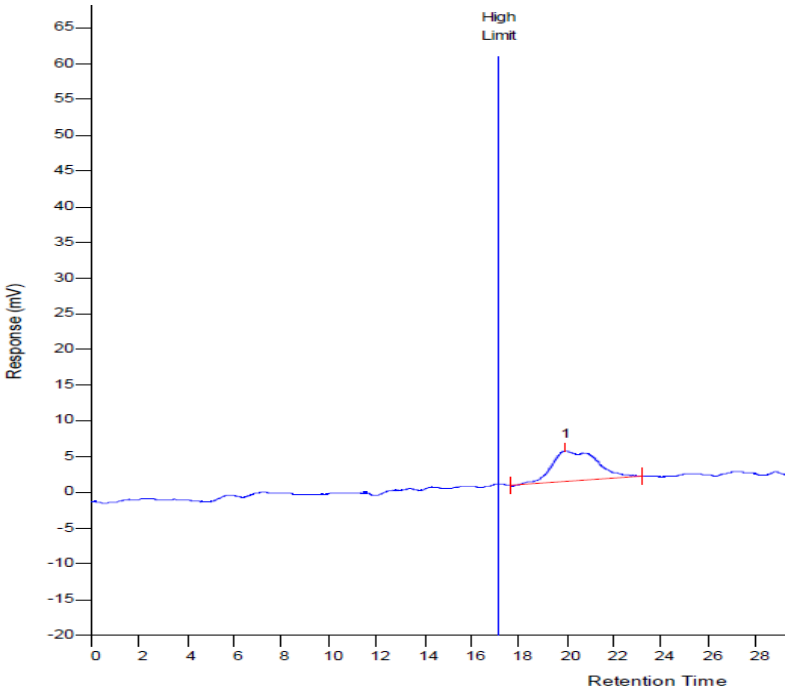

Figure A. 30 - SEC chromatogram of the polycaprolactone obtained at 25ºC, of Run 6, Table 2 (THF with polystyrene calibration at 40 ° C).

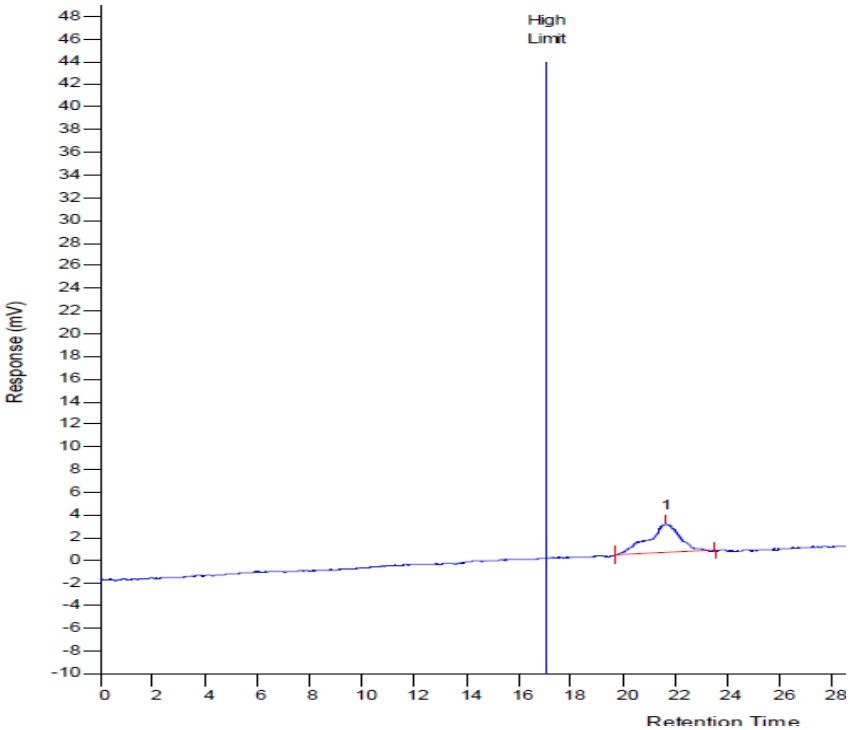

Figure A. 31 - SEC chromatogram of the poly(caprolactone-co-butyrolactone) obtained at 25ºC, of Run 2, Table 5 (THF with polystyrene calibration at 40 ° C).

p

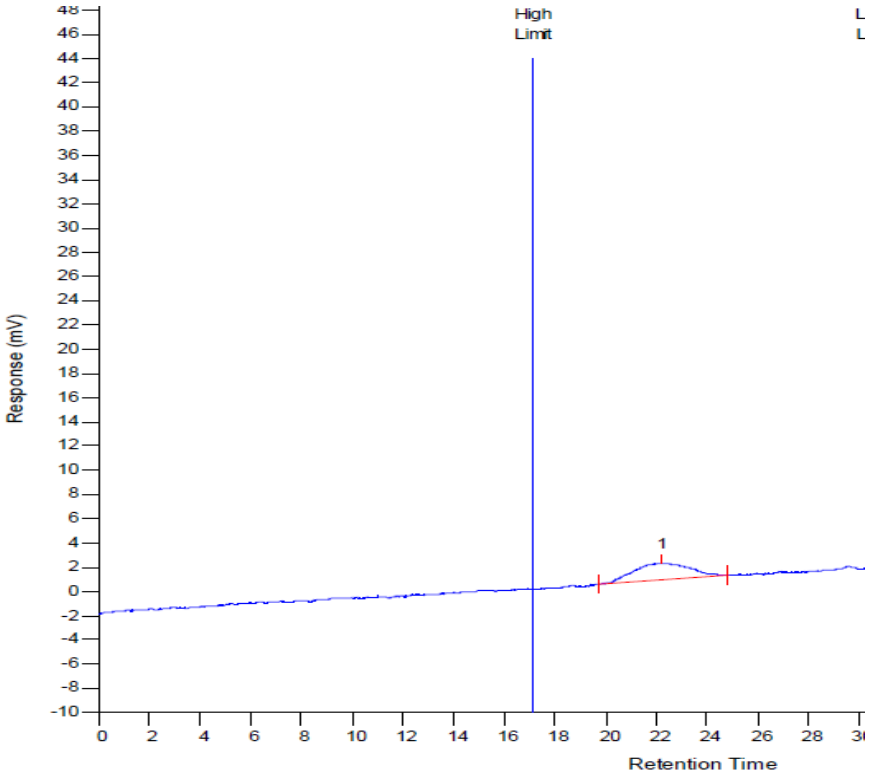

Figure A. 32 - SEC chromatogram of the poly(caprolactone-co-butyrolactone) obtained at 25ºC, of Run 1.1, Table 6 (THF with polystyrene calibration at 40 ° C).

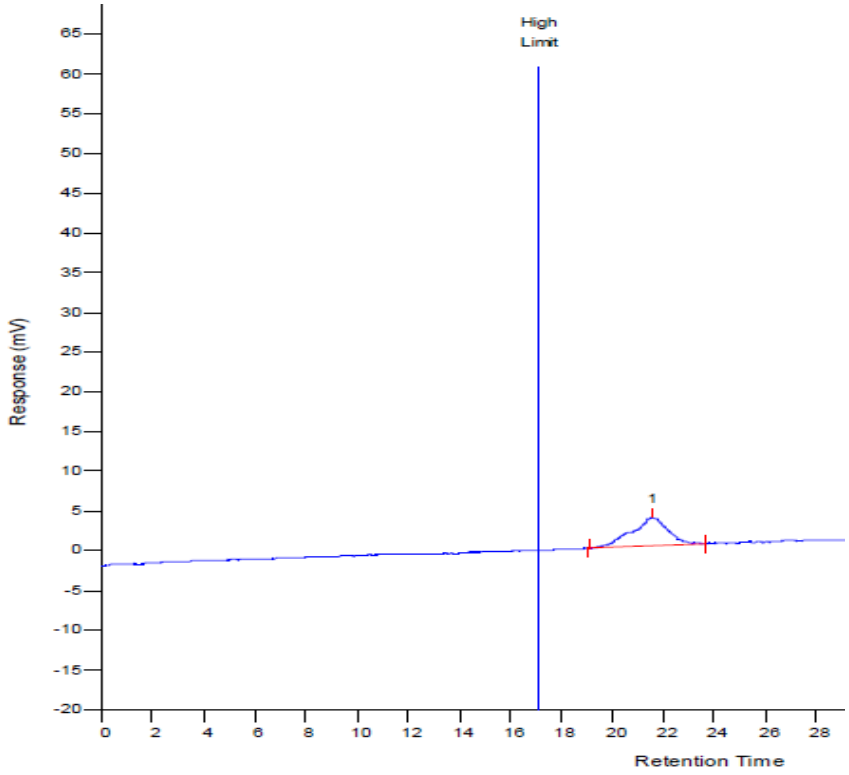

Figure A. 33 - SEC chromatogram of the poly(caprolactone-co-butyrolactone) obtained at 25ºC, of Run 1, Table 7 (THF with polystyrene calibration at 40 ° C).

q

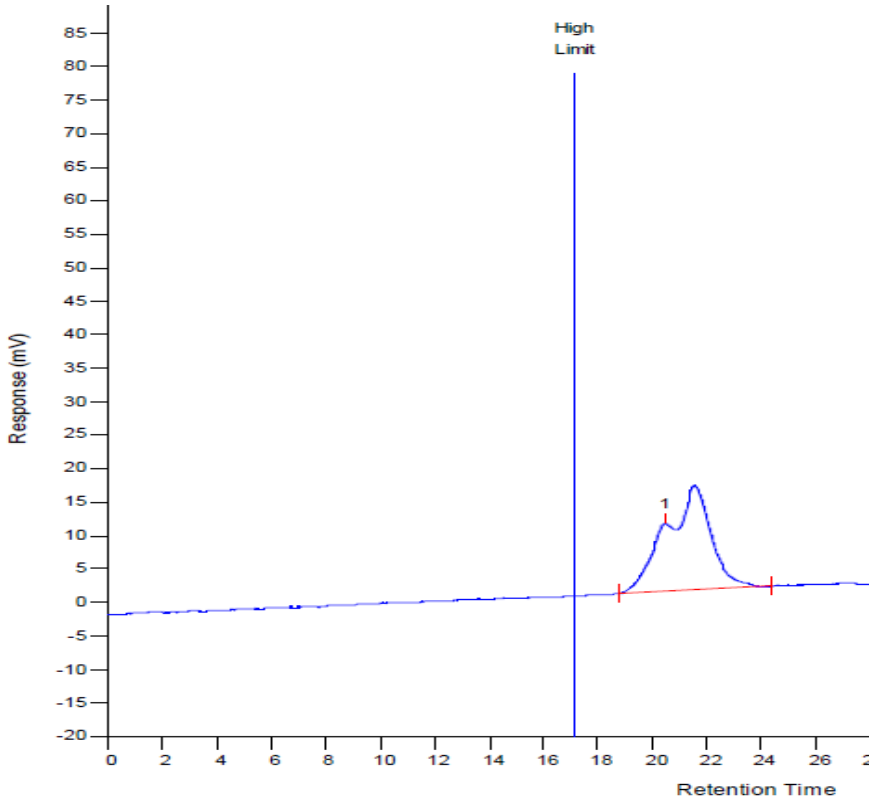

Figure A. 34 - SEC chromatogram of the poly(caprolactone-co-butyrolactone) obtained at 25ºC, of Run 2, Table 7 (THF with polystyrene calibration at 40 ° C).

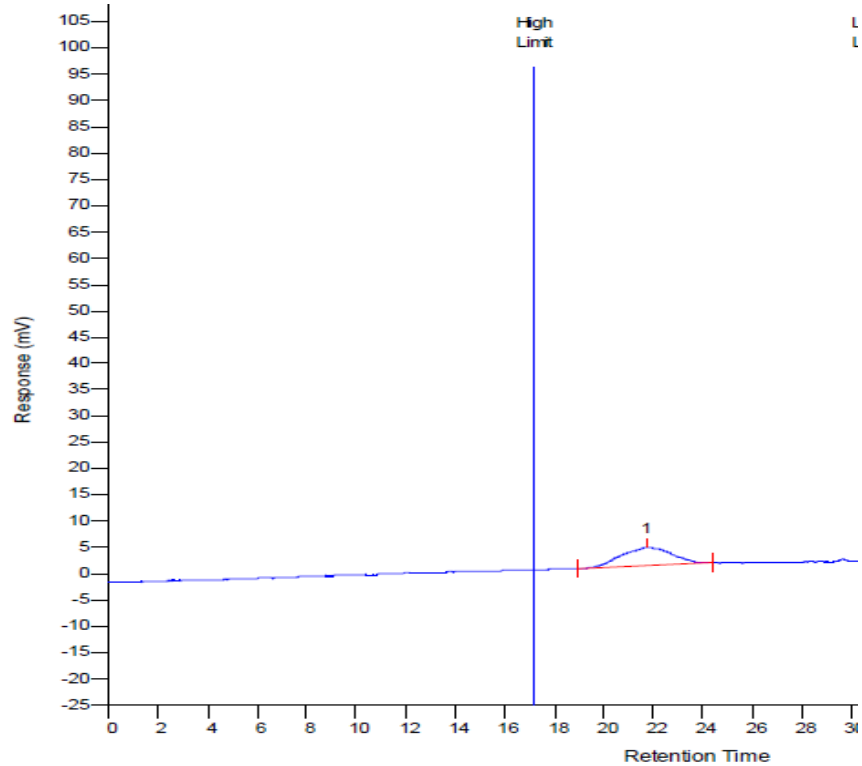

Figure A. 35 - SEC chromatogram of the poly(caprolactone-co-butyrolactone) obtained at 25ºC, of Run 1.1, Table 8 (THF with polystyrene calibration at 40 ° C).

r

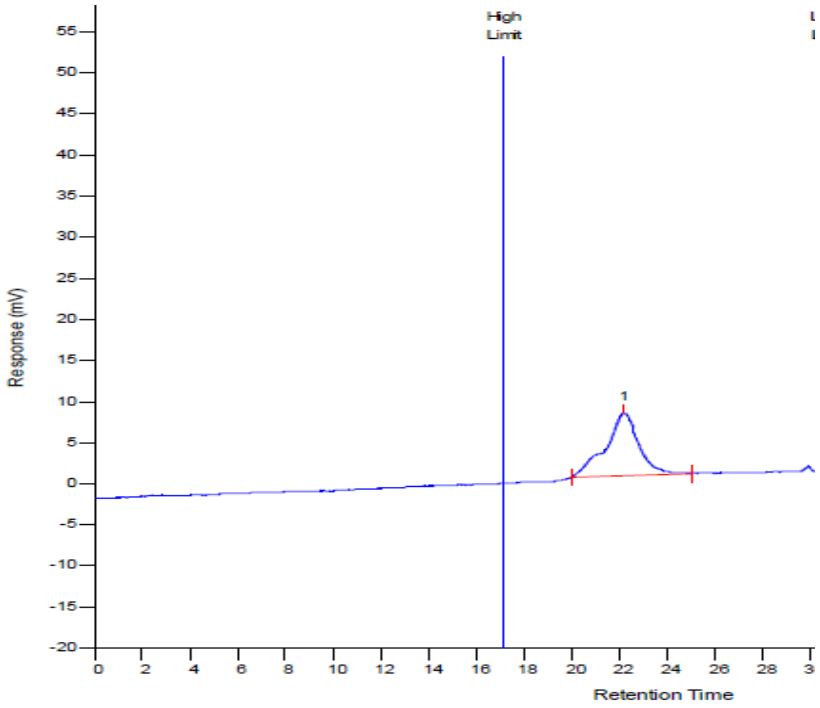

Figure A. 36 - SEC chromatogram of the poly(caprolactone-co-butyrolactone) obtained at 25ºC, of Run 1, Table 9 (THF with polystyrene calibration at 40 ° C).

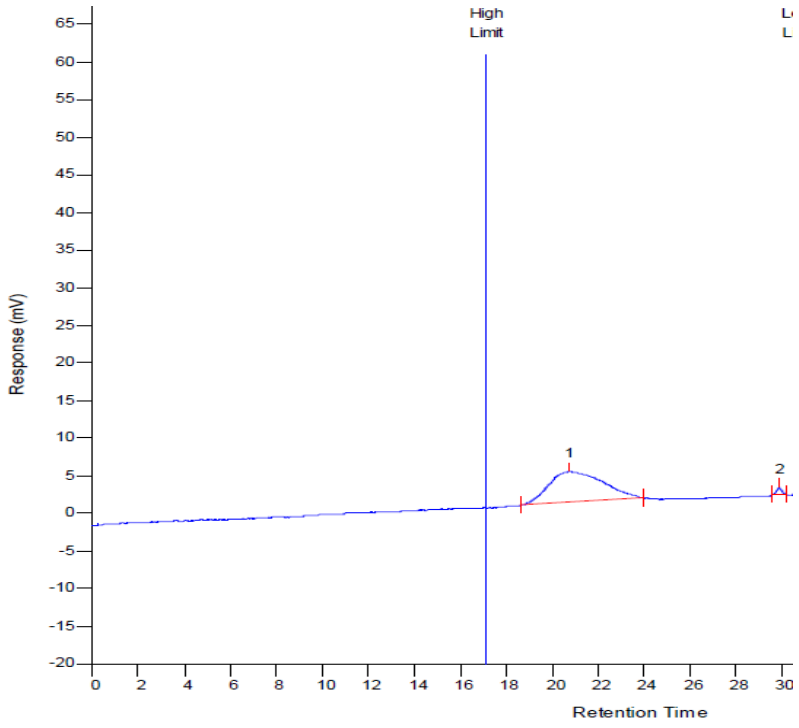

Figure A. 37 - SEC chromatogram of the poly(caprolactone-co-butyrolactone) obtained at 25ºC, of Run 2, Table 9 (THF with polystyrene calibration at 40 ° C).

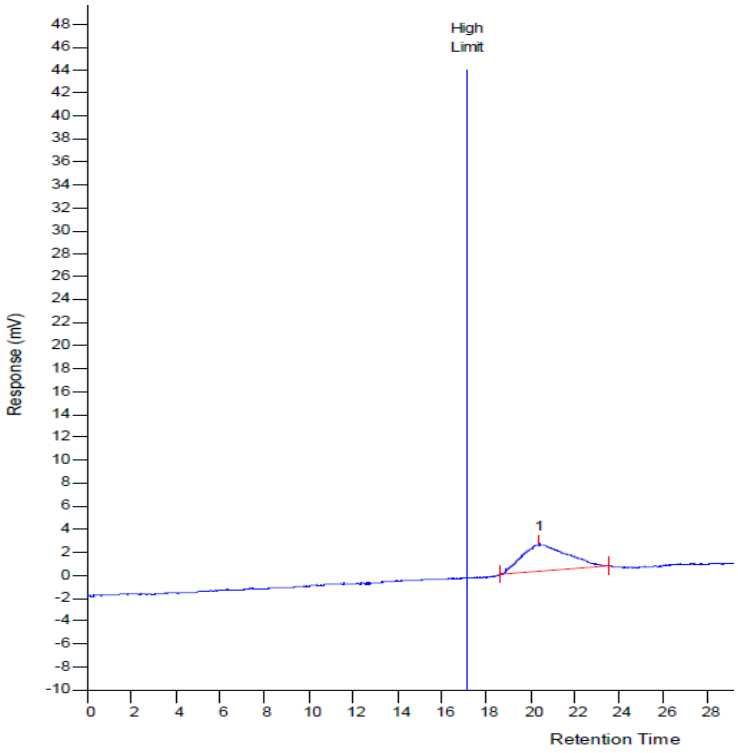

Figure A. 38 - SEC chromatogram of the poly(caprolactone-co-butyrolactone) obtained at 25ºC, of Run 3, Table 9 (THF with polystyrene calibration at 40 ° C).

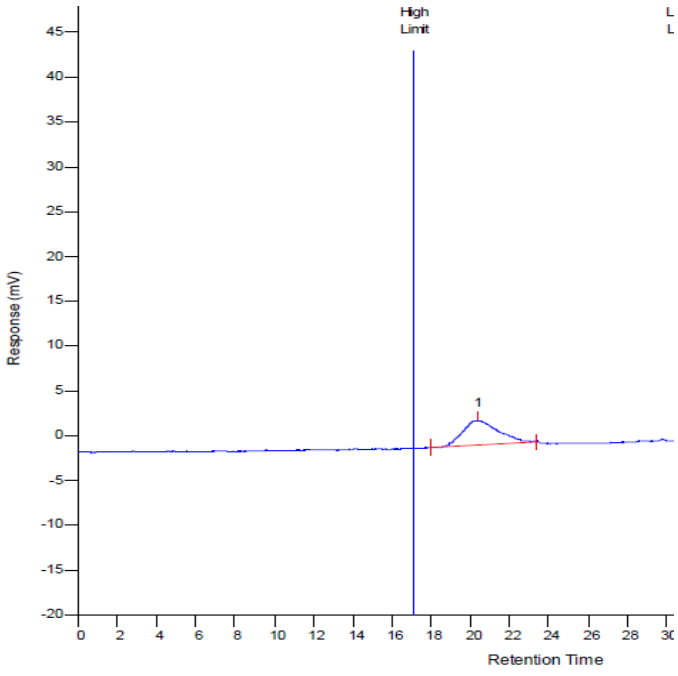

Figure A. 39 - SEC chromatogram of the poly(caprolactone-co-butyrolactone) obtained at 25ºC, of Run 1, Table 10 (THF with polystyrene calibration at 40 ° C).

t

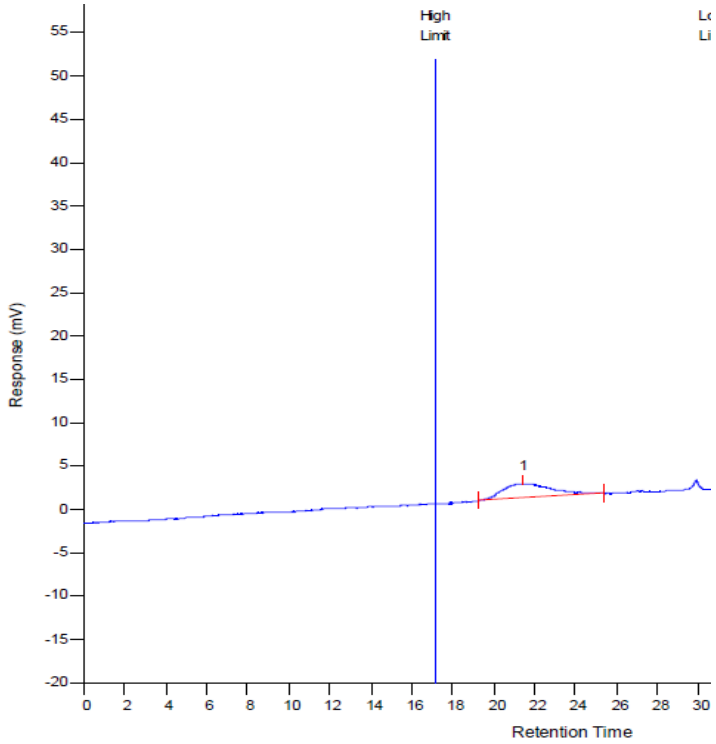

Figure A. 40 - SEC chromatogram of the poly(caprolactone-co-butyrolactone) obtained at 25ºC, of Run 2, Table 10 (THF with polystyrene calibration at 40 ° C).

u